Models of Epsilon-Sarcoglycan Gene Inactivation and their Implications for the Pathology of Myoclonus Dystonia

Alexis Given, B.Sc.

This thesis is submitted as a partial fulfillment of the M.Sc. program in Neuroscience

August 31, 2012

University of Ottawa, Ottawa, Ontario

Abstract

Myoclonus Dystonia (MD) is an autosomal dominant movement disorder characterized by bilateral myoclonic jerks paired with dystonia [1]. Mutations have been mapped to the ε-sarcoglycan (*SGCE*) gene in about 40% of patients [2,92]. The purpose of this project was to examine the properties of SGCE in the central nervous system (CNS) and use this knowledge to elucidate the pathology of MD. Although Sgce is a member of the sarcoglycan complex (SGC) in other tissues, little is known about its interactions in the CNS. The vast majority of mutations in SGCE alter the translational reading frame. Proteins arising from these rare mutations are less stable than the wild type (WT) and undergo preferential degradation via the ubiquitin proteasome system [3]. As this locus is maternally imprinted, patients with MD are effectively null for sgce expression [73,91]. Therefore, *Sgce* knock out (KO) models should approximate MD conditions both *in vivo* and *in vitro*.

As there are no current treatments for MD, in sight into the pathology of the disease will aid in eventual treatments and help bring patients some relief by finally understanding their disease. Since a large percentage of MD patients are without the sgce protein, identifying what this protein's function is and how its absence effects normal processing in the brain should help to identify the underlying cellular pathology which produces the MD phenotype.

This research was performed under the hypothesis that, in neuronal cells, sgce interacts with a group of proteins that together play a role in stabilization and localization of ion channels and signaling proteins at the cell membrane. The aims were to: (1) Build a MD mouse model with either a conditional knock-out (cKO) or a conditional gene

repair (cGR) mutation; (2) Use neuroblastoma cells to identify the other proteins which interact with sgce in neurons, and; (3) Determine if there is a disruption of the localization of the sgce-complex members due to the loss of sgce.

Recombineering was used to complete the constructs for two transgenic mouse models: One model for the KO of exon 4 of sgce and one for the cGR in intron 1. Primary neurosphere lines from two previously generated chimeras were developed, as well as from a WT mouse. These neurosphere cell lines allowed comparisons of RT-PCR results from a heterogeneous neurological cell population to neuroblastoma cell lines.

mRNA is present in neuronal cells for many of the DGC associated proteins. It was confirmed that the KD of sgce results in a reduction of nNOS protein and in increased proliferation of NIE cells. By using a nitrite/nitrate assay as well as studies with L-NAME, it was confirmed that this increased proliferation was in fact due to a lack of nNOS function. These proliferation changes did not occur in N2A cells, which do not express high levels of nNOS during proliferation, further confirming nNOS's role in the proliferation changes. Using qRT-PCR, KD of sgce was shown to result in significant changes in the transcript levels for many DGC associated proteins. This suggests that a DGC-like complex is forming in neuronal cells. Also, as a result of difficulties with the research, it became clear that over-expression of sgce causes cell death. This observation was quantified using cell counts and TUNEL staining, both showing significant results.

Additionally, several new constructs were created which will hopefully be of use for future students wanting to study sgce's functions. New shRNA targeting sgce and

sgcb have been made and both constructs result in reducing the expression of sgce. Seven different flag-tagged sgces have been created and some of these have been transferred into a tet-inducible system, which should circumvent the problem of over-expression. Finally GFP-tagged constructs for sgce and sgcb have been made and pooled clones have been developed. These tools will hopefully enable future students to continue to tease apart sgce's function(s).

Table of Contents

Index of Tables

Index of Figures

Abbreviations

AD	Autosomal Dominant
AR	Autosomal Recessive
Amp	Ampicillin
BDNF	Brain Derived Neurotrophic Factor
BG	Basal Ganglia
Cam	Chloramphenicol
Cav1,2,3	Caveolin 1, 2 or 3
cGR	Conditional Gene Repair
cKO	Conditional Knock-Out
CNS	Central Nervous System
DEPC	Diethylpyrocarbonate
DG	Dystroglycan
DGC	Dystrophin Glycoprotein Complex
DMEM	Dulbecco's Minimal Essential Medium
DOPAC	3,4-Dihydroxyphenylacetic acid
DP#	Dystrophin Isoforms
Dtn(s)	Dystrobrevin(s)
Dyf	Dysferlin
Dys	Dystrophin
ES	Embryonic Stem
FBS	Fetal Bovine Serum
GABA	Gamma-Aminobutyric Acid
Glu	Glutamax
GPe	Globus Pallidus externa
GPi	Globus Pallidus interna
HVA	Homovanillic acid
IHC	Immunohistochemistry
Kan	Kanamycin
KO	Knock-Out
LB	Luria Bertani
LGMD	Limb Girdle Muscular Dystrophy
LIF	Murine Leukemia Inhibitory Factor
LR-PCR	Long Range PCR
MD	Myoclonus Dystonia
MOI	Multiplicity of Infection
NADPH	Nicotinamide Adenine Dinucleotide Phosphate
NaPy	Sodium Pyruvate
NCBI	National Centre for Biotechnology Information

NEAA	Non-Essential Amino Acids
NMDA	N-Methyl-D-Aspartic Acid
nNOS	Neuronal Nitric Oxide Synthase
NO	Nitric Oxide
O/N	Overnight
OCD	Obsessive Compulsive Disorder
OD	Optical Density
pBSK	pBluescript
PCR	Polymerase Chain Reaction
Pen/Strep	Penicillin Strptomycin
PNS	Peripheral Nervous System
PTD	Primary Torsion Dystonia
qRT-PCR	Quantitative RT-PCR
R	Recessive
RE	Restriction Enzyme
RT	Room Temperature
RT-PCR	Reverse Transcriptase PCR
SB	Southern Blot
SGC	Sarcoglycan Complex
sgc	Sarcoglycans
sgca	alpha-Sarcoglycan
sgcb	beta-Sarcoglycan
sgcd	delta-Sarcoglycan
sgce	epsilon-Sarcoglycan
sgcg	gamma-Sarcoglycan
sgcz	zeta-Sarcoglycan
SNc	Substantia Nigra pars compacta
SNr	Substantia Nigra pars reticulata
Snt(s)	Syntrophin(s)
Sspn	Sarcospan
STN	Subthalamic Nucleus
Tet	Tetracycline
WB	Western blot
WT	Wild Type

1. Introduction

1.1 Dystonia Subtypes and Sarcoglycanopathies

Of the six sarcoglycans (sgc), disorders are associated with the dysfunction of five of them. There are no reported links between ζ-sarcoglycan (sgcz) and any disorders. Mutations in sarcoglycans are often associated with limb girdle muscular dystrophy (LGMD) [60]: Sgca with LGMD2D, sgcb with LGMD2E, sgcg with LGMD2C, and sgcd with LGMD2F [81]. LGMD is usually inherited and is an autosomal class of muscular dystrophy. It most severely effects the muscles around the hips and shoulders. As the sarcoglycans associated with LGMD are all known members of a heterotetrameric sub-complex formed predominantly in muscle, it suggests that the disruption of this complex may be important in the disease pathology. Other LGMD subtypes are associated with mutations in many other genes however.

The last sarcoglycan associated disorder is due to mutations in the sgce gene and causes the neurologically based disorder myoclonus dystonia. This sarcoglycanopathy is set apart from the others by being neurologically based. Mutations leading to the loss of functional sgce protein do not create muscular deficiencies but do cause involuntary jerks and torsions via the CNS.

Dystonias in general are neurologically based movement disorders characterized by sustained muscle contractions causing repetitive movements and twisting, or torsions. Within the dystonia family there is a wide variety of clinical features, age of onset, mode of inheritance and associated genetic loci (Table 1). Dystonias are not

exclusively hereditary and may also arise from other factors such as trauma, infection, poisoning or drug reactions [37].

Table 1: Dystonia sub-types

Name	OMIM	Gene	Locus	Alternative Names	Clinical features	Age of onset	Mode of inheritance
DYT1	128100	TOR1A	9q34.11	Early-Onset Torsion Dystonia, Dystonia Musculorum Deformans 1	Early onset primary torsion dystonia (PTD) starts in limb and often generalizes	Mid- to late-Childhood, occasional Adult	AD ~30% penetrance
DYT2	224500	unknown	unknown	Autosomal Recessive Torsion Dystonia	Early onset, generalized or segmental PTD	Childhood to Adolescence	AR
DYT3	314250	TAF1	Xq13.1	X-linked Dystonia-Parkinsonism, Torsion Dystonia-Parkinsonism, Filipino Type	Segmental or generalized PTD with parkinsonism progressive neurodegenerative syndrome	Adult; avg. 35 yrs	X-linked R
DYT4	128101	unknown	unknown	Autosomal Dominant Torsion Dystonia	Whispering dystonia	13-37 yrs	AD
DYT5	128230	GCH1	14q22.2	Dopamine-Responsive Dystonia, Segawa Syndrome	Most often dystonia with parkinsonism, treated with levodopa	Usually Childhood	AD incomplete penetrance
DYT6	602629	THAP1	8p11.21	Adolescent-Onset PTD of mixed type, Torsion Dystonia	Focal or generalized; cranial, cervical or limb dystonia	Late Childhood; avg. 19 yrs	AD
DYT7	602124	unknown	18p	Primary Cervical Dystonia, Adult Onset Focal PTD Torsion Dystonia, Focal Adult-Onset	Adult onset focal dystonia and postural tremor	Adult; 28 to 70 yrs	AD incomplete penetrance
DYT8	118800	MR1	2q35	Paroxysmal Nonkinesigenic Dyskinesia 1, Mount Reback Syndrome	Attacks of dystonia, athetosis, chorea precipitated by hunger, caffeine, alcohol and emotional stress	Infancy to Childhood	AD incomplete penetrance

Name	OMIM	Gene	Locus	Alternative Names	Clinical features	Age of onset	Mode of inheritance
DYT9	601042	possibly KCNA3	1p	Episodic Choreoathetosis /Spasticity	Involuntary movements and dystonia following exercise, stress and alcohol; spastic paraplegia between attacks	Childhood; 2-15 yrs	AD
DYT10	128200	PRRT2	16p11.2	Episodic Kinesigenic Dyskinesia 1, Paroxysmal Kinesigenic Choreoathetosis /Dyskesia	Attacks of dystonia/ choreoathetosis brought on by sudden movements	Childhood or Adolescence increased male to female ratio of 3.5 to 1	AD incomplete penetrance
DYT11	159900	SGCE	7q21	Myoclonic Dystonia, Alcohol Responsive Dystonia	Myoclonic jerks in combination with dystonia, responsive to alcohol	Early Childhood or Adolescence	AD incomplete penetrance
DYT12	128235	ATP1A3	19q13.2	Rapid-Onset Dystonia-Parkinsonism	Acute or subacute onset of generalized dystonia with parkinsonism	Adolescence to Adulthood, rarely Childhood	AD incomplete penetrance
DYT13	607671	unknown near D1S2667	1p36.32 -p36.13	Early and Late Onset Focal or Segmental Dystonia	Focal or segmental dystonia with onset either in the cranial-cervial region or in the upper limbs; mild course	Early Childhood to Adulthood; avg. 15 yrs	AD incomplete penetrance
DYT14	See DYT5	unknown	14q13		Generalized dystonia and parkinsonism	Adult	AD
DYT15	607488	unknown	18p11	Myoclonic Dystonia	Myoclonus dystonia, highly similar to Dyt11	5 to 15 yrs	AD incomplete penetrance
DYT16	612067	PRKRA	2q31.3	N/A	Progressive disorder, early-onset dystonia-parkinsonism, orofacial dystonia is a prominent feature	Childhood to Adolescence	AR
DYT17	612406	unknown near D20S107	20p11.2 -q13.12	Torsion Dystonia	Begins as focal dystonia, later becomes segmental or generalized, progressive dystonia	Adolescence	AR
DYT18	612126	SLC2A1	1p34.2	GLUT1 Deficiency Syndrome 2	Highly variable phenotype	Childhood	AD incomplete penetrance

Name	OMIM	Gene	Locus	Alternative Names	Clinical features	Age of onset	Mode of inheritance
DYT19	611031	unknown	16q13-q22.1	Episodic Kinesigenic Dyskinesia 2	Episodic, symptoms precipitated by sudden movements, often remits with age	Childhood to Adolescence	AD
DYT20	611147	unknown	2q31	Paroxysmal Nonkinesigenic Dyskinesia 2	Episodic, typically lasting 2 to 5 minutes, occurring daily to several times per month	Childhood to late Adulthood	AD reduced penetrance

Mode of Inheritance: AD = autosomal dominant, AR = autosomal recessive, R= recessive

This data was derived from OMIM [36]

1.2 Myoclonus Dystonia

Myoclonus Dystonia (MD) is a neurologically based non-degenerative movement disorder [72]. Patients with this disorder have a prevalence of myoclonic jerks along with dystonic torsions, predominantly of the torso, neck and arms [69]. They do not however show any signs in skeletal or myocardial muscles of muscle disease [60,80]. The severity of these symptoms varies widely, even amongst a single family [78,84]. MD patients may also express co-morbid psychological symptoms, such as obsessive compulsive disorder (OCD) and some reports indicate increased depression and anxiety [64,87].

Currently there are no effective treatments for MD, however ethanol ingestion has been shown to ameliorate symptoms in a subset of patients [98]. Unfortunately this amelioration is followed by a rapid rebound of symptoms [88]. Alcoholism rates are increased in MD patients but it is not clear if alcohol dependence is a symptom of MD, is due to obsessive behaviour or to self medication. Increased alcohol dependance even in sgce-mutation carriers who do not display motor symptoms has been shown however [64,87]. It is unknown why alcohol results in an amelioration of symptoms but ethanol has been shown to up-regulate mRNA transcripts of sgce and both α- and β-laminin 1 in neurospheres [4].

MD is an inherited autosomal dominant trait with variable penetrance [90]. Approximately 40% of patients present with mutations in the SGCE gene [2,92]. The majority of these mutations alter the translational reading frame resulting in a premature termination of translation. SGCE protein arising from genes containing mutations undergo preferential degradation via the proteasome [3]. Since this locus is maternally imprinted, most patients inherit MD paternally and are effectively sgce nulls [73]. Another

locus on chromosome 18p11 has been linked to MD, but this gene has yet to be identified [5,76].

Not much is known about the neuronal activities of sgce, so the sarcoglycan complex (SGC) in muscle has been used as a paradigm to begin building a neuronal model.

1.3 Dystrophin Glycoprotein Complex

In muscle, the dystrophin glycoprotein complex (DGC) links the actin cytoskeleton to the extracellular matrix and is important for cell membrane stability and ion channel clustering. The SGC is one component in a greater complex (Figure 1A). The dystroglycans (DG) work together to span the membrane and give structural integrity to the muscle tissue. αDG is located extracellularly and binds to laminin in the basement membrane while βDG spans the cell membrane and binds to dystrophin (Dys) in the cytoskeleton [6].

There are a number of other associated proteins, including Sarcospan (sspn), which forms a complex with the SGC and functions to anchor αDG to the sarcolemma. Sspn also contributes to the stability of the sarcolemma and over-expression has been shown to promote utrophin binding to the extrasynaptic sarcolemma in Dys null, or *mdx,* mice [7]. This over-expression of sspn in *mdx* mice also restores the localization of the sarcoglycans (sgc) and DGs [7]. Other associated proteins include the syntrophins (Snt), adaptor proteins which aid in localization of signaling proteins, the dystrobrevins (Dtn), and likely various channels and signaling proteins [8,94]. Integrins, receptors who mediate the cell's attachment to the extracellular matrix, are also associated with the DGC

through the sarcoglycans. In muscle, integrin α7 increases at the membrane in response to sarcoglycan deficiency and mice lacking both integrin α7 and sgcg exhibit profound rapid muscle degeneration leading to death [67]. In myocytes, it was shown that the removal of alpha and gamma sarcoglycan leads to significant reductions of focal adhesion proteins and a 50% reduction of cell adhesion [68].

Previous studies have shown that, in muscle, that the removal of either alpha-, beta- or delta-sarcoglycan (sgca, sgcb, or sgcd) is sufficient to prevent the formation of the SGC at the membrane. As mutations in the corresponding genes for these proteins are known to result in LGMD, this suggests that the lack of this complex is involved in the pathology. In these sgc KO models, as well as in Dys KO models, a 50% decrease of neuronal nitric oxide synthase (nNOS) has been observed [9,93]. It is thought that without the SGC nNOS cannot anchor properly to the membrane and is therefore degraded.

Many of the DGC associated proteins are also present in the brain. Thus far, little is known about the exact function and complex formation of these proteins in neurons or glia [8] (Figure 1B, C). There are, however, several reasons to suspect that novel DGC-like complexes reside in the brain. For example distinct Dys isoforms are present in the brain. Also sgce and zeta-sarcoglycan (sgcz) are more highly expressed in the brain than the other sgcs, which are predominantly expressed in striated and smooth muscle. This altered stoichiometry of the sgcs would support a novel SGC in the brain. Additionally there is evidence that there may be many different neuronal DGC-like complexes in different neuronal tissues and cell types. In the case of Dys, the full length isoform, DP427, is expressed in neurons while Dp71 and Dp140 are located in glial

cells. The different Dys isoforms present in the brain are also distinctly localized [38,39,40,41,42,43,44]. Dp71 is the most abundant product in the CNS and it is also expressed throughout the body. While the Dp427p isoform is expressed specifically in the cerebellar Purkinje cells and yet a different isoform, Dp427c, is expressed in the cortex and subcortical regions including the hippocampus [8]. Dp140 is found in the cerebellum, kidneys and microvasculature, and Dp260 is found in retina [8,40,41].

In the cerebellar Purkinje cells, Dys is associated with post-synaptic gamma-aminobutyric acid (GABA) A receptor clusters, specifically the α2 subunit. The *mdx* mouse shows a significant reduction in the number of these clusters, suggesting a role for one of these DGC-like complexes at inhibitory synapses. Additionally, the DGs are also found at these inhibitory synapses and are likely key elements in the formation of the DGC-like complex here. Further supporting the association with inhibitory synapses, other DGC members are associated with inhibitory synapses in hippocampal neurons [8]. It has also been demonstrated that αDG binds neurexin, a membrane bound protein which helps stabilize the synapse and keep it together and facilitates signaling across the synapse [34]. As in muscle, αDG also binds laminin, specifically laminin1, in neuronal tissues [35]. Laminin1 also interacts with other surface receptors, including the integrins.

The dystrobrevins (dtns) bind directly to Dys. These proteins then bind directly to the syntrophins (snts). α-Dtn is found in striated muscle while β-Dtn is found in many non-muscle DGC-like complexes including those found in the brain [10]. The Snts have a PDZ domain which has been shown to bind proteins such as nNOS, aquaporin-4 and the neuroligins [94]. Specifically α-Snt has been shown to bind nNOS but it has been

suggested that the Snts may have a compensatory role for each other, as KO models for specific Snts have not produced any obvious CNS phenotypes [8].

Disruption of members of the DGC in muscle often results in muscle based movement disorders. As mentioned, disruptions with α–, β–, δ– or γ–sarcoglycan are associated with LGMDs. Mutations in the gene for caveolin 3 (Cav3), a membrane scaffolding protein, and dysferlin (Dysf), a protein linked to skeletal muscle repair, have also been associated with LGMD [45,46]. In addition, the absence of dystrophin is the cause of DMD [47]. These are all based in the muscle however, making the pathology markedly different from MD, which is neurologically based. MD patients maintain healthy muscle tissue.

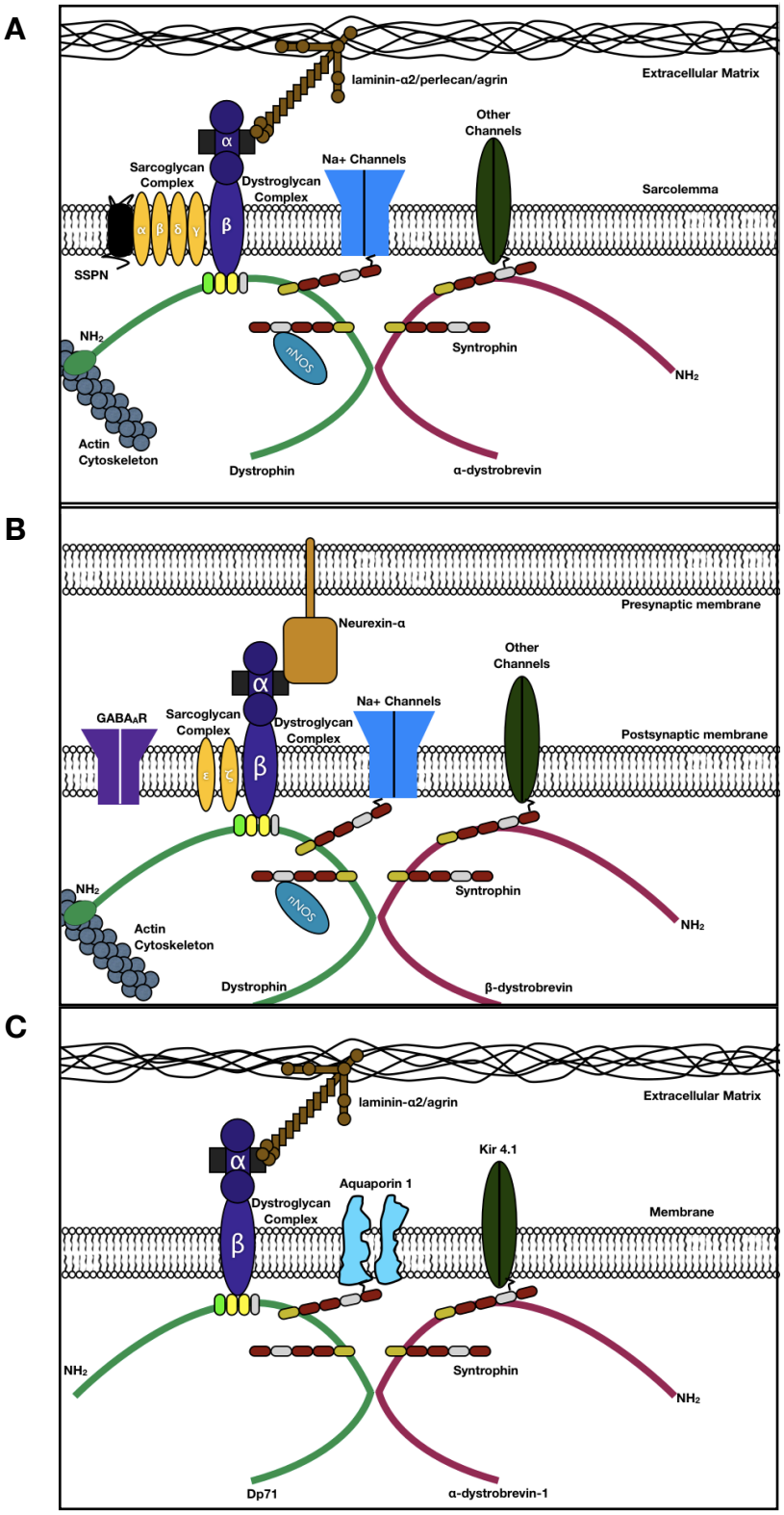

Figure 1: The Dystrophin Glycoprotein Complex [8]: as determined in muscle from direct biochemical purifications (A), as inferred in neurons from different studies (B), and as inferred in glia from different studies (C)

1.4 Sarcoglycans

The sarcoglycans (sgcs) are a family of transmembrane proteins. There are six known family members: α–, β–, δ–, ε–, γ– and ζ– sarcoglycan, also designated as sgca, sgcb, sgcd, sgce, sgcg and sgcz, respectively. The composition of sgcb is unique, while sgcd, sgcg and sgcz are 68% similar to each other, and alpha and epsilon are 62% similar [11] (Figure 2A). Both sgca and sgce take the same position within the known SGC and it has been shown that loss of alpha in the muscle or cardiac tissue can be compensated for by over-expression of sgce [12,13].

All six sarcoglycans are expressed in muscle where they form two heterotetrameric sub-complexes or SGCs (Figure 2B). The first complex consists of sgca, sgcb, sgcd, and sgcg. This is the predominant complex in skeletal and cardiac muscle. The second complex consists of sgce, sgcb, sgcd and sgcz. This complex is the more dominantly expressed complex in smooth muscle, retina and likely the peripheral nervous system (PNS). At least in muscle, these sub-complexes contribute to the greater DGC and help maintain its stability. They also maintain sspn at the sarcolemma and help stabilize signaling molecules, such as nNOS. The formation of this SGC happens in a stepwise process [14]. Sgcb initiates and associates with sgcd, which is essential for correct localization. Sgca is next incorporated and then sgcg. It is likely that sgce and then sgcz are added, in lieu of sgca and sgcg, in tissues expressing this heterotetramer.

In the PNS sgce, sgcb and sgcd appear to form a complex together and associate with αDG and βDG [15]. It is not clear if these three sarcoglycans are forming the heterotetrameric complex with sgcz or perhaps a novel nervous system specific

complex. In the CNS both sgce and sgcz are highly expressed but it is unclear what complexes they form. In Schwann cells and the sciatic nerve mRNA transcript is present for sgce, sgcb, sgcd and sgcz, suggesting that one of the known complexes is formed [15]. Studies have suggested the presence of the DGC at some postsynaptic membranes, possibly contributing to the proper localization of GABA receptors. αDG binds neurexin, possibly mediating interactions between pre- and post-synaptic membranes [16, 34]. This may also contribute to cell adhesion in the brain [17].

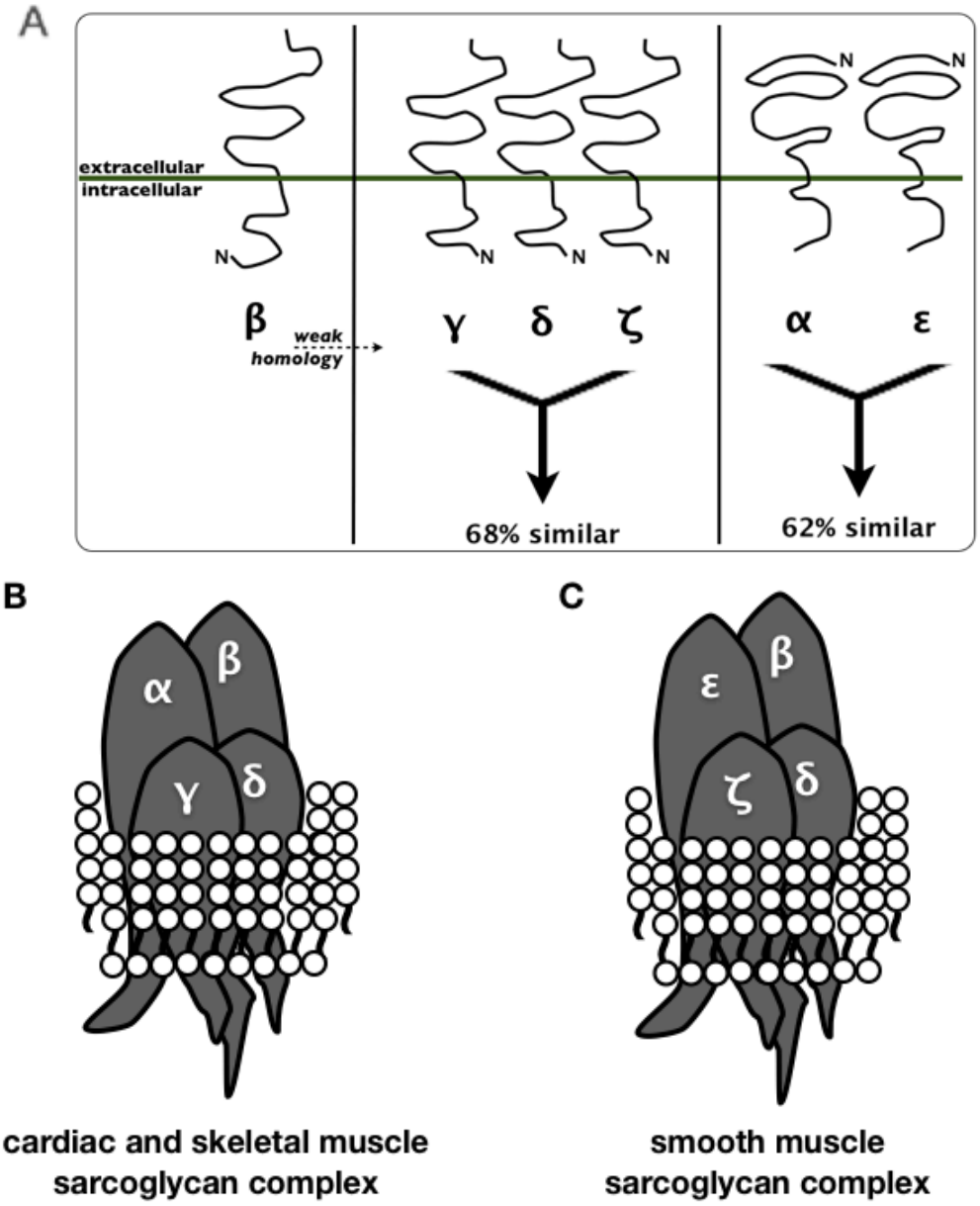

Figure 2: The sarcoglycans: Their structural similarities [11] (A) and two known heterotetramers [12] (B, C)

1.5 SGCE

SGCE, the protein which is absent in many MD patients, is the most widely expressed sgc. It is expressed throughout development. In rats, expression has been shown to peak at embryonic day 20 before rapidly dropping off towards adulthood [18]. Although it is almost ubiquitous in its expression pattern, its highest expression is in the lungs and the CNS. In the brain it appears to be expressed in the olfactory bulb, hippocampus, pons and cerebral cortex [20]. Sgce has also been associated with dopaminergic neurons in the substantia nigra and the ventral tegmental area [8].

Sgce has two main isoforms (Figure 19C). The first isoform contains exon 8 but lacks exon 11b and is predicted at 47 kDa. This isoform is expressed in all tissues and organs, including the brain. The second isoform lacks exon 8 but does include exon 11b and is slightly larger at 49 kDa. This isoform is only expressed in the brain [20]. Recently a third isoform was discovered including the exon 11c [65]. This isoform was also shown to be brain specific. Both isoforms one and two isoforms have been found throughout the brain in similar quantities, with the one exception of high expression of isoform 1 in the olfactory bulb [20]. Interestingly this second isoform appears to by pre-synaptic, while the first isoform is post-synaptic [65]. It is unclear as of yet whether these isoforms will play different roles or form novel complexes in the brain.

The sgce gene in mice shares 95.9% of it's amino acid identity with the human SGCE. It has a conserved N-terminus which targets it to the cell membrane. Extracellularly, sgce has asparagine residues for glycosylation, 4 cysteine residues and six potential phosphorylation sites [19,80]. Sgce has been implicated in playing a role in cell matrix adhesion [19,55].

1.6 nNOS

Members of the nitric oxide synthase (NOS) family include neuronal (nNOS), endothelial (eNOS), and inducible (iNOS). nNOS is highly expressed in neurons of the CNS and PNS, but it has also been described in other cell types including skeletal muscle myocytes, lung epithelial cells, and skin mast cells [57]. In the brain the nNOS isoform is located in several populations of neuronal cells in the cerebellum, olfactory bulb, hippocampus, and is also highly expressed within neurons of the hypothalamus [57]. eNOS is highly expressed by endothelial cells and may also be found in neurons, dermal fibroblasts, and smooth muscle cells among others. iNOS is expressed in a wide range of cell types including chondrocytes, epithelial cells, glial cells, and several immune system cell types [30].

nNOS is a signaling protein activated by an influx of Ca^{2+} through N-Methyl-D-aspartic acid (NMDA) receptors. In the brain, nNOS has been implicated in mediating neurotransmitter release and in long term potentiation. It is also linked to brain derived neurotrophic factor (BDNF) [96], which has been associated with OCD. nNOS acts to synthesize nitric oxide (NO) via the reaction of L-Arginine, Nicotinamide adenine dinucleotide phosphate (NADPH), and oxygen to NO and Citrulline. NO influences cell proliferation and differentiation. It is also involved in development and triggers neural progenitor cells to differentiate in response to a drop in phosphorylated CREB [21]. NO only has a half life of a few seconds, making it difficult to detect. For this reason levels of the more stable NO metabolites, nitrite (NO_2^-) and nitrate (NO_3^-), can be used as an indirect measurement of NO in biological fluids

The DGC complex has been shown to anchor signaling proteins, such as nNOS, to the membrane. Studies have shown that in muscle the removal of either sgca, sgcb or sgcd is sufficient to prevent the formation of the SGC at the membrane. In these sgc KO models, as well as in Dys KO models, a 50% decrease of nNOS has been observed [9,93]. It is hypothesized that the removal of the SGC causes conformational changes within the DGC, specifically to the PDZ domain of Snt, which interferes with the anchoring of nNOS.

1.7 ε-Sarcoglycan Knock-Out

A previous sgce KO mouse model demonstrated that removal of sgce expression *in vivo* is sufficient to produce MD symptoms. These mice demonstrated 28 times more myoclonic jerks than WT mice [22]. In addition, the sgce null mice showed impaired fine motor coordination, motor learning and vertical hyperactivity. It has been suggested that the vertical hyperactivity could mimic OCD, showing perhaps an obsessive predator checking behaviour. Females also displayed an increase in horizontal activity and depression while increased anxiety was only seen in male mice [22].

It has been suggested that MD may be a hyperdopaminergic dystonia. These KO mice showed an increase in dopamine levels in the striatum. Increased levels of DA metabolites DOPAC and HVA were also present. OCD has been associated with reduced serotonin transmission. While no changes were seen in overall serotonin levels of the KO mice, the ratio of serotonin metabolite 5-H1AA to serotonin tended to be higher in KO mice. Additionally, correlation between DOPAC and 5-H1AA metabolites

was seen and these levels inversely correlated with vertical movement [22]. This indicates that changes in serotonin should be further investigated.

Removal of sgce also resulted in abnormal nuclear envelopes in cerebellar Purkinje cells and striatal medium spiny neurons [62,63]. Interestingly, when sgce was specifically removed from either type of cell they did not show abnormalities in their nuclear envelopes or MD phenotype. KO in cerebellar Purkinje cells only resulted in motor learning deficits while KO in the striatal medium spiny neurons only resulted in some motor deficits [62,63]. This suggests that the loss of sgce in these cerebellar cells may account for motor learning disabilities and loss of sgce in these striatal neurons may account for motor deficits but that other regions are responsible for nuclear envelope abnormalities as well as the major MD symptoms.

Another mouse model of sgce KO was created by replacing sgce's exons 6-9 with Neo + β-gal cassette. These mice maintain maternal imprinting and no sgce, or hybrids of sgce-β-gal or sgce-Neo are expressed from the paternal allele. These mice have been used up to this point to create sgce/sgca double KO mice for research on cardiomyopathy [13].

1.8 Neurological Pathway

The specific area or pathway within the brain responsible for MD has yet to be elucidated. It has been proposed however that MD may be a hyperdopaminergic dystonia and increased dopamine (DA) was found in the striatum of sgce KO mice [22,70]. Sgce has been associated with dopaminergic neurons in both the substantia nigra and the ventral tegmental area, which are members of the basal ganglia (BG) [8].

Furthermore, the nigrostriatal pathway is involved in the motor loop of the BG, making it an interesting area for further MD research. MD has been classified as a cortical phenomena with one study showing increased cortical membrane excitability, fitting with the BG's affect on cortical inhibition [69,71,83].

The BG are a collection of nuclei located at the base of the forebrain. They work together cohesively for a variety of functions including the control of voluntary movement. The BG are also known to play a role in reward learning and emotional functions. If malfunctions are occurring in this area of the brain in MD patients, this could explain the increased incidences of alcoholism and OCD as learned behaviours. There are two pathways through the BG; the direct pathway and the indirect pathway [52] (Figure 3). Stimulation of the direct pathway results in a hyperkinetic state, while stimulation of the indirect pathway produces a hypokinetic state. In Parkinson's disease, where patients develop difficulty in producing voluntary movements, it is thought to be the deterioration of DA producing neurons in the substantia nigra. Parkinson's disease is often treated with Levodopa to increase the amount of DA and the common side effect of Levodopa, usually occurring only when the drug is at it's peak brain concentration, are dyskinesias [48]. Mainly these side effects take the form of chorea and

A

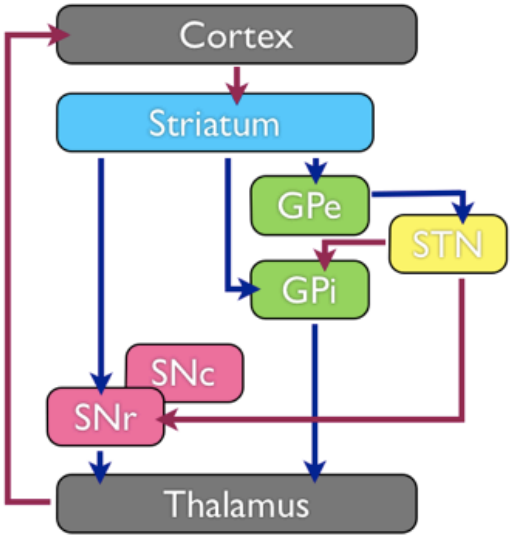

B **Direct Pathway:**

Cortex (stimulates) → **Striatum** (inhibits) → **SNr-GPi complex** (less inhibition of thalamus) → **Thalamus** (stimulates) → **Cortex** (stimulates) → **Muscles etc.** → **Hyperkinetic State**

C **Indirect Pathway:**

Cortex (stimulates) → **Striatum** (inhibits) → **GPe** (less inhibition of STN) → **STN** (stimulates) → **SNr-GPi complex** (inhibits) → **Thalamus** (is stimulating less) → **Cortex** (is less stimulating) → **Muscles etc.** → **Hypokinetic State**

Figure 3: The pathways of the Basal Ganglia. Basal ganglia model (A) with red arrows depicting stimulation and blue arrows inhibition. Two pathways exist through the basal ganglia: the direct pathway (B) and the indirect pathway (C).

Abbreviations
Globus Pallidus externa (GPe), Globus Pallidus interna (GPi), Subthalamic Nucleus (STN), Substantia Nigra pars compacta (SNc), Substantia Nigra pars reticulata (SNr).

dystonia but myoclonus, although less common, is also seen. This supports the suggestion that increased DA, potentially in the substantia nigra, may play a role in MD.

Changes in the BG have been seen in MD patients. One study found a strong correlation between the severity of the dystonia symptom and the increase in the volume of gray matter in the bilateral putamina [74]. It was suggested by these authors that this may increase the activation of the direct putamen-pallidal pathway, in turn decreasing the inhibitory output of the internal globus pallidus. This would increase the thalamic input to the pre-motor cortex. Magnetic resonance imaging of the cortical activation patterns in MD patients carrying sgce mutations indicated disorganized sensorimotor integration [77].

It has been further suggested that dystonia may be produced from hypofunction of dopamine's D2 receptor-mediated inhibition of the indirect pathway of the BG [49,86]. One large MD family was in fact shown to have a disease segregating mutation (Val154-Ile) within the D2 receptor gene [51]. Although this mutation was not found in other families screened this may still be important information towards the pathology of MD [50].

1.9 Hypothesis and Objectives

This research was performed under the hypothesis that, in neuronal cells, sgce interacts with a group of proteins that together play a role in stabilization and localization of ion channels and signaling proteins at the cell membrane. The aims were to: (1) Build a MD mouse model with either a conditional knock-out (cKO) or a conditional gene repair (cGR) mutation; (2) Use neuroblastoma cells to identify the other proteins which interact

with sgce in neurons, and; (3) Determine if there is a disruption of the localization of the sgce-complex members due to the loss of sgce.

2. Establishment of an *In Vivo* model for Myoclonus Dystonia

2.1 Materials and Methods

2.1.1 Bacterial Culture and Reagents for development of *In Vivo* Models

Escherichia coli (E. coli) strains DY380 and EL350 and plasmids, pL253, pL451 and pL452 were gifts from Dr. Neal Copeland (National Cancer Institute, Frederick, MD) [23]. DY380 and EL350 were maintained in Luria Burtani (LB) broth (1.0% Bacto-Tryptone 0.5% Yeast Extract 1.0% NaCl, pH 7.5) or solid medium (LB with 1.5% agar) at 32°C. DH5α competent *E. coli* cells (Invitrogen, Carlsbad, CA) were maintained on LB-broth or solid medium at 37°C. When required, antibiotics were used at a final concentration of 12.5 μg/ml Chloramphenicol (Cam), 12.5 μg/ml Tetracycline (Tet), 25 μg/ml Kanamycin (Kan), or 100 μg/ml Ampicillin (Amp) (Sigma-Aldrich,Oakville, ON).

2.1.2 Cloning of the retrieval vector

The BAC clone RP22-237K16 from the RPCI-22 (129S6/SvEvTac) mouse BAC library was obtained from The Centre for Applied Genomics (Toronto, ON). DNA from this clone had been previously isolated in the lab using the GenElute Plasmid Mini-Prep Kit (Sigma-Aldrich, Oakville, ON) and sent for sequencing [2].

PCR primers for the amplification of the 5', or AB, and 3', or YZ, homology arms were designed with *NotI/HindIII* and *HindIII/SpeI* restriction enzyme (RE) sites,

respectively, using the software program Primer 3 (www.frodo.wi.mit.edu) (Table 2). These RE sites were included to facilitate cloning into the pL253 vector and creation of the retrieval vector. The AB and YZ homology arms were PCR amplified from the BAC clone RP22-237K16 as described below. The resulting PCR products were sequenced to confirm their identity using the Big Dye 3.1 Cycle Sequencing kit (Applied Biosystems, Foster City, CA) according to manufacturers instructions. All resulting sequences were analyzed using the software program DS gene (Accelrys, San Diego, CA) and aligned to the mouse genomic sequence which had been downloaded from the NCBI database (www.ncbi.nlm.nih.gov/gene/), which corresponded to the *Sgce* gene and surrounding region.

The AB and YZ PCR products were purified using the Illustra GFX PCR DNA and Gel Band Purification Kit (GE Healthcare, Baie d'Urfe, PQ) and digested with either *SpeI* and *HindIII* or *HindIII* and *NotI* REs respectively (Invitrogen, Carlsbad, CA). The digested PCR products were again purified by spin column and quantified by comparison of band intensities to the Highranger Plus 100 bp DNA Ladder using gel electrophoresis (Norgen Biotek, St Catherines, ON) and by Nanodrop Spectrometer ND1000 (Thermo Scientific, Asheville, NC).

The pL253 vector contains the *MC1-TK* gene for negative selection with ganciclovir in mouse embryonic stem (ES) cells [31]. The pL253 plasmid was digested with *NotI* and *SpeI* REs. The linearized plasmid was then purified by spin column and quantified by gel electrophoresis and Nanodrop Spectrometer as previously described. Once the homology arm fragments and backbone were quantified, it was possible to

determine the relative amounts of these products for ligation reactions using the following equation:

$$\text{Insert V } (\mu\text{l}) = \frac{\text{plasmid amount (ng)} \times [\text{insert size (bp)} / \text{plasmid size (bp)}]}{\text{concentration of insert (ng/}\mu\text{l)}} \times \text{molar ratio}$$

The ligation of the homology arms into the pL253 vector was performed at 16^{o}C overnight (O/N) with 1U of T4 DNA ligase (Invitrogen, Carlsbad, CA) according to manufacturer's instruction. Ligation reactions were then transformed into DH5α competent cells according to the manufacturer's protocol and incubated on LB-Amp plates. DNA from resulting Amp^{r} clones was screened by RE digest and confirmed by sequencing. This plasmid was then designated as the retrieval vector.

2.1.3 Cloning of the mini-targeting vectors

Mini-targeting vectors were designed to place the floxed-neomycin resistance cassettes within the introns both 5' and 3' of exon 4 of the *Sgce* gene. The homology arms for each of the two cassettes, CD/EF and GH/IJ respectively, were amplified by PCR from the BAC clone RP22-237K16 (Table 2). Each homology arm was confirmed by sequencing. The CD and EF homology arms were digested with *SalI/EcoRI* and *BamHI*/*NotI* respectively, and the GH and IJ homology arms were digested with *NotI*/*EcoRI* and *BamHI*/*SalI* respectively. Following appropriate RE digestion, the PCR products were purified by spin column and quantified as described previously.

For generation of the 5' mini-targeting cassette, the pL452 plasmid was digested with *BamHI* and *EcoRI* REs to excise the *loxP-PGKNeo-loxP* cassette. For the 3' mini-targeting cassette, the pL451 plasmid was digested with *EcoRI* and *BamHI* REs to excise the *loxP-frt-PGKNeo-frt* cassette. The digested products were subject to gel electrophoresis to separate the cassette from the backbone and the band corresponding to the cassette was excised and purified as described previously . The resulting product was quantified as previously described. Each set of the homology arms along with their respective *PGKNeo* cassettes were ligated into an appropriately digested and purified pBluescript (pBSK) backbone. As described, resulting $kana^r$ clones were screened by RE digest and confirmed by sequencing.

2.1.4 Recombineering to generate Gap-Repaired Retrieval vector

Previously BAC DNA from *E. coli* containing the clone RPCI22-237K16 had been collected and electroporated into DY380 cells. A resulting Cam^r/Tet^r clone was chosen, screened and expanded for use in recombineering experiments [2]. This clone was re-screened prior to use, using the PCR primers for the AB and YZ homology arms to ensure the desired genomic DNA was still present.

The confirmed BAC containing clone was grown in 5 ml of LB-Tet-broth O/N at 32^{o}C with shaking. The next morning, the O/N culture was added to 250 ml of LB-Cam-Tet-broth and grown at 32^{o}C with shaking until the culture reached an optical density (OD) of 600 nm. OD measurements were taken of the subculture after 3 hrs and then every half hr until the desired density was obtained. One hundred mls of the culture was

transferred to a clean 250 ml Erlenmeyer flask and incubated at 42^{o}C for 15 minute (min) to induce the expression of the λ Red recombination proteins. The remaining 150 ml of culture was returned to the 32^{o}C incubator to act as an “un-induced”

Table 2: Primers for the generation of the cKO construct for exon 4 of Sgce.

Name	SEQUENCE
sgce-A ex4-Not1	ATAA**GCGGCCGC**TCAAAACCATGACGGTAGCA
sgce-B ex4-HindIII	GTC**AAGCTT**TCCACGTACTTCCCTTCACC
sgce-C ex4-SalI	GTC**GTCGAC**TCAGCGAAATGCACTGTAGG
sgce-D ex4-EcoRIKpnI	GTC**GAATTCGGTACC**CATGCCATCCACATTGAGTC
sgce-E ex4-BamHI	ATA**GGATCC**ATTTCAATGCCTGGAAGCAG
sgce-F ex4-NotI	ATAA**GCGGCCGC**TGCCGAGTCAGTTTCAGATG
sgce-G ex4-NotIPstI	ATAA**GCGGCCGCCTGCAG**AGTGGCTTCGCTTCAGGTAA
sgce-H ex4-EcoRI	GTC**GAATTC**GCAAGTTCCAGAACCTCCAG
sgce-I ex4-BamHI	ATA**GGATCC**TCGGGACTTGATTCTTCTGT
sgce-J ex4-SalI	GTC**GTCGAC**CAAGGGACCAAAGTCACCAT
sgce-Y ex4-HindIII	GTC**AAGCTT**CCAATCCACTGGCCTACTGT
sgce-Z ex4-SpeI	TCT**ACTAGT**CACCTTTCCCATGCCTAGAA

Colour Code: **NotI, SpeI, EcoRI, KpnI, SalI, HindIII, BamHI, PstI,**

control. Following the 15 min incubation, both of the flasks were transferred to an ice slurry and cooled as quickly as possible while shaken gently for 10 min. The bacteria were then collected by centrifugation in pre-chilled glass centrifuge tubes, with rubber adaptors, at 4000 rpm for 10 min at 4^{o}C. The bacterial cell pellet was then washed 3 times with 1 ml of ice-cold ddH_2O, and centrifuged again at 4000 rpm at 4^{o}C in order to remove any traces of LB.

The bacterial cell pellet was resuspended in 50 µl of ice-cold ddH_2O. Twenty nanograms of *HindIII* digested, linearized, and purified retrieval vector was then added to the bacteria. The bacteria and DNA mixture was transferred to a pre-chilled 0.4 cm gap electroporation cuvette (Bio-Rad, Mississauga, ON), subjected to electroporation at 175 Kv, 25 µFD and 200 ohms, and allowed to recover in SOC-broth (0.5% Yeast Extract, 2% Tryptone, 10 mM NaCl, 2.5 mM KCl, 10 mM $MgCl_2$, 10 mM $MgSO_4$, 20 mM Glucose) for 1 hr at 32^{o}C with shaking. After recovery, the induced and un-induced bacteria was plated onto LB-Amp/Tet plates and incubated at 32^{o}C O/N. Amp^{r}/Tet^{r} clones were selected for plasmid DNA collection.

The GenElute Plasmid Mini-prep Kit (Sigma-Aldrich,Oakville, ON) was used to collect and purify the now recombined retrieval vector, called pLM103. The vector was checked by RE digest and gel electrophoresis and confirmed by sequencing. Due to the possibility of rolling replication and the generation of long concatamers if the plasmid remained in the induced DY380, pLM103 was transformed into DH5α bacteria according to the manufacturer's protocol.

2.1.5 Targeting the first loxP site into pLM103

The 3' mini-targeting cassette was designed to incorporate a *loxP* site upstream of exon 4 of the *Sgce* gene. The 3' mini-targeting cassette was digested with *NotI* and *SalI* to excise the *loxP-PGKNeo-loxP* cassette along with the flanking CD and EF homology arms. The digest products were subject to gel electrophoresis and the corresponding band was excised and purified as described. DY380 cells that contained the recombined retrieval vector, pLM103, were prepared in the same manner as was described for generation of the recombined retrieval vector. Thirty five nanograms of the digested and purified 3' mini-targeting cassette was transformed into these bacteria by electroporation using the same conditions as previously described. Bacteria which underwent recombination to integrate the 3' mini-targeting cassette into pLM103 were Amp^r/Kan^r, due to the Amp resistance cassette on the vector backbone and the presence of the *PGKNeo* gene. Recombination resulted in a mixed population of integrated and non-integrated plasmids, so this population was retransformed into DH5α bacteria and $Kana^r$ colonies were selected.

Only one of the loxP sites was required in the intron upstream of exon 4. To excise the *PGKNeo* cassette, 5 ng of the targeted plasmid DNA was electroporated into *E. coli* EL350, in which Cre recombinase expression had been induced by arabinose. Resulting Amp^r colonies were re-plated onto Kan plates and incubated O/N at 32°C to test for the excision of the Neo gene and therefore loss of Kan resistance. The excision of the *PGKNeo* cassette was confirmed by RE digest and sequencing. The resulting plasmid was called pLM106.

2.1.6 Targeting the second loxP site into pLM106

The 5' mini-targeting cassette was designed to integrate the *loxP-frt-PGKNeo-frt* cassette downstream of exon 4 of the *Sgce* gene as described above. The *loxP-frt-PGKNeo-frt* cassette along with GH and IJ homology arms was excised by digestion with *NotI* and *SalI* and purified as previously described. DY380 cells which contained pLM106 were prepared in the same manner as described previously. One-hundred ng of the purified 5' mini-targeting cassette was transformed by electroporation and bacteria was selected for on LB-Amp/Kan plates. This again resulted in a mixed population of plasmids, so DH5α cells were transformed and selected for with Kan. To confirm that the second targeting had been successful, plasmid DNA from these colonies were screened by RE digestion and confirmed by sequencing. This plasmid was called pLM108, or the final conditional knockout (cKO) construct.

2.1.7 Generating the cGR construct

This construct was again developed using recombineering techniques (Figure 4). Only one vector was necessary in this case however. The plasmid pBS302 was digested with *SpeI* and *EcoRI* to extract the loxP-flanked SV40 splice-terminator fragment. Two homology arms, AB and YZ, were designed to recombine within the first intron of sgce (Table 3). An extra *KpnI* site was included for later Southern blot (SB) genotyping. Once the homology arms were amplified, RE digested and band purified, a 4 way ligation was performed with the terminator fragment into a pBSK back bone. This ligation was transformed in DH5α cells according to manufacturer's instructions. Amp^r

clones were screened using RE digest and confirmed by sequencing, now called pLM206.

In order to add the desired neomycin drug resistance, the *loxP-frt-PGKNeo-frt* cassette was amplified from pl451. Primers were designed with *EcoRI* RE sites to allow for ligation into the pLM206 (Table 3). This did not allow for direction specific cloning as the resistance should be effective in either direction. The ligation was then transformed into DH5α cells according to manufacture's instructions. Amp^r/Kan^r clones were screened using RE digest and confirmed by sequencing, now called pLM208 or the final conditional gene repair (cGR) construct. The final cGR construct used in proceeding experiments contained the *loxP-frt-PGKNeo-frt* cassette in the opposite orientation to sgce.

Table 3: Primers for the generation of the cGR construct for intron 1 of Sgce.

Name	SEQUENCE	SIZE
cKI-A-NotI-F	ATAA**GCGGCCGC**GGCAGCTTGTTAGGATGAGC	393 bp
cKI-B-SpeI-R	TCT**ACTAGT**ATGACTGTGGCTCTCCTGCT	
cKI-Y-EcoRI-KpnI-F	GTC**GAATTCGGTACC**TTGCAATTCCTTGAGTGCAG	420 bp
cKI-Z-SalI-R	GTC**GTCGAC**AACAGATGCTGGGTGATTCC	
pl451-FRT-EcoRI-5'	GTC**GAATTC**GTTTTCCCAGTCACGACGTT	2104 bp
pl451-FRT-EcoRI-3'	GTC**GAATTC**ACCATGATTACGCCAAGCTC	
Colour Code: **NotI, SpeI, EcoRI, KpnI, SalI**		

2.1.8 Preparation of pLM108 and pLM208 for electroporation into mouse ES cells

To obtain enough of the final cKO and cGR constructs, pLM108 and pLM208 respectively, for the targeting experiments in ES cells the construct containing DH5α cells were grown in 150 ml LB-Kan and collected using the Genelute HP Plasmid Maxiprep Kit (Sigma-Aldrich,Oakville, ON) according to manufacturer's instructions. The concentration and purity of the preparations was confirmed by gel electrophoresis and by nanodrop spectrometer. The resulting plasmids were again screened by RE digestion and confirmed twice by sequencing. Resulting plasmid stock was stored at -20^{o}C in TE. One-hundred μg of pLM108 was digested with *NotI*, and pL208 with *SalI*, purified by spin column and resuspended in phosphate buffered saline (PBS). The concentration of the digested product was determined by gel electrophoresis and by Nanodrop Spectrometer.

2.1.9 Preparation of Cre recombinase expressing *E. coli*

Prior to electroporation of the final linearized constructs into ES cells, the constructs were tested for their appropriate response in the presence of Cre recombinase. EL350 *E. coli* was grown in LB-Tet-broth O/N at 32^{o}C with shaking. The next morning, 5 ml of the O/N culture was subcultured into 250 ml of LB-Cam-Tet-broth and grown at 32^{o}C with shaking until the culture reached an optical density (OD) of 600 nm. At this point 2.5 ml 10% L$^{(+)}$ arabinose was added, resulting in a final concentration of 0.1% arabinose, and incubated for 1 hr. The cells were collected by centrifugation at 4000 rpm for 5 min at 0°C and washed with cold ddH_2O twice, before resuspension

twice in 15% glycerol. The last resuspension was aliquoted across 40 eppendorf tubes and stored at -80°C.

2.1.10 Preparation of feeder MEF cells

A vial with $5x10^6$ p3 neomycin resistant primary mouse embryonic fibroblasts (MEF) (Chemicon International, Billerica, MA) was thawed at 37°C for 2 min. Cells were resuspended in MEF medium (Dulbecco's modified eagle medium (DMEM) with glucose, 10% Fetal bovine serum (FBS), 1% Penicillin Streptomycin (Pen/Strep) and 1% Glutamax (Glu)). To remove freezing medium, cells were then centrifuged at 300 xg for 5 min and resuspended in fresh medium. Cells were plated onto dishes pretreated with 0.01% gelatin, then allowed to proliferate until approximately 80% confluent. Cells were passaged 4 times, until the attainment of 64x 225 cm^2 flasks with approximately 90% confluency.

To stop proliferation and create a stock of feeder cells, these cells were irradiated. Cells were detached from the plate using trypsin, as described previously. Cells were collected by centrifugation at 300 xg for 5 min and resuspended in fresh medium to obtain a total volume of 100 ml, divided across two 50 ml conical tubes. The cells were quantified by a Reichert Bright-Line Metallized Hemocytometer (Hausser Scientific, Horsham, PA), according to manufacturer's instructions, and then exposed to 30 Gy of gamma-irradiation. Irradiated cells were collected by centrifugation and resuspended in freezing medium (DMEM with glucose, 20% FBS and 10% DMSO). Aliquots of $2.55x10^6$ cells were frozen for future use as feeders.

2.1.11 Toxicity testing of serum

One vial of approximately $2X10^6$ P16 J1 ES stem cells was thawed and seeded into a 10 cm dish of previously thawed MEF feeder cells on 0.1% gelatin. After 48 hrs, another vial of feeders was thawed into six 65mm gelatin coated dishes (Falcon, BD Biosciences, San Jose, CA). The dish of J1 ES cells was then split equally across the 65mm dishes. After 24 hrs the medium was changed to one of five different media that had been prepared containing concentrations of Fetal Bovine Serum (FBS) (Hyclone, Logan, UT) ranging from 10% to 35%. The medium was changed every 24 hrs and the cultures were split when the ES cells appeared to reach a confluency of approximately 60%. The cells were observed daily for 7 days to determine if there appeared to be any toxicity associated with increasing concentrations of serum.

2.1.12 ES cell tissue culture

Both J1 (129S4/SvJae) and V6.5 (129S4 x C57BL/6) ES cells were a gift from Dr. Michael Rudnicki (Ottawa Hospital Research Institute). The ES cells were maintained in filter sterilized ES complete medium (DMEM with glucose, 10% FBS, 1% Pen/Strep, 1% non-essential amino acids (NEAA), 1% sodium pyruvate (NaPy), 1% Glu, 0.1% murine leukemia inhibitory factor (LIF) and 0.1 M β-mercaptoethanol) (Sigma-Aldrich, Oakville, ON, Hyclone, Logan, UT, Chemicon International Inc, Temecula, CA). Prior to plating of ES cells, dishes were gelatin coated and a MEF feeder layer was seeded. This was accomplished by pipetting a small amount of 0.1% w/v gelatin (Sigma-Aldrich, Oakville, ON) 1X PBS solution into the dish and then swirling the dish until the entire surface was coated. Excess gelatin solution was removed prior to plating the MEF feeder layer.

To preserve ES cells they were frozen. Medium was removed and the dish was rinsed with PBS. Trypsin was added to the dish and allowed to sit until cells began to detach, less than 5 min. ES cell medium was added to wash the cells off the plate, then collected and centrifuged at 1000 xg for 5 min. Resulting cells were resuspended in ES freezing medium (DMEM with 20% FBS and 10% DMSO). Vials were placed in a Nalgene Cryo 1°C Freezing Container (Nalgene,Rochester, NY) at -80°C O/N to allow for slow cooling of 1°C/minute. Vials were then placed in liquid nitrogen for long term storage.

2.1.13 Electroporation

Early passage J1 (129S4/SvJae) or V6.5 (129S4 x C57BL/6) ES cells were grown on a Neo^r MEF feeder layer until approximately 60% confluent. Medium was changed 4 hrs prior to electroporation procedure and new dishes of MEFs were plated between 4-24 hrs in advance. ES cells were collected from the dish as previously described then centrifuged at 4°C 1000 rpm for 5 min. The resulting cell pellet was resuspended in 9 ml cold PBS, centrifuged a second time and resuspended in 1 ml cold PBS. 30 μg linearized DNA, either cKO or cGR construct, was added and mixed before transferring to a pre-chilled 0.4 cm gap electroporation cuvette. The cells were electroporated as previously described, incubated on ice for 20 min, then removed from the cuvette by resuspension with room temperature ES medium. Cells were plated across 2 large plates of fresh MEFs. Selective medium containing 2 μM Ganciclovir and 400 μg/ml G418 was added 24 hrs later and resistant clones were harvested between 7-12 days later.

2.1.14 Effectene transfection

As an alternative to electroporation, a protocol using the liposome based transfection agent Effectene (Qiagen, Mississauga, ON) was used. The protocol was adapted from the literature [24]. ES cells were seeded on a bed of feeder MEFs the day before transfection, so that plates were approximately 80% confluent at the time of transfections. 2 µg of linearized DNA was diluted with the EC buffer, provided by the manufacturer. The enhancer solution, also provided, was added and mixed by vortexing for 1 sec and allowed to incubate for 5 min at RT. Effectene was added to the DNA solution, vortexed for 10 s then allowed to sit for 10 min at RT. During this time, cells were rinsed with PBS and covered in fresh ES cell medium. Several mls of medium were added to the DNA-effectene solution and then it was added drop-wise to the cells. The plate was gently swirled and left to incubate O/N.

Three different DNA samples were used. As a control for transfection rates, a non-linearized GFP-plasmid, pEGFP-N1 was transfected in one dish. The experimental DNA, either the cKO construct linearized with *NotI* or the cGR construct linearized with *SalI*, were added to other dishes. The dishes containing the linearized constructs were split 1:10 approximately 36 hrs later. Selective medium, containing 2 µM Ganciclovir and 400 µg/ml G418, was applied 24 hrs after that. Fluorescence microscopy was used to assess the transfection efficiency of GFP at 18.5 and 30 hrs post effectene treatment. These plates were not split.

Dishes under G418/Ganciclovir selection were left between 7-12 days, until individual resistant colonies could be picked out. Dishes were placed on a microscope in a tissue culture hood and single colonies were scraped off and sucked up using a

pipette. Each single colony was given its own well on a 96-well plate and allowed to grow until approximately 60% confluent. Proliferating colonies were then expanded into 2 wells from a 6 well plate, one with MEFs and one without. The sample on MEFs was grown until approximately 60% confluent and then frozen for later use. The well without MEFs was grown until approximately 90% confluency and then DNA was extracted for genotyping.

2.1.15 DNA extraction

Different methods of DNA extraction were used for different experiments. To genotype the offspring from the chimeras containing the mutation for the cKO of sgce's exon 1, tail or ear snips were used with HotShot DNA extraction [29]. This was an expedient method of DNA extraction. The tail or ear snip was placed in a PCR tube with 75 μl of Alkaline Lysis Reagent (25 mM NaOH, 0.2 mM disodium EDTA, pH 12) and the sample was heated to 95°C for 30 min then cooled to 4°C. 75 µl of Neutralizing Reagent was then added (40 mM Tris-HCl, pH 5) and the sample was quickly vortexed. The resulting DNA-containing solution was used for polymerase chain reaction (PCR) with primers corresponding to WT sequence, as a positive control, as well as primers specific for the cKO mutation.

Cellular DNA extraction from tissue culture dishes used a different method. The cell monolayer was rinsed in 1X PBS. Then an appropriate amount of 5% trypsin EDTA (Sigma-Aldrich,Oakville, ON) was added to release the cells from the dish. They were left with trypsin until they came easily off the plate, less than 5 min. Cells were then resuspended in medium and triturated gently to separate. With cells, such as

neurospheres, which do not adhere, this step was skipped and the medium containing the cells was simply collected. The cell-medium solution was then centrifuged at 300 xg for 5 min to remove the medium. Cells were then washed by resuspension in PBS and centrifugation at 300 xg for 5 min two times. The cells were lysed by adding enough Lysis Buffer (100 mM Tris-HCl pH 8.5, 5 mM EDTA, 0.2% SDS, 200 mM NaCl, 100 µg/ml Proteinase K) to cover the cell pellet. Cells were left at 37°C with agitation for 15 min and then placed in a 37°C water bath for several hours (hrs).

To extract the DNA, the lysis reaction was then subject to isopropanol precipitation. An equal volume of isopropanol to lysis buffer was added and the solution was agitated until viscosity was gone. The resulting DNA precipitate was removed from the solution with a pipette tip and left in a fresh eppendorf tube to air dry.

To further purify the DNA for Southern Blot (SB), phenol:chloroform extractions were performed. A 1:1 volume of phenol and chloroform equal to half the volume of the DNA was added to the DNA solution and mixed well. The DNA was centrifuged at 16000 xg for 2 min and the upper aqueous phase was transferred to a new eppendorf tube. A volume of 7.5 M NH_4Ac equal to half the original DNA volume was added, then 4 times that volume of 95% ice-cold ETOH. The extraction was kept at -20 ^oC O/N, then centrifuged at 16000 xg for 15 min at 4 ^oC . The resulting pellet was kept, rinsed twice in 70% ETOH, and allowed to air dry. Finally DNA was resuspended in TE (Tris-HCl, 0.1 mM EDTA pH 8.0) and left at 37 ^oC until fully dissolved. DNA concentration was determined with the Nanodrop Spectrometer and confirmed visually using gel electrophoresis.

2.1.16 Southern Blots

Southern blots (SB) were used to genotype the G418^r/Ganciclovir^r ES clones. Probes were amplified from the BAC clone RP22-237K16 using PCR primers (Table 4). Primers were used as described below, with a 1 minute elongation period and a 57°C annealing temperature. Both cKO probes were amplified best with 0.2 mM $MgCl_2$ concentration in the PCR buffer while the cGR probe was optimal with 0.15 mM $MgCl_2$. Amplified probes were purified using the PCR Pure kit (Qiagen, Mississauga, ON) then quantified as described previously.

High molecular weight DNA was isolated from mouse tails as described above. DNA (3 ug) was then digested O/N with the appropriate restriction enzymes (New England Biolabs, Ipswich, MA), and resolved on 0.8% agarose gels by electrophoresis. Following electrophoresis, DNA was transferred to polyvinylidene fluoride membranes (Millipore, Billerica, MA) by using capillary transfer method [53].

Radioactive DNA probes were prepared using NEBlot kit (New England Biolabs, Ipswich, MA) for random priming [54]. [α-^{32}P] dCTP with specific activity >3,000 Ci/mmol was used (Amersham Biosciences, Fairfield, CT). The probe was then mixed with salmon sperm, heated to 95°C for 5 min, and added to hybridization solution (10% PEG, 1.5x SSPE, 7% SDS). Hybridization of DNA was performed at 65 °C for 16 hours. Following hybridization the membranes were washed at 65 °C in 2X SSC buffer (0.3 M sodium chloride, 0.03 M sodium citrate, pH 7.0, 0.5 % SDS) followed by 0.5X SSC.

Autoradiography was performed at -80°C, with intensifying screens and Kodak XAR films (Sigma-Aldrich,Oakville, ON). If membranes were to be re-probed they were stripped in 0.5% SDS for 1 hr at 60 °C.

To test the SB process and the specificity of the probes, small aliquots of each of the purified probe PCR products were resolved on a gel. This gel was then used for SB and hybridized with one labeled probe at a time. In each case, a band was clearly seen on the membrane where the corresponding probe should be. No bands were seen for the non-corresponding probes.

Table 4: Primers for the amplification of SB probes.

NAME	SEQUENCE	SIZE of Probe	RE	SB WT band	SB Mut band
cKI-KpnI-probe-F	GTAAGAAGGCAGGGGTTTCC	904 bp	KpnI	16 Kb	12 Kb
cKI-KpnI-probe-R	GGAAAGAGAAGCGTCCTGTG				
5'-KpnI-probe-ex4-F	CACCCCCGTTAGCACTTAAA	764 bp	KpnI	20 Kb	16Kb
5'-KpnI-probe-ex4-R	GTGCTCTGCCAGATGTGAAA				
3'-PstI-probe-ex4-F	TCTAGCCTCACACAGCATGG	875 bp	PstI	6 Kb	8 Kb
3'-PstI-probe-ex4-R	CCTTCTTGGAAGCGTCTTTG				

2.1.17 PCR conditions

The polymerase chain reaction (PCR) conditions for each primer pair were determined individually (Table 5). Reaction buffers with 1.0, 1.5 and 2.0 mM $MgCl_2$ were all used with a range of annealing temperatures between 55-65°C for each primer set to determine optimal conditions. PCR amplification was performed using a MBS Satellite 0.2G Thermo Cycler (Thermo Electron Corporation, Whaltham, MA). Generally, the amplification conditions were: (1) 95°C for 5 min; (2) 95°C for 1 min; (3) determined annealing temperature for 1 min; (4) 72°C for 1 min; and (5) 72°C for 2 min, with steps 2 through 4 being repeated for 25-30 cycles. Step 4 was modified according to the desired product using the approximate rule of 1Kb of amplification per minute. Resulting products were subjected to gel electrophoresis and optimal conditions were determined by the clarity and intensity of the expected band.

The genomic DNA sequence of sgce as well as cDNA sequences of each gene to be amplified was downloaded from the National Center for Biotechnology Information's (NCBI) gene site (www.ncbi.nlm.nih.gov/gene/). Primers were designed using Primer 3 (www.frodo.wi.mit.edu/). If primers were desired for the use with cDNA, primer pairs were selected which amplified across multiple exons to avoid amplifying any contaminant genomic DNA.

Table 5: Primers for cDNA

Gene	Primer Name	SEQUENCE (5'-3')	Annealing Temp °C	$MgCl_2$ concentration (mM)
Biglycan	Bgn-ex3-F	GCCCTGGTCTTGGTAAACAAT	55-65	1.0-2.0
	Bgn-ex3-R	ACTTTGCGGATACGGTTGTC		
Caveolin 1	Cav1-ex2-F	CATCTCTACACTGTTCCCATCC	55-60	1.0-2.0
	Cav1-ex2-R	ACGTCGTCGTTGAGATGCTT		
Caveolin 2	Cav2-ex2-F	TCGAGGATCTGATTGCAGAG	55-63	1.0-20
	Cav2-ex2-R	ACAGGATACCCGCAATGAAG		
Caveolin 3	Cav3-ex2-F	TCCTGTTCGCCTGTATCTCC	55-65	1.0-2.0
	Cav3-ex2-R	CTTCGCAGCACCACCTTAAT		
Dysferlin	Dysf-ex19-F	TCCCTCTTTGCTGCCTTCTA	55-63	1.0-2.0
	Dysf-ex19-R	TGTCGAACTTGTTCCCGTAG		
Dystroglycan, alpha	Dag1-C-term-F	CGAGACCACTCCTCTGAACC	57-63	1.0-2.0
	Dag1-C-term-R	TCGGTATGGGGTCATGTTCT		
Dystroglycan, beta	Dag1-N-term-F	TGTGAGGGACTGGAAGAACC	55-65	1.0-2.0
	Dag1-N-term-R	GGCAATTAAATCCGTTGGAA		
Dystrobrevin, alpha iso 1	Dtna-iso1-F	GGAGAGAGCTGATGGTCCAG	63	1.5-2.0
	Dtna-iso1-R	TACCCCAGTGAGGGAGTCCT		
Dystrobrevin, beta	Dtnb-ex3,4-F	AGACCGTCATCTCGTCCATC	57-63	1.5-2.0
	Dtnb-ex3,4-R	CATTTTTCCACCACACATGG		
Dystrophin, all isoforms	DPcommon-F	CAGCACAACCTCAAGCAAAA	60	1.5
	DPcommon-R	CAGGGAAATGATGCCAGTTT		
nNOS	Nos1-F-051606	AGGAATCCAGGTGGACAGAG	66	1.5
	Nos1-R-051606	TCCTTGAGCTGGTAGGTGCT		
Sarcospan	Sspn-ex3-F	GCAGTTTACCTGCGAGACCT	55-65	1.0-2.0
	Sspn-ex3-R	GAGGCCACAGACCAGGTTTA		
Sgca	sgca-ex3-F	ACTCACCTACCACGCTCACC	55-65	1.0-2.0
	sgca-ex3-R	GGTACCCACGATCTTCTGGA		
Sgcb	sgcb-F-051606	GCAACTTAGCCATCTGCGTG	55	1.5
	sgcb-R-051606	TCTCATAGTCCGTGCTGAAC		
Sgcd	sgcd-ex1-F	GTATTCCCACCACAGGAGCA	65	1
	sgcd-ex1-R	TGAGAATCCAGATGGTCATGG		
Sgce	M-SGCE-F	CGCCATAAATCATCACGTCAG	57-60	2
	M-SGCE-R	AGCCAGGGTAACGAGGAAATC		
Sgcg	Sgcg-ex1-280507-F	GAGAACAGTACACCACGGTCA	55-65	1.0-2.0
	Sgcg-ex1-280507-R	TGAGAGCGAGATTCACAACG		
Sgcz	Sgcz-ex1-280507-F	CCACACAGCAGAACAACCTG	60	1.5
	Sgcz-ex1-280507-R	TGGTAACCAACAGCAGAAGG		

2.1.18 PCR Genotyping of Transgenic mouse models

In conjunction with SB screening PCR primers were designed to screen potential cKO or cGR ES cell clones (Table 6). These were designed so one primer would sit within the desired area of recombination and the other just outside in the WT genomic DNA. Primers could not be optimized as there was no positive control, so they were used at a Tm-5°C.

Lack of success with the first set of primers prompted the design of Long Range PCR (LR-PCR) primers (Table 7). These primers were designed to sit on either side of the area of homology between the conditional constructs and the genomic DNA. PCR was performed using SequalPrep Long Range PCR kit with dNTPs (Invitrogen, Carlsbad, CA). Primers were designed, as instructed by the kit, to be between 18-35 nucleotides in length with between 45-65% CG content and at least 2 Gs or Cs at the 3' end.

Primer sets were optimized using 10 ng of DNA from WT V6.5 ES cells. Both sets performed optimally with the inclusion of Enhancer B provided by the kit. Resulting products were run on a 0.7% gel with 0.001% ETBr. The amplification conditions for the cKO primers were (1) one cycle of 94°C for 2 min (2) ten cycles of 94°C for 10 s, 53°C for 30 s, 68°C for 14 min 10 s (3) twenty cycles 94°C for 10 s, 53°C for 30 s, 68°C for 14 min 10 s with the addition of 20 s each cycle, and (4) one cycle of 72°C for 5 min. The amplification conditions for the cGR primers were (1) one cycle of 94°C for 2 min (2) ten cycles of 94°C for 10 s, 54.5°C for 30 s, 68°C for 5 min 30 s (3) twenty cycles 94°C for 10 s, 54.5°C for 30 s, 68°C for 5 min 30 s with the addition of 20 s each cycle, and (4) one cycle of 72°C for 5 min.

Table 6: Primers for genotyping ES clones.

NAME	SEQUENCE
5‘cKI-GenT-F	TTGCCTTCCTCTTCCTCAGA
STOP-GenoT-R	ATAACAACAACGGCGGCTAC
Neo-GenoT-F	GGGGAACTTCCTGACTAGGG
3‘cKI-GenT-R	AGCTGCCTATCTCCCAAACA
3‘cKO-GenoT-F	ATTGCATCGCATTGTCTGAG
3‘cKO-GenoT-R	CACCTTTCCCATGCCTAGAA
Neo-F	GATCGGCCATTGAACAAGAT
Neo-R	CCACCATGATATTCGGCAAG

Table 7: Primers for LR-PCR genotyping ES clones

NAME	SEQUENCE	SIZE
cKI-LRPCR-F	CCTTAGTCTTAACTGTCTTCCCAGAGCC	2.1 kb (WT) 5.3 kb (cKI)
cKI-LRPCR-R	GTGGGATAGCTCAGACCACCTATTACCC	
cKO-LRPCR-F	CTCAAAGCTATCTTCCTACCAGTCTCC	12.2 kb (WT) 14.1 kb (cKO)
cKO-LRPCR-R	CACTAGATACCAGAGATTTGGTGAGGG	

2.1.19 Development of Neurosphere cell lines

Neurosphere cell lines were developed from a WT CD1 mouse as well as two chimeras containing the mutation for the cKO of sgce's exon 1 (Chimera 1 and 2) [2]. Mice were anesthetized with CO_2 gas then culled by cervical dislocation. The brain was quickly removed and placed in PBS with 2% glucose. The area containing the hippocampus and subventricular zone (SVZ) was dissected in the PBS-glucose solution and then placed in a 50 ml conical tube (Falcon, BD Biosciences, San Jose, CA) with Neurosphere medium (NeuroCult NSC Basal Medium, 10% NeuroCult NSC Proliferating Supplements, 20 ng/ml rh EGF, 10 ng/ml rh FGF-b, $2.0x10^{-4}$ % Heparin, 1x penicillin, 1x streptomycin, 1x mycin). The tissue was triturated using a glass pipette, which had been run through the flame of a bunsen burner to round the tip so as to prevent cell shearing. The dissociated tissue was then allowed to settle for 2 min. The supernatant, containing the single cells, was collected and the tissue was re-triturated in fresh medium. Again the tissue was allowed to settle for 2 min before the supernatant was collected and combined with the first. This single cell solution was centrifuge at 800 rpm for 5 min. Cells were resuspended in fresh media and run through a 200 μM filter to remove any remaining tissue and obtain a single cell filtrate. Filtrate was centrifuged once more and the resulting cell pellet was resuspended in new medium and incubated at 37°C with 5% CO_2.

Within 2 weeks, spherical neurospheres became clearly visible. These spheres were collected under a microscope using wide tipped pipette tips. The neurospheres were then gently dissociated and transferred to a new dish to obtain a more homogenous population of cells. The neurospheres derived from the chimeras were

grown with G418 selective media, to ensure a population of cells containing the cKO mutation.

2.1.20 Cre recombinase expression in Neurospheres

The neurospheres developed from the chimeras 1 and 2 contain the cKO mutation for exon 1 of sgce [2]. An adenovirus able to infect neurospheres with cre, MA26Cre, was a gift from Dr. Robin Parks (Ottawa Hospital Research Institute). It was used to remove exon 1 of sgce and attempt to create a sgce-KO cell line.

First, the correct multiplicity of infection (MOI) was determined using an adenovirus expressing red fluorescing protein, this virus was also a gift from Dr. Robin Parks (Ottawa Hospital Research Institute). WT neurospheres were chemically dissociated using the NeuroCult Chemical Dissociation Kit (Mouse) (StemCell Technologies, Vancouver, BC) according to manufacture's instructors. These cells were split across 4 conditions and used with MOIs of 10, 50, 100 and 500. To accomplish this, cells were centrifuged at 1800 rpm for 10 min, and resuspended in 500 µl fresh medium, then the desired amount of the virus was then added. The cells were incubated O/N with the virus, centrifuged at 1800 rpm for 10 min and resuspended in fresh medium. Cells were incubated at 37°C in 5% CO_2 for 72 hrs before pictures were taken under fluorescence light. A 10xMOI was sufficient to infect all the cells.

The neurospheres with the cKO mutation were infected in the same manner with a 10xMOI of a cre-containing adenovirus, MA26Cre. Unfortunately, the infected cells never recovered enough to grow up for further experimentation. The control cKO neurospheres, not exposed to the cre-adenovirus, continued to expand healthily.

2.2 Results

2.2.1 Development of the cKO construct

A conditional knock-out (cKO) of sgce in mice would allow for tissue specific and temporal specific studies. Constructs were designed using the principles of recombineering [23] (Figure 4).

Initially a construct had been designed for the conditional removal of exon one by a previous student [2]. Unfortunately, the resulting chimeras did not produce any mutant pups. Four chimeras were generated, two of which produced few offspring, denoted chimeras 3 and 4. The other two chimeras, both males and denoted chimeras 1 and 2, were bred for one year with multiple WT females. All resulting 325 pups were genotyped with PCR and appeared WT themselves. It is hypothesized that interference with the neighboring, also maternally imprinted, PEG10 gene by one of the LoxP sites caused difficulties during embryonic development. Removal of PEG10 is known to be embryonically lethal causing defects in the placenta [32,85].

It is worth noting however, that although all offspring were genotyped, the mutant pup was expected to have a brown coat coloring. ES cells had been used to create the clone which would result in brown color. They were injected into blastocysts which should result in white colored mice. Even if the mutation was disrupting development we would have expected a number of WT pups, from the other non-mutation carrying chromosome, with brown coat coloring to emerge as well. Of all 325 WT pups only one displayed brown coat coloring. To ensure that the cells containing the mutation were distributed throughout the germ line tissue, this tissue was dissected, cut into eight

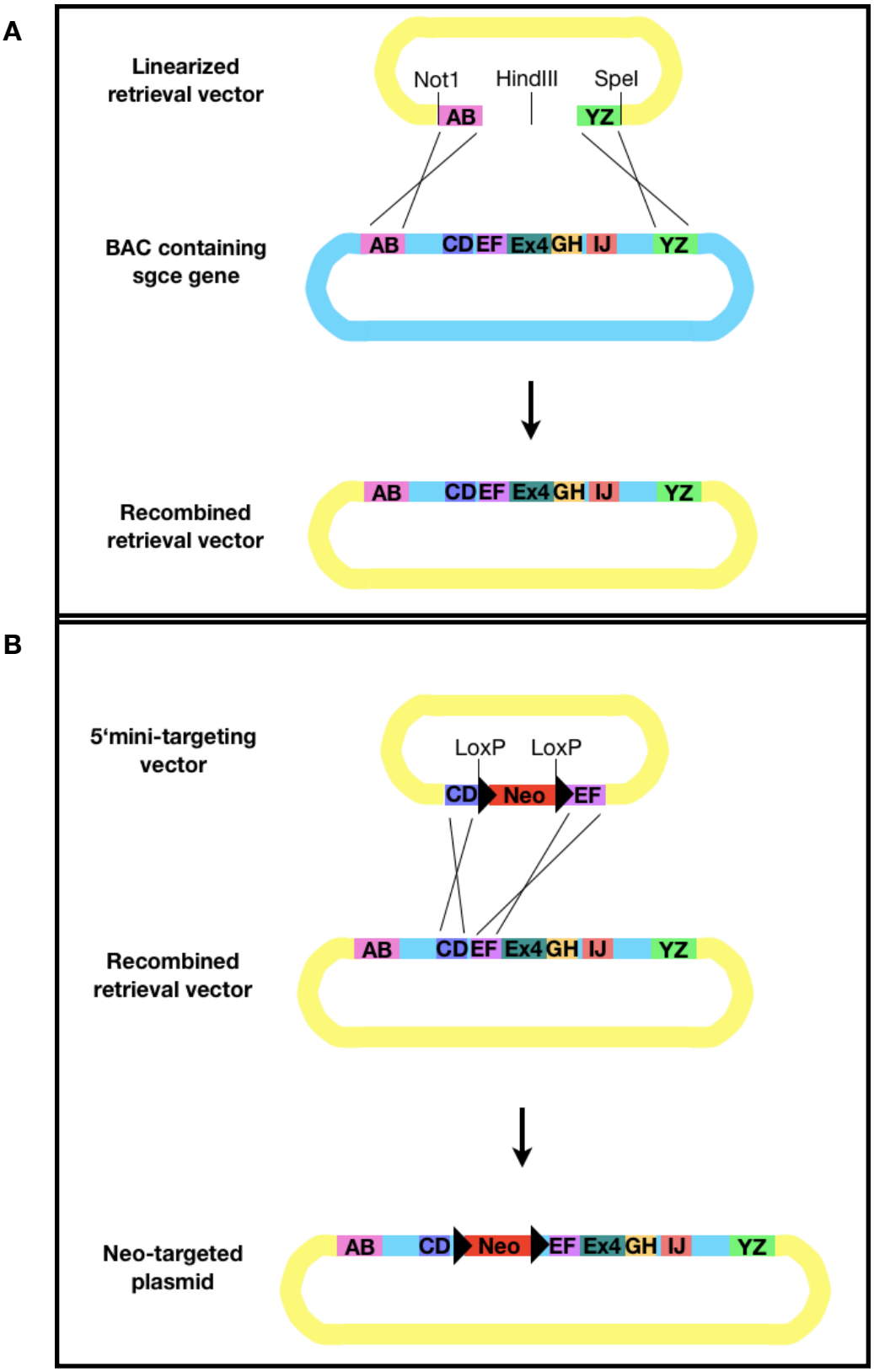

Figure 4: Recombineering Principle [23]: An example of the retrieval of the DNA of interest (A) and the mini-targeting of LoxP sites (B).

pieces and used for multiple DNA extractions. PCR revealed that the mutant DNA was present throughout the different sections of germ line tissue (Figure 5C). This suggests that there may have been other difficulties preventing germ line transmission of the mutation other that PEG10 interference.

The next construct was designed for the conditional removal of sgce's exon five. Unknown problems prevented the insertion of the 5'mini-targeting vector during construction of this construct.

The current cKO construct was designed to conditionally excise exon 4 from the sgce gene. Exon four was chosen for several reasons: it is in the middle of the gene and should therefore not interfere with neighboring genes; the removal will result in a frameshift that should cause early termination and degradation [75]; and finally the previous KO model of exon four produced MD symptoms. Following the recombineering protocol, six homology arms were picked using the designators consistent with Figure 4: AB, CD, EF, GH, IJ, YZ (Table 2). The size of the arms varies between 354bp to 498bp, well within the suggested 200-500bp range for recombineering. Primers to amplify these arms were designed with RE sites to facilitate directed ligation. Extra RE sites were included in the primers at the 3' of CD and the 5' GH for later SB screening.

The retrieval vector was constructed by ligating pBSK with the homology arms AB and YZ. This vector was confirmed by digestion and sequencing, and then used to pull out the portion of chromosome six containing exon 4 of sgce from BAC Rp22-237K16 (Figure 4A). This was accomplished by electroporating the BAC into electrocompetent EL350 bacteria, which had been induced for expression of the red genes to promote homologous recombination. Single colonies grown under Cam

selection were then expanded. The retrieval vector was linearized by cutting between the homology arms, then purified and electroporated into the BAC containing EL350 cells. Homologous recombination between the AB and YZ homology arms and the BAC yielded a 7.1kb fragment of the mouse sgce gene, which was the subcloned plasmid, pLM103.

Two mini-targeting vectors were used to insert the LoxP sites on either side of exon 4 (Figure 4B). The 5' mini-targeting vector was constructed by ligation of a floxed Neo resistance cassette between the CD and EF homology arms into pBSK. The floxed Neo gene, along with the homology arms, was excised, purified, and coelectroporated with the subcloned plasmid into electrocompetent EL350 cells. The Neo cassette was then selected for. Once the 5‘ mini-targeting vector had recombined with the subcloned plasmid DNA, the resulting construct was isolated and confirmed by both digest and sequencing. Cre recombinase was then used to excise the Neo cassette. This was accomplished by electroporating the vector into EL350 cells that had been induced to express Cre recombinase under an arabinose promoter, resulting in a single LoxP site on the 5‘ side of exon 4. This was called pLM106.

The 3' mini-targeting vector was constructed by ligation of a FRT flanked Neo gene with a single LoxP site between the homology arms EF and GH into pBSK. Again this vector was purified and confirmed by sequencing. It was then digested and the fragment containing the Neo and loxP was co-electroporated with the subcloned vector now containing the 5' LoxP site.

The final cKO construct, pLM108, has been confirmed by multiple RE digests and sequenced twice (Figure 5A). It has also been exposed to Cre recombinase within

bacteria to show the correct removal of the area between the LoxP sites, including exon 4. The FRT flanked Neo cassette can be used for selection for now but, if a positive clone is identified, the option to remove this Neo gene before blastocyst injections is available using FRT recombination.

2.2.2 Development of the cGR construct

A conditional gene repair (cGR) of sgce would also allow for tissue specific and temporal specific studies. A construct was designed to insert an artificial splice-terminator site, or STOP-cassette, from pBS302 into intron one, between exon 1 and 2, of sgce. This should result in a premature stop site during transcription after exon 1 and eventual degradation of that transcript. The theory for this construct was taken from the literature [59] and this construct was also made using the principles of recombineering [23] (Figure 4).

Only two homology arms were necessary for the creation of this construct: AB and YZ (Table 3). Arms were close together within intron 1 of the sgce gene and RE sites were included on both ends to facilitate ligation. One additional RE site was included at the 5' end of the YZ arm for later SB experiments. The LoxP flanked SV40 splice-terminator fragment was removed from pBS302 by RE digest and fragment purification. The splice-terminator site was ligated between the two homology arms into pBSK.

In order to provide drug selection, an FRT flanked Neo resistance cassette was amplified from pl451. The primers for amplification contained RE cut sites to allow for ligation into the area between homology arms.

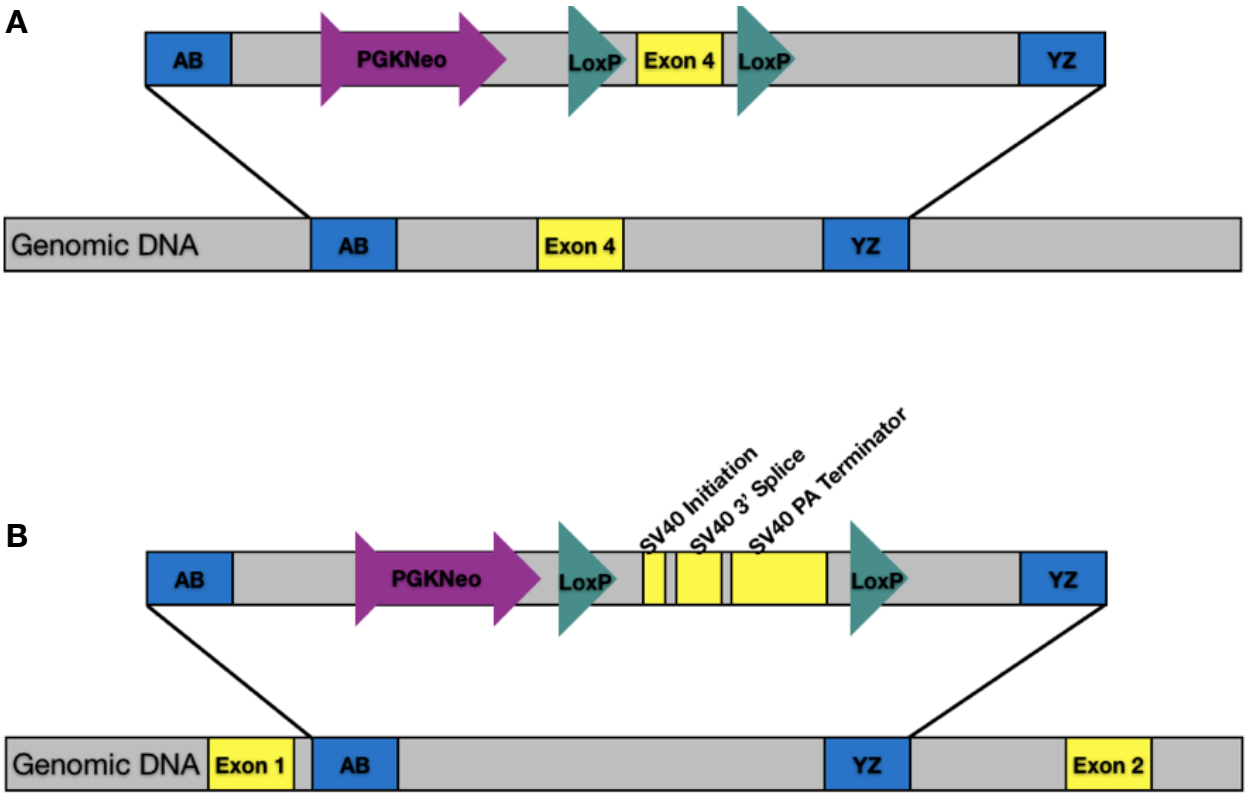

Figure 5: Final MD mouse model constructs as they would recombine into the sgce gene of a mouse ES cell. The cKO (A) and cGR (B). PCR using DNA from the testis of chimera 1 from the attempted cKO of exon 1 of sgce (C).

The final cGR construct has been confirmed by multiple RE digests and sequencing (Figure 5B). It has also been exposed to Cre recombinase which results in the correct removal of the artificial splice-terminator sequence between the LoxP sites. The FRT flanked Neo cassette can be used for selection. Once a positive ES clone is identified, the option to remove this Neo gene before blastocyst injections is again available.

2.2.3 Development of Recombinant Mouse lines

In order to develop the recombinant cKO or cGR mouse lines, the DNA of interest between the AB and YZ homology arms must recombine into the genome of a mouse ES cell (Figure 5). To achieve this, both constructs were linearized by RE digest and then purified before use. The linearized construct was used for electroporation.

The gene targeting results in two possible outcomes, the more common result is random integration of the cassette and the less common would be the desired homologous integration of the cKO or cGR cassette at the appropriate location within the sgce gene. Homologous recombination may occur anywhere along the targeting cassette and the corresponding region of the genome. The presence of the positive selection marker, the PGKNeo cassette, confers resistance to G418, which is likely to be retained in both random and homologous integration events. Hence the necessity to screen any resistant clone by SB or PCR. The *MC1-TK* gene, which lies outside of the region of homology, provides negative selection in the case of random integration of the cKO cassette by conferring sensitivity to Ganciclovir. Homologous incorporation of the targeting cassette results in the retention of the positive selection cassette, while the

MC1-TK gene is lost due to a lack of surrounding homology. This double selection strategy should reduce the number of surviving clones by 5 to 10-fold [2].

Unfortunately recombination of neither the cKO nor the cGR construct has yet to be successful (Figure 7). Both constructs have been electroporated into early passage ES cells five times. This has produced a total of 34 cKO and 123 cGR clones. These clones were screened using SB and LR-PCR. Thus far all appear WT.

To investigate the low number of clones, a non-linearized GFP plasmid was used for electroporation to determine the rate of DNA entry into the ES cells. This electroporation resulted in about 4% of cells with visible GFP expression (Figure 6A). This is in accordance with the ratios in the literature, but increasing the number of cells receiving DNA should increase the chances of the construct recombining properly.

To increase the rate of DNA entry I used effectene, a non-liposomal lipid-based transfection method. For delivery of genes into mouse ES cells this method was adapted based on the literature for the cKO and cGR constructs [24]. This method was beneficial in that the cells were left on the dish in their usual growth medium, resulting in less trauma to the cells from handling. A test transfection with the non-linearized GFP demonstrated an increase in the transfection efficiency as well as healthier looking colonies over all (Figure 6B). The percentage could not be exactly determined as the cells were not in a single cell state during the transfections and only parts of the individual colonies fluoresced.

Transfection using effectene was performed twice with each linearized construct. The first round resulted in 58 cKO clones and 41 cGR clones, all of which appear WT when screened with LR-PCR. The second round of effectene gave rise to 15 cKO and 5

cGR clones. It is possible that the reduced number of clones from the second experiment was due to the DNA preparation. The linearized DNA had been frozen and thawed, which may have affected its quality. All clones screened from the effectene method have also appeared WT, although the increased number of clones makes this protocol potentially useful for future experiments.

2.2.4 Screening of ES Single Colonies

Southern blot (SB) was initially employed for the screening of the clones from the cKO and cGR electroporation attempts. Probes were amplified from the BAC Rp22-237K16 using PCR, then purified using spin columns and sequenced before being labeled with P^{32}. As a test for the labeling and purification procedures, probes were radioactively labeled and used for SB against themselves successfully. This showed successful labeling of the probe and specificity between the probe sequences.

DNA for SB was digested using the appropriate RE, the cut site for which was included in the cKO and cGR constructs for this purpose. If the construct has successfully recombined into the genome it will contain this extra cut site, producing a smaller sized labelled band compared to the WT (Table 4). In both cases the mutant bands were expected to show approximately a 4kb shift. Many of the clones from electroporation were determined to be WT using this method (Figure 7A).

Due to the time required for SB screening, this method was replaced with the more efficient LR-PCR protocol for the initial screen. Primers were designed to sit outside the homology arms. In both cases, due to the inserted LoxP sites and Neo resistance cassette, the PCR products would be approximately 2kb longer for positive

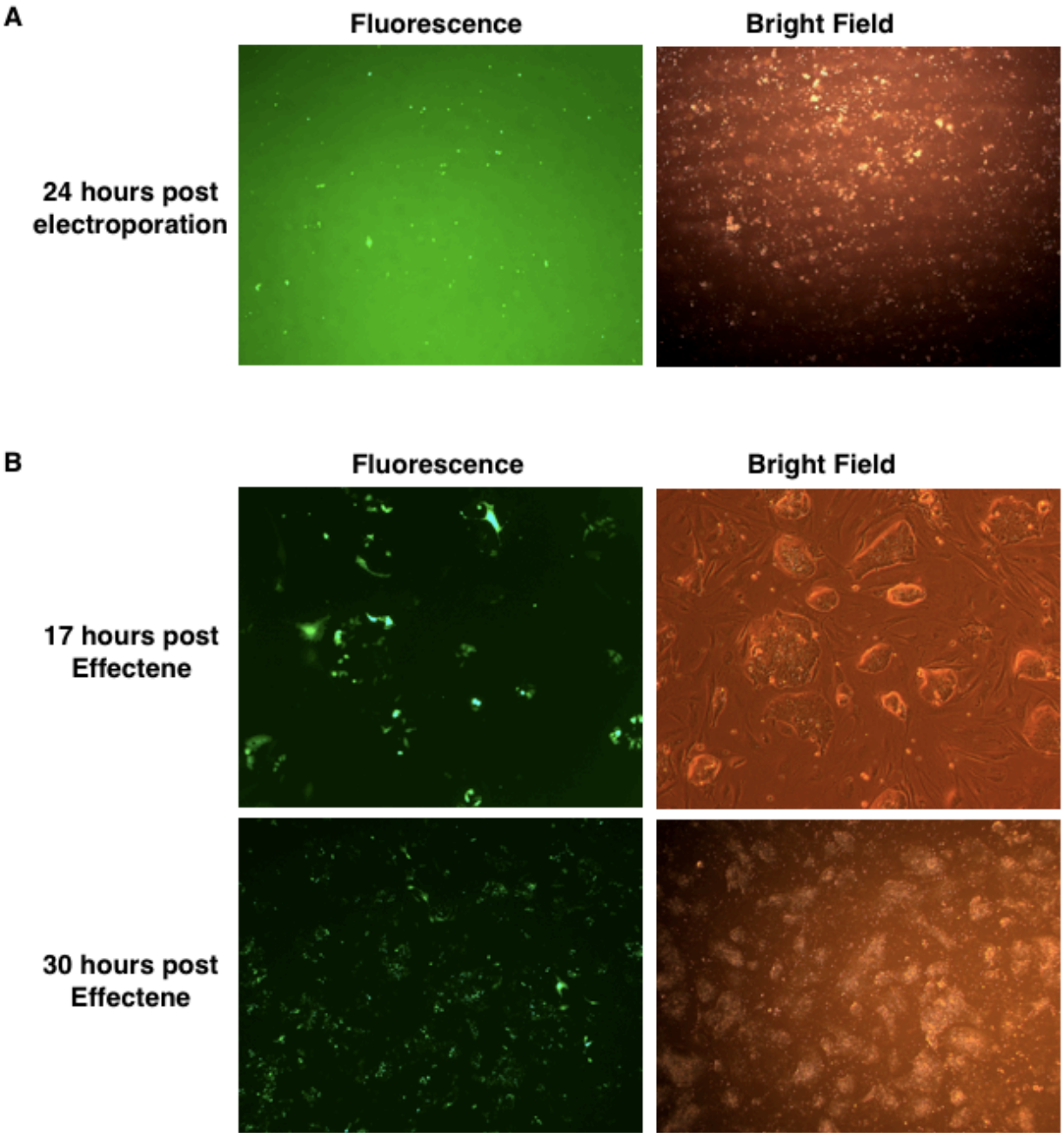

Figure 6: Determining the efficiency of DNA inclusion into ES cells with electroporation (A) and Effectene transfection (B).

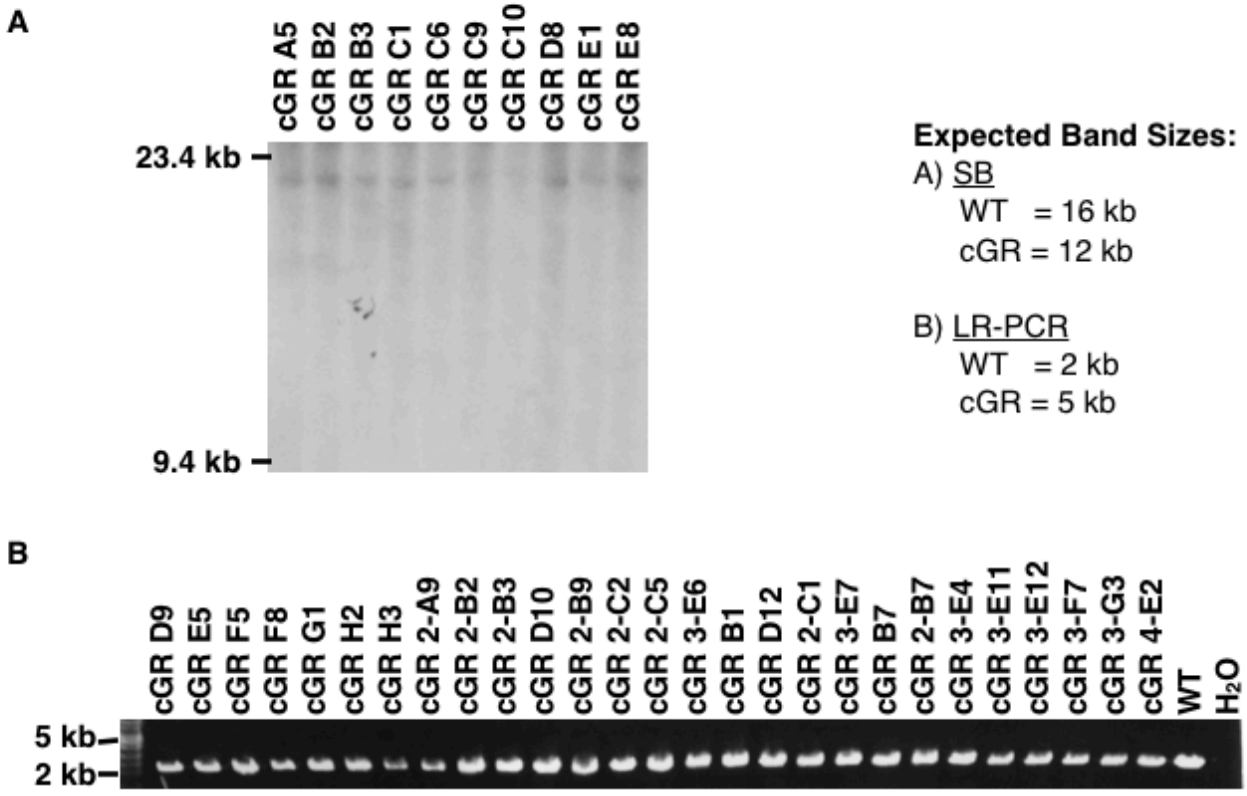

Figure 7: Genotyping tests to screen potential cKO or cGR ES cell clones. An example of a Southern Blot (A) and LR-PCR (B) screens for some of the cGR clones.

clones. All clones screened with this new protocol appear to be WT as well (Figure 7B). The clones were also screened by PCR for the inclusion of the Neo gene to check for non-specific recombination. This resulted in all clones appearing positive, likely due to the Neo-resistant MEFs that the ES cells are grown on.

2.2.5 Development of Neurosphere Cell Lines

To test if these original chimeras for the cKO of sgce's exon 1 might play a useful role, despite the lack of a mutant pup, they were used for the development of cKO neurospheres lines. Both chimeras were dissected for their SVZ and used to grow neurospheres as described previously. These cell lines were expanded under drug selection to remove any wild type cells and they were screened by PCR for inclusion of the cKO mutation around exon 1 of sgce and for the inclusion of the neomycin resistance cassette. Neurospheres were then exposed to cre, to excise exon 1 and create sgce-KO cells. Unfortunately the cells exposed to Cre recombinase did not survive. This perhaps could be due to the loss or disruption of *PEG10* expression.

2.3 Discussion

2.3.1 Trouble Shooting

The majority of the technical problems which occurred during this project revolved around attaining a positive homologous recombinant clone for one of the conditional MD mouse models. Many troubleshooting attempts were made.

The first construct made was successful in producing four chimeras [2]. As previously described, these mice were unsuccessful at producing a pup heterozygous for the mutation. After designing a construct to conditionally remove exon 5 of sgce, making the retrieval vector and two mini-targeting vectors, as well as retrieving the correct portion of the sgce gene, the 5‘mini-targeting vector was unable to homologously recombine into the subcloned-retrieval vector. Both the subcloned vector and the mini-targeting vector were sequenced and re-purified. All steps in the process were double checked and solutions re-made. This was to no avail and I was unable to determine the reason why homologous recombination did not occur.

The next construct was designed for the conditional excision of exon 4 of sgce. This construct went together properly and responded to Cre recombinase by excising exon 4 between the loxP sites. The electroporation protocol took several attempts before yielding single colonies. It became clear that best results were achieved with freshly digested and purified construct DNA. Once colonies were expanded and DNA was extracted, they were used for SB. Several different protocols were used for DNA extraction in order to get high concentration DNA which appeared contaminant free when subject to gel electrophoresis. As well, the digestion of this DNA had to be

optimized. Different concentrations of DNA and RE were left for varying amounts of time with different enhancing agents to produce DNA that was completely digested and produced a proper looking smear when subjected to gel electrophoreses. All probes amplified were gel purified and then sequenced. Several protocols were used to radioactively label and then purify the labeled probe. Changes made included changing labeling kits, spin columns, and film exposure times. Unfortunately much trial and error resulted in at best ambiguous results.

Finally a new SB protocol was adopted from the CHEO diagnostic lab. All aspects of the SB protocol were switched and WT bands became clearly visible as a result. Changes in protocol included switching from a Church and Gilbert hybridization buffer to a PEG based buffer, using new blotting paper for the transfer, changing probe labeling kits and using different spin columns for the purification of the probe. As a result of switching so many aspects at once, it is still unclear where the problem lay with the original protocol but at least consistent results were obtained from then on.

Once SB and LR-PCR were both working, it became clear that the cKO and cGR ES clones all appeared WT. For this reason increasing the transfection efficiency became a priority. Electroporation has low efficiency. This has been seen previously in our lab and similar efficiencies have been reported in the literature [2,24]. Therefore effectene was used as an alternative method to raise transfection efficiencies.

Despite the increased transfection efficiency, finding a positive clone for either mouse model remains elusive. The construct sequences have been screened using BLAST (www.blast.ncbi.nlm.nih.gov/Blast.cgi) to look for similar sequence in the mouse

genome, but they are unique to the mouse sgce gene. Constructs were also sequenced a second time at Sequencing-Genome Quebec (McGill University, Montreal, PQ).

To assess the effectiveness of the neo cassette used in the constructs, ES cells were electroporated with one of four conditions: a negative control using no plasmid, pl451 containing the PGK-Neo used in the constructs, and two positive controls, pD1106, containing a Neo gene under a SV40 promoter, and pD1107, containing a Neo gene under a PGK promoter. All were selected with either 0, 200, 300 or 400 ug/ml G418. All cells in the negative condition were killed, while similar sized populations of the other conditions remained across the different transfections. This demonstrated that the Neo cassette from pl451 was effective.

2.3.2 Future Experiments

As a possible alternative, some future experiments may be completed with a sgce KO mouse which has just become available. The original exon 4 KO by the Li lab is unavailable but recently a new sgce null mouse was described, where exon 6-9 of sgce has been replaced with β-gal and Neo [13]. This mouse line is available from the Nigro lab. This model can be used for many of the behavioral and molecular studies proposed, either as a compliment model or in lieu of the conditional models.

Once a positive cKO or cGR clone is identified it can be used to create chimeras and eventually more versatile mouse models for MD. As sgce is maternally imprinted, once these mouse lines are backcrossed only the male mice should be used for breeding experimental mice. Using heterozygous mice with a WT sgce inherited maternally will best exemplify the human condition.

First, to develop a complete KO line, the mutant cKO mouse should be crossed with mice which express Cre recombinase ubiquitously. The cGR sgce mouse will be a heterozygous KO in which the wild type allele is not expressed due to imprinting. It would be important to compare these mice to the previously published sgce exon four KO mouse. Based on the sgce KO paper, I would predict that there will be approximately 30 times more myoclonic jerks, as well as differences in motor activities, anxiety and depression as compared to control animals [22]. Two control models should be used: Both WT mice of the same strain as well as het cKO mice for whom the mutation was inherited from the mother and is therefore imprinted.

In addition, spatial memory can be tested using a Morris water maze. Sgce has been reported in the hippocampus, an area of the brain strongly involved in the learning of spatial memory tasks. The Morris water maze should therefore identify if the loss of sgce is affecting hippocampal neurogenesis and/or spatial memory. The KO mice should also be scrutinized for gross morphological and developmental changes of the brain, muscle and cardiac tissue. No gross changes are expected, given that neither the previous KO mice nor the human patients lacking sgce show any. If any changes are seen this may indicate confounding factors. The mice should then be scrutinized more carefully and perhaps only used for tissue specific or *in vitro* experiments.

Differences in protein expression should be analyzed using a combination of quantitative RT-PCR (qRT-PCR), Western blot (WB), and immunohistochemistry (IHC). It will be crucial to first demonstrate that the expression of sgce is in fact removed in all tissues. Only then can the effects of this loss on the expression of other transcripts and

proteins be analyzed. In response to the loss of sgce there may be feedback loops which indicate to other proteins in the same pathway(s) to up- or down-regulate.

It will also be of interest to look at nitric oxide (NO). Previous studies in muscle have indicated that the loss of one of the sarcoglycans is sufficient to reduce the amount of nNOS protein, likely reducing the amount of NO which is synthesized. Additionally, KD of sgce *in vitro* results in the reduction of nNOS protein. NO production may be assessed by looking at its metabolite levels in the urine or blood. However, due to the expected normal levels of nNOS in many tissues and the diffuse nature of NO, this may not be an informative experiment.

In the future these mutant mice can also be crossed with strains expressing Cre recombinase only in the CNS or skeletal muscle. Since Sgce is present in both skeletal muscle and the CNS, but its interactions and function(s) are unknown, these crosses should aid in elucidating Sgce's separate roles in these tissues. This would also confirm that MD is in fact a neurological disease, assuming that KO in the CNS is itself sufficient to produce the MD phenotype. Conversely, experiments can be done where the cGR mouse only restores sgce expression to these particular cre-expressing tissues. Using the two conditional MD models in tandem with increasingly specific cre-expression, will allow for the exact cell type or tissue responsible in the disease pathology to be distinguished.

These mouse models can also be used for developmental studies, by either knocking out or repairing the gene at different time points. Combining these models will elucidate whether repair must occur prior to a certain point in development to be effective. Conversely it can be determined whether the removal of the gene expression

is necessary prior to a particular point in development in order for MD symptoms to develop. This type of knowledge has potential to aid in diagnostics and future treatment courses for MD patients.

3. Generation of *In Vitro* models for Myoclonus Dystonia

3.1 Materials and Methods

3.1.1 Tissue Culture

The N1E-115 and N2A mouse neuroblastoma cell lines were a gift from Dr. David Picketts (Ottawa Hospital Research Institute). Neuroblastoma cells were stored in liquid nitrogen and thawed at 37°C for approximately 2 min. Cells were resuspended in growth medium (DMEM with glucose, 10% FBS, 1x Glu, 1x antibiotic-antimycotic), centrifuged at 1500 xg for 5 min to remove all freezing medium and then seeded with fresh medium. To expand, cells were incubated at 37°C with 5% $C0_2$ and medium was changed every 1-3 days, as needed.

Neuroblastoma cells were allowed to proliferate until approximately 80% confluency and were then split. As these cells adhere to the dish, the cell monolayer was rinsed in PBS and an appropriate amount of 5% trypsin EDTA was added to release them from the dish (Table 8). Cells were left with trypsin until they came easily off the plate, less than 5 min. They were then resuspended in medium and triturated gently to separate before centrifugation at 300 xg for 5 min. Finally cells were resuspended and split appropriately, usually 1:4.

Neuroblastoma cells are grown in an undifferentiated state to promote proliferation. To differentiate into neuron-like morphology, cells were grown in a differentiating medium (DMEM with glucose, 1% FBS, 1x Glu, 1x antibiotic-antimycotic) containing low FBS until neurite outgrowth was seen, approximately 7 days.

To freeze cells for long term storage, cells were detached from the plate with trypsin as described above. They were then centrifuged at 800 rpm for 5 min to remove the growth medium. Cells were resuspended in 1 ml of freezing medium (DMEM with glucose, 20% FBS and 10% DMSO), and then placed in a Nalgene Cryo 1°C Freezing Container (Nalgene, Rochester, NY) at -80°C O/N to allow for slow cooling of 1°C/ minute. Vials were then kept in liquid nitrogen for long term storage.

Other cell lines were thawed, split and frozen in a similar fashion. The HEK293 cell line was a gift from Dr. Robin Parks (Ottawa Hospital Research Institute) and the Cos-1 cell line was a gift from Dr. Rashmi Kothary (Ottawa Hospital Research Institute). Both cell lines were maintained in growth medium (minimal essential medium (MEM) with glucose, 1X glu and 10% FBS).

3.1.2 RNA Extraction

To obtain RNA from tissue, the desired tissue was quickly dissected and weighed. RNA extraction from tissue culture was performed by collecting cells, as described previously. TRI Reagent (Sigma-Aldrich,Oakville, ON) was added in the ratio of 1ml:50-100mg of tissue and homogenized by pipette. In the case of tissue culture 1 ml of TRI Reagent was used. The solution was allowed to stand at RT for 5 min and then chloroform was added in a ratio of 0.2 ml:1 ml TRI Reagent. The mixture was shaken vigorously for 15 s, allowed to stand at RT approximately 10 min, then centrifuged at 12000 xg for 15 min at 4°C. The aqueous solution was transferred to a new eppendorf tube and isopropanol was added in a ratio of 0.5 ml:1 ml TRI Reagent. Solution was mixed and allowed to stand for 5-10 min before collecting the pellet by

centrifuging at 12000 xg for 10 min at 4°C. The supernatant was discarded and the pellet was washed with 1 ml of 75% ETOH, then recollected by centrifugation at 7500 xg for 5 min at 4°C. The supernatant was removed and pellet was allowed to air dry before being resuspended in Diethylpyrocarbonate (DEPC) treated H_2O. Concentration was determined by the Nanodrop Spectrometer and then stored at -80°C.

3.1.3 cDNA

cDNA was amplified from RNA samples obtained from mouse tissue as well as cell lines. One µg of RNA was used per reaction. DEPC treated H_2O was used to adjust the volume of RNA to 10 µl before addition of 10U DNAseI (Invitrogen, Carlsbad, CA). This mixture was incubated at 37°C for 20 min and 70°C for 10 min. One µl of pDN6 random hexamers was added and the mixture and incubated for 5 min at 70°C, then placed on ice for 1 min. Finally, 4 µl of 5x first strand buffer, 2 µl 0.1 mM DTT, 1 µl 10 mM dNTP, and 1 µl SuperScript II Reverse Transcriptase (Invitrogen, Carlsbad, CA) was added. The mixture was incubated at RT for 10 min, 42°C for 45 min, and 95°C for 5 min. The resulting cDNA was used for PCR. cDNA samples were tested using control or housekeeping primers prior to use for experimentation.

Table 8: Tissue Culture parameters.

Plate	Surface Area (mm^2)	Seeding Density of Cells	Cells at Confluency	Trypsin (ml)	Growth Medium (ml)
100 mm dish	7854	2.2 $x10^6$	8.8 $x10^6$	1	10
150 mm dish	17671	5.0 $x10^6$	20.0 $x10^6$	2	20
6-well plate	962	0.3 $x10^6$	1.2 $x10^6$	0.2	3

3.1.4 qRT-PCR

Primers for quantitative RT-PCR (qRT-PCR) were designed to amplify between 100-400 bp products from mouse cDNA (Table 9). As with primers used for cDNA, these primers spanned more than one exon to avoid amplification of any contaminant DNA. Optimization was performed as previously described except for the use of a PCR buffer with 3 mM $MgCl_2$. SYBR Green Super mix Buffer (Bio-Rad, Mississauga, ON) was used according to manufacturer's instructions for quantitative reactions. To ensure viability of primers for quantitative analysis between samples, standard curves were first performed with each set of primers. To accomplish this WT cDNA was serially diluted across seven tubes and cycle threshold-values, the number of cycles required for the fluorescent signal to cross the threshold or exceed the background level, were determined for each dilution. Primer sets were only used for qRT-PCR if their standard curves yielded a value of $r > 0.8$.

Once primers were determined as appropriate for qRT-PCR, they were used to amplify experimental cDNA samples. Each reaction, along with control primers (GAPDH, 18S), was completed in triplicate.

Table 9: Primers for qRT-PCR

qRT-PCR	Name	SEQUENCE (5'-3')
BDNF	BDNF-Mus-F	GCGGCAGATAAAAAGACTGC
	BDNF-Mus-R	CTTATGAATCGCCAGCCAAT
Biglycan	Bgn-ex3-F	GCCCTGGTCTTGGTAAACAAT
	Bgn-ex3-R	ACTTTGCGGATACGGTTGTC
Dystroglycan, alpha	Dag1-C-term-F	CGAGACCACTCCTCTGAACC
	Dag1-C-term-R	TCGGTATGGGGTCATGTTCT
Dystroglycan, beta	Dag1-N-term-F	TGTGAGGGACTGGAAGAACC
	Dag1-N-term-R	GGCAATTAAATCCGTTGGAA
Dystrobrevin, beta	Dtnb-ex3,4-F	AGACCGTCATCTCGTCCATC
	Dtnb-ex3,4-R	CATTTTTCCACCACACATGG
nNOS	nNOS-ex1-230307-F	CCAGTAACGGACCTCAGCAT
	nNOS-ex1-230307-R	CCACCTGGATTCCTGTGTCT
Sgcb	Sgcb-ex2,4-F	GCAACTTAGCCATCTGCGTG
	Sgcb-ex2,4-R	TCTCATAGTCCGTGCTGAAC
Sgce	M-SGCE-F	CGCCATAAATCATCACGTCAG
	M-SGCE-R	AGCCAGGGTAACGAGGAAATC
Snta1	snta1-ex2-F	CGGGAAAACAAGATGCCTAT
	snta1-ex2-R	CCTCCTTGCCTGTCTTCTTG
Sarcospan	Sspn-ex3-F	GCAGTTTACCTGCGAGACCT
	Sspn-ex3-R	GAGGCCACAGACCAGGTTTA
Synapsin	M-Syn1-F 032106	CAGCACAACATACCCTGTGG
	M-Syn1-R 032106	AGTTCCACGATGAGCTGCTTG

3.1.5 Protein Extraction from Tissue

To obtain proteins from tissue, the tissue was frozen in liquid nitrogen directly after dissection. It was then transferred to a cold mortar containing a small amount of liquid nitrogen and powdered using a pestle. The powdered tissue was vortexed in radioimmunoprecipitation (RIPA) buffer (1x PBS, 1% NP40, 0.1% SDS, 0.5% Sodium deoxycholate, mini protease inhibitor (Roche, Laval, PQ)), then left on ice for 45 min. A polytron homogenizer was used 2 times for 15 s to homogenize the tissue further. Remaining tissue debris was removed by centrifugation at 4°C for 10 min at 14000 xg. The supernatant solution, or protein containing lysate, was then quantified using the Bradford assay with Bio-Rad Protein Assay Dye Reagent Concentrate (Bio-rad Laboratories, Mississauga, ON) and by BioPhotometer (Eppendorf, Mississauga, ON).

3.1.6 Protein extraction from cells

For whole cell lysate the plate was rinsed with cold PBS twice while on ice to remove the medium. Cells were scraped in 1 ml of cold PBS then collected in a pre-chilled eppendorf tmM ube which were centrifuged at 3000 xg for 3 min at 4°C to remove PBS. A volume of protein extraction Buffer A (10 mM Tris-HCl pH 7.9, 0.1 M NaCl, 1.5 mM $MgCl_2$, 0.18% NP-40, Protease inhibitor tablet (Roche, Laval, PQ)) approximately equal to the volume of the cell pellet was added. The cells were then mixed by pipette to homogenate, before adding that same volume of protein extraction Buffer B (50 mM Tris-HCl pH 7.9, 0.6 M NaCl, 1.5 mM $MgCl_2$, 25% glycerol, Protease inhibitor tablet (Roche, Laval, PQ)) and again mixing by pipette. The extraction was left on ice for 30 min and then centrifuged at max for 10 min at 4°C. The supernatant, or cell

lysate, was transferred to a fresh pre-chilled eppendorf tube and stored at -80°C. Protein concentration was determined using the Bradford assay and by BioPhotometer (Eppendorf, Mississauga, ON).

For fractionated protein samples, a fractionation protocol was used. This allowed for the enrichment of cytosolic soluble proteins, organellar plasma membrane proteins, nuclear proteins, and cytoskeletal RAFT proteins. The protocol was taken directly from the literature [33].

3.1.7 Protein Analysis

Western blot (WB) was used to check for the presence and determine relative quantification of proteins. Protein samples from cell lines and mouse tissues were used. Equal quantities of protein from each sample being analyzed (between 15-50 µg) were mixed with Laemmli Buffer (2% SDS, 10% glycerol, 5% 2-mercaptoethanol, 0.002% bromphenol blue, 0.0725 M Tris HCl pH 6.8). The samples were then heated to 95°C for 10 min and loaded on a precast NuPage 4-12% Bis-Tris gel (Invitrogen, Carlsbad, CA). Precision Plus Protein Standards (Bio-Rad, Mississauga, ON) were used as a size reference and the gel was run in MOPS Running Buffer (50 mM MOPS, 50 mM Tris base, 1 mM EDTA, 0.1% SDS) at 100V until the dye front ran off the gel.

The protein from the resulting gel was transferred onto a Hybond-P PVDF membrane (Amersham Biosciences, Fairfield, CT) for 1 hr at 100 V in Transfer Buffer (48 mM Tris Base, 39 mM Glycine, 0.0375% SDS). The membrane was then blocked in 5% powdered milk in 1X Tris-Borate Saline Tween-20 (TBST) (10 mM Tris-HCl pH 8.0, 0.15 M NaCl, 0.05% Tween-20) for 1 hr at RT with gentle shaking. Primary Ab was

diluted in blocking milk and the membrane was incubated O/N at 4°C. The next day, the membrane was rinsed with TBST and then washed 5x for 10 min at RT with gentle shaking. The species specific HRP conjugated secondary Ab (Sigma-Aldrich, Oakville, ON) was diluted in 5% milk in TBST and the membrane was incubated for 1 hr at RT with gentle shaking. The membrane was then rinsed and washed 5x in TBST followed by a final wash with TBS for 10 min.

The ECL Plus Western Blotting Detection System (GE Healthcare, Baie d'Urfe, PQ) was used to develop the membrane according to manufacture's instructions. The membrane was then placed between a plastic covering in a developing cassette and the Kodak XAR film was exposed to the membrane for variable amounts of time.

If re-use of the membrane was desired, it was incubated in Stripping Solution (0.02% SDS, 62.5 mM Tris-HCl pH 6.7) for 30 min at 50°C. The membrane was washed in TBST twice for 10 min, left to soak for at least 1 hr in TBST, and then blocked O/N.

3.1.8 Generation of FLAG-tagged constructs

For ease of sgce detection in co-immunoprecipitation (co-IP) experiments the flag-tag, DYKDDDK, was placed in the cytoplasmic region of sgce, 18 amino acids away form the transmembrane domain. A plasmid containing the coding region of sgce in the pCMV-sport6 backbone, called MGC13836, was used for the excision of sgce. This was accomplished by RE digest with *KpnI* and *NotI*. The resulting product was subject to gel electrophoresis, band purified and ligated into a pcDNA3 backbone. The resulting sgce-pcDNA3 ligations was transformed as previously described and resulting

kan^r clones were screened by RE digest. This construct was used for In situ mutagenesis as described below and confirmed by sequencing.

After difficulties with this first flag-tagged sgce construct, 6 new constructs were designed. In Situ mutagenesis was used to place 3 different flag tags either just after C-terminus or just before the signal peptide of sgce (Table 10). The 3 tags were (1) a short flag DYKD, (2) the standard flag DYKDDDDK and (3) a 3xflag DYKDHDGDYKDHDIDYKDDDDK, resulting in the design of 6 plasmids total. The plasmid containing sgce in pCMV-Sport6, MGC13836, was grown from glycerol stock in Amp-LB. The plasmid was then collected using the Qiagen Spin Miniprep Kit (Qiagen, Mississauga, ON) and concentration was determined by gel electrophoresis and Nanodrop Spectrometer. During quantification by gel electrophoresis the relative percentage of supercoiled DNA was estimated at approximately 80%.

In situ mutagenesis for each construct was performed by mixing 50 ng MGC13836 with 200 ng of F and R primers in 1x Buffer, provided by the manufacturer. This mixture was heated to 95°C for 2 min then cooled to RT and put on ice. One µl dNTP mix and 1 µl of the high fidelity Pfu Ultra Polymerase (Agilent Technologies, Mississauga, ON) was added before subjecting the sample to PCR amplification. The mixture was heated to 68°C for 5 min then cycled 18 times through (1) 95°C for 1 min (2) 55°C for 1.5 min (3) 68°C for 12 min. The mixture was iced for 2 min before addition of 1 µl *DpnI* RE, then left at 37°C for 1 hr.

The product was transformed into XLI-Blue *E. coli* cells (Stratagene, Agilent Technologies, Mississauga, ON), according to manufacturer's instructions. The flask was then allowed to recover in a 37°C shaker at 225 rpm for 1 hr before being left O/N

on Amp-LB plates at 37°C. Resistant colonies were expanded and then DNA was collected using the Qiagen Spin Miniprep Kit (Qiagen, Mississauga, ON). Confirmation of the cloning steps was done by sequencing.

3.1.9 Immunohistochemitry

Immunohistochemistry (IHC) was used with mouse tissue as well as cell lines. Tissues were embedded directly after dissection. The tissue was rinsed 3 times in PBS and then left O/N at 4°C submerged in 30% sucrose. The next day the tissue was placed in 50% OCT compound (Sakura, Torrance, CA) with 15% sucrose O/N. The tissue was then frozen in OCT-sucrose solution by immersing in liquid Nitrogen. Tissue was then sectioned on a Leica CM 1850 cryostat (Leica, Concord, ON) and tissue slices were placed directly on a slide and allowed to dry for 1 hr before being submerged in 70% ETOH for 10 min and washed 3 times with PBS for 5 min. A water repellant Dako Pen (Dako, Carpinteria, CA) was then used to trace the edge of the tissue or slide.

Next tissue was denatured by placing the slide in 1x Sodium Citrate and heating in the microwave twice for 5 min at 60% power. The slide was allowed to cool to RT before neutralizing for 10 min in neutralizing solution (0.1 M Tris pH 8.8, 0.01 M Triton X). The slide was then rinsed twice with PBS for 5 min and incubated in a humidity chamber for 1 hr with blocking solution (PBS with 10% FBS and 0.001% triton X). Primary Ab was diluted in blocking solution and left on the tissue O/N at 4°C. The next day, the slide was washed 3 times with PBS for 10 min before incubation for 1 hr at RT in the dark with secondary Ab in TBLS (25 ml 1 M Tris-HCL pH 7.4, 4.25g NaCl, 5g BSA, 4.5g L-lysine, 5 ml 10% NaN_3, fill to 500 ml H_20). The slide was rinsed once with

Table 10: Primers for Flag-Tag In Situ Mutagenesis.

Name	SEQUENCE
FLAGtag-F	CAGTGATATC**GACTACAAGGACGACGATGACAAGCA**GCTTGTCCATCACAGCTC
FLAGtag-R	GAGCTGTGATGGACAAGC**TGCTTGTCATCGTCGTCCTTGTAGTC**GATATCACTG
SP-FLAG DYKD	CCAAGGTGCACTCT**GACTACAAAGAC**GACCGGAACGTG
SP-FLAG-anti DYKD	CACGTTCCG**GTCGTCTTTGTAGTC**AGAGTGCACCTTGG
SP-FLAG	CCAAGGTGCACTCT**GACTACAAAGACGATGACGACAAGGA**CCGGAACGTG
SP-FLAG-anti	CACGTTCCGG**TCCTTGTCGTCATCGTCTTTGTAGTC**AGAGTGCACCTTGG
SP-3xFLAG	CTCCAAGGTGCACTCT**GACTACAAAGACCATGACGGTGATTATAAAGATCATGA CATCGATTACAAGGATGACGATGACAAGGA**CCGGAACGTGTACCC
SP-3xFLAG-anti	GGGTACACGTTCCGG**TCCTTGTCATCGTCATCCTTGTAATCGATGTCATGATCTT TATAATCACCGTCATGGTCTTTGTAGTC**AGAGTGCACCTTGGAG
C-Terminus FLAG DYKD	GGTAAATGGTATCCC**GACTACAAAGAC**TGAAGAAAGAAAGC
C-Terminus FLAG-anti DYKD	GCTTTCTTTCTTCA**GTCTTTGTAGTC**GGGATACCATTTACC
C-Terminus FLAG	GGTAAATGGTATCCC**GACTACAAAGACGATGACGACAAGGA**AGAAAGAAAGC
C-Terminus FLAG-anti	GCTTTCTTTCTT**ACCTTGTCGTCATCGTCTTTGTAGTC**GGGATACCATTTACC
C-Terminus 3xFLAG	GGTAAATGGTATCCC**GACTACAAAGACCATGACGGTGATTATAAAGATCATGAC ATCGATTACAAGGATGACGATGACAAGTGA**AGAAAGAAAGCTGACAGAAGC
C-Terminus 3xFLAG-anti	GCTTCTGTCAGCTTTCTTTCT**TCACTTGTCATCGTCATCCTTGTAATCGATGTCAT GATCTTTATAATCACCGTCATGGTCTTTGTAGTC**GGGATACCATTTACC
Colour Code: **FLAG-tag**	

PBS for 10 min, incubated for 3 min in the dark with 1:10000 dapi stain, and rinsed 3 times with PBS for 10 min. Finally the slide was sealed by placing a coverslip over Fluorescence Mounting Medium (Dako, Carpinteria, CA), removing any bubbles and sealing the edges with Advanced Hard as Nails nail polish (Sally Hansen, New York City, NY).

Cellular IHC was accomplished by allowing the cells to grow on a multi-chamber slide (Thermo Fisher Scientific, Rochester, NY). At desired confluency, approximately 60-80%, cells were rinsed with PBS and fixed with ice cold MeOH for 5 min at -20°C. The slide was then incubated for 30 min at RT in blocking solution (PBS with 10% FBS). Primary Ab was diluted in blocking solution at left on the slide O/N at 4°C. The next day, the slide was washed 4 times in PBS for 5 min, incubated in the dark for 1 hr with secondary Ab in blocking solution and then washed 3 times for 5 min in PBS with 1:5000 Hoechst. The coverslip was again mounted with mounting medium and sealed with nail polish.

3.1.10 Generation of Tet-Inducible Plasmids

The Tet-inducible system allows for dose dependent control of the transcript under the control of the TRE promotor. The pTRE2 plasmid was obtained from Dr. Picketts (Ottawa Hospital Research Institute) and employed for the creation of a system for inducible expression of sgce. Sgce was extracted from the sgce-pcDNA3 plasmid, described previously, by digestion with *SalI* and *XbaI*. The TRE2 plasmid was digested similarly and the resulting products were band purified, quantified, and ligated as previously described. A final sgce-TRE2 plasmid was confirmed by RE digest and

sequencing. For future studies with this inducible system, pTK-Hyg and pTet-On were also obtained from Dr. Picketts, grown up and stored as stocks.

To create an inducible sgce flag-tag system the plasmids containing the correct sgce-flag sequence in pcDNA3, described above, were digested with *KpnI* and *NotI* for ligation into the TRE2 backbone. All digests were subjected to gel electrophoresis and the desired product was purified. Concentrations were determined using gel electrophoresis and Nanodrop Spectrometer. Ligations were performed as previously described, then transformed into DH5α cells and incubated on Amp-LB plates. DNA was extracted from the Amp^r clones using spin columns and the final plasmids were confirmed by RE digestion and sequencing.

3.1.11 Generation of GFP-Tagged Sarcoglycans

To visualize the sgcs in the absence of specific Abs, constructs were designed to express GFP-tagged sgcs. Primers were created for PCR amplification of the sgcs from neuroblastoma cDNA (Table 11). The primers were designed so as to remove the stop codon from the end of the sgcs and to include RE sites on either end to facilitate ligation into the pEGFP-N1 plasmid. Attention was also paid to the resulting reading frame during the transition between the sgc and the GFP coding sequence and between 0-2 filler nucleotides were added as necessary.

cDNA from N1E cells was used for amplification and primers were optimized, as previously described, using the HotStarTaq Plus Polymerase kit (Qiagen, Mississauga, ON). Annealing temperatures were determined as 68°C for sgcb, 60°C for sgce and

53°C for sgcg primers. The PCR cycling was programmed as previously described except with 35 cycles and an extension time of 1 min and 30 s.

Amplified sgc product and pEGFP-N1 were digested with the appropriate REs (*HindIII* with either *BamHI* or *SmaI*) then subject to gel electrophoresis and band purification using the illustra GFX PCR DNA and Gel Band Purification Kit (GE Healthcare, Baie d'Urfe, PQ). Resulting product's concentration was determined by gel electrophoresis and by Nanodrop Spectrometer.

Ligation reactions were prepared and transformed into DH5α *E. coli* as described previously. Kana^r colonies were screened by RE digest and sequencing.

Table 11: Primers for the generation of sgce-GFP constructs

	NAME	SEQUENCE
Sgca	Sgca-mRNAamp-HindIII-F	GTC**AAGCTT**ATGGCAGCAGCAGTAACTTGGATAC
	Sgca-mRNAamp-BamH1-R	ATA**GGATCCCA**GTGCTGGTCCAGGATAAGAGGC
Sgcb	Sgcb-mRNAamp-HindIII-F	GTC**AAGCTT**ATGGCGGCAGCGGCGGCGGCGGCGG
	Sgcb-mRNAamp-BamH1-R	ATA**GGATCCCA**ATGAGTGTTCCCACAAGGGTTG
Sgcd	Sgcd-mRNAamp-HindIII-F	GTC**AAGCTT**ATGCCTCAGGAACAGTATTCCCACC
	Sgcd-mRNAamp-Sma1-R	ATA**CCCGGGA**AAGGCAGACACTTGTGTTTATC
Sgce	Sgce-mRNAamp-HindIII-F1	GTC**AAGCTT**ATGAGCCCCGCGACCACTGGCACAT
	Sgce-mRNAamp-BamH1-R	ATA**GGATCCCA**GGGATACCATTTACCTGTAGTC
Sgcg	Sgcg-mRNAamp-HindIII-F	GTC**AAGCTT**ATGGTTCGAGAACAGTACACCACGG
	Sgcg-mRNAamp-BamH1-R	ATA**GGATCCCA**AAGACAGACGTGGCTGTGTTCC
Sgcz	Sgcz-mRNAamp-HindIII-F	GTC**AAGCTT**ATGACTCGAGAACAATACATACTAG
	Sgcz-mRNAamp-BamH1-R	ATA**GGATCCCA**GTTCCACAAGCAAATGCTACTA
	Colour Code: **HindIII**, **BamH1**, **SmaI**, **Filler**	

3.1.12 Generation of shRNA plasmids

Oligonucleotides (oligos) were designed for the production of shRNA using the program sirnawizard (www.sirnawizard.com) (Table 12). They were designed with REs at either end to facilitate ligation into a cloning vector from The RNAi Consortium, pLKO. 1 (Addgene, Cambridge, MA). Sgce-shRNA3 was based on a previous oligomer designed against the rat genome and the equivalent mouse sequence was used, both for sgce-shRNA3 and the control scrambled-shRNA3 [2]. The oligo sequences were run through the BLAST program to determine homology. All were 100% identical and specific for the desired gene with no other homologous hits. The scrambled sequence did not return any homologous matches.

To anneal the oligos, 100 µM of both oligo 1 and 2 were mixed with NEB buffer #2 (New England Biolabs, Ipswich, MA). This mixture was heated for 4 min at 95°C, 10 min at 70°C, then cooled from 70°C to 37°C in 1°C increments every 4 min. The annealed oligos and pLKO.1 were then digested with *AgeI* and *EcoRI* O/N, band purified and quantified as described previously. Ligations and DH5α transformation were also completed as previously described and the resulting Amp^r colonies were screened by RE digest and confirmed by sequencing.

3.1.13 Transfection and Establishment of Stable Cell Lines

Once final constructs for the above experiments were confirmed by sequencing, they were transfected into either N1E or N2A neuroblastoma cells. This was achieved with Lipofectamine 2000 (Invitrogen, Carlsbad, CA), which was used according to manufacture's instructions. Constructs were used for either transient transfections into

Table 12: Oligos for the generation of shRNA constructs

NAME	SEQUENCE
Scrambled shRNA3	**CCGG**GGAACTAAGTGTCATACATTA**TCAAGAG**TAATGTATGACACTTAGTTCC**TTTTTG**
	AATTCAAAAAGGAACTAAGTGTCATACATTA**CTCTTGA**TAATGTATGACACTTAGTTCC
Sgce shRNA3	**CCGG**GAAGCAATGAGTTTATAATCA**TCAAGAG**TGATTATAAACTCATTGCTTC**TTTTTG**
	AATTCAAAAAGAAGCAATGCGTTTATAATCA**CTCTTGA**TGATTATAAACTCATTGCTTC
Sgcb shRNA1	**CCGG**GCGTGATCGTCCTCCTGTTTA**TCAAGAG**TAAACAGGAGGACGATCACGC**TTTTTG**
	AATTCAAAAAGCGTGATCGTCCTCCTGTTTA**CTCTTGA**TAAACAGGAGGACGATCACGC
Sgcb shRNA2	**CCGG**GGGAGTACCTGAATGAGTTAT**TCAAGAG**ATAACTCATTCAGGTACTCCC**TTTTTG**
	AATTCAAAAAGGGAGTACCTGAATGAGTTAT**CTCTTGA**ATAACTCATTCAGGTACTCCC
Sgcb shRNA3	**CCGG**GATGAAGAGGAGACCACTAAA**TCAAGAG**TTTAGTGGTCTCCTCTTCATC**TTTTTG**
	AATTCAAAAAGATGAAGAGGAGACCACTAAA**CTCTTGA**TTTAGTGGTCTCCTCTTCATC
Sgcd shRNA1	**CCGG**GACCAGGTAATGCCCTATACT**TCAAGAG**AGTATAGGGCATTACCTGGTC**TTTTTG**
	AATTCAAAAAGACCAGGTAATGCCCTATACT**CTCTTGA**AGTATAGGGCATTACCTGGTC
Sgcd shRNA2	**CCGG**GAGCTGAGAGATTGAGAGTCT**TCAAGAG**AGACTCTCAATCTCTCAGCTC**TTTTTG**
	AATTCAAAAAGAGCTGAGAGATTGAGAGTCT**CTCTTGA**AGACTCTCAATCTCTCAGCTC
Color Code: **Age1**, **EcoR1**, **Loop**, **Terminal**	

the cells or for the development of stable pooled or single clones. If transient expression was desired, the cells were incubated with the lipofectamine and DNA for 48 hrs. After this time cells were harvested or used for experimentation.

If the development of stable cells lines was desired, the cells were incubated with the lipofectamine and DNA for 24 hrs prior to the addition of fresh medium along with the appropriate antibiotic selection. Medium was changed every 24-48 hrs for approximately 7 days to obtain a pooled stable line. If stable single clones were the goal, then cloning rings were employed to isolate each single colony. The single colonies were moved to a 96-well plate and surviving resistant clones were expanded and stored as previously described.

3.1.14 L-NAME Treatment of Neuroblastoma Cells

Neuroblastoma cells were treated with N^G-Nitro-L-Arginine Methyl Ester (L-NAME) to chemically inhibit nNOS. Cells were seeded into 12 dishes, or wells, at the suggested density (Table 8). L-NAME was added to media to create concentrations of 0M, 10^{-5}M, 10^{-4}M, and 10^{-3}M. Each concentration was applied to cells in triplicate. Media was changed daily and cells were observed, so as not to exceed 70% confluency in any given dish. Cells were then counted using a Reichert Bright-Line Metallized Hemocytometer (Hausser Scientific, Horsham, PA) and re-seeded at the suggested density. Total cell count values were calculated after 7 to 9 days.

3.1.15 Nitrate and Nitrate assay

To assess the activity of nNOS, NO metabolite levels were measured using the Nitrate/Nitrite Colorimetric Assay Kit (Cayman Chemicals, Ann Arbor, MI). This was done according to manufacturer's instructions using medium from WT, KD, and L-NAME treated N1E cells. Medium alone was used as a control. All samples were tested in triplicate.

3.1.16 Cell Death and TUNEL staining

In order to quantify cell death in response to over-expression of sgce, N1E cells were grown and transfected using Lipofectamine as previously described. Cells were either transfected with the sgce-pcDNA3 plasmid or with and empty-pcDNA3 vector. Both plasmids were co-transfected with a pEGFP-N1, which was used as a visual control for transfection efficiencies.

The number of surviving cells in each condition was counted 24 and 48 hrs after transfections using Trypan Blue (StemCell Technologies, Vancouver, BC) and a Hemocytometer according to manufacturer's instructions. After the first count, an equal number of cells were re-plated for each condition. This prevented changes in proliferation rates due to over-crowding. Additionally, aliquots of cells from each condition were transferred to a multi-chamber slide for TUNEL staining with The In Situ Cell Death detection kit, TMR red (Roche, Laval, PQ). Staining was done according to the manufacturer's protocol and the resulting slide was preserved as previously described.

3.2 Results

3.2.1 DGC expression in the CNS

In order to determine which, if any, members of the DGC interact with sgce in the CNS, it is necessary to first identify which of these proteins are present in neuronal cells. If a similar complex is being formed in neurons, many of the complex members will be present in neuronal cell lines. Using N1E-115 (N1E) and Neuro-2A (N2A) mouse neuroblastoma cells as a model for neurons, as well as neurospheres (NeuroS) and oligodendrocytes (OligoD) to look at other neuronal cell types, RT-PCR was used to show that many transcripts from the DGC are present (Figure 8A, B). The presence or absence of these proteins was confirmed by WB where possible. Staining for the present sgcs and other proteins known to co-localize in the model outside of the CNS was the first step towards revealing Sgce's interactions and functions.

In neuronal cells the transcripts for sgcb, sgce and sgcz are clearly present (Figure 8C, D). Contrary to the findings presented here, a previous study had indicated that there may be Sgcg in the CNS [2]. It is unclear whether sgcd is or is not present in these cells [2] (Figure 9), which may indicate a low or variable level of expression.

Other neuronal cell lines were also examined for DGC members. Sgce is expressed predominantly in the brain. It is functionally absent in MD patients and MD patients display normal muscle. For these reasons MD is considered a neurologic disorder, but it is unclear which neuronal cell type, or combination of cell types, is responsible. Neurospheres were grown from the SVZ of WT mice and represent mainly

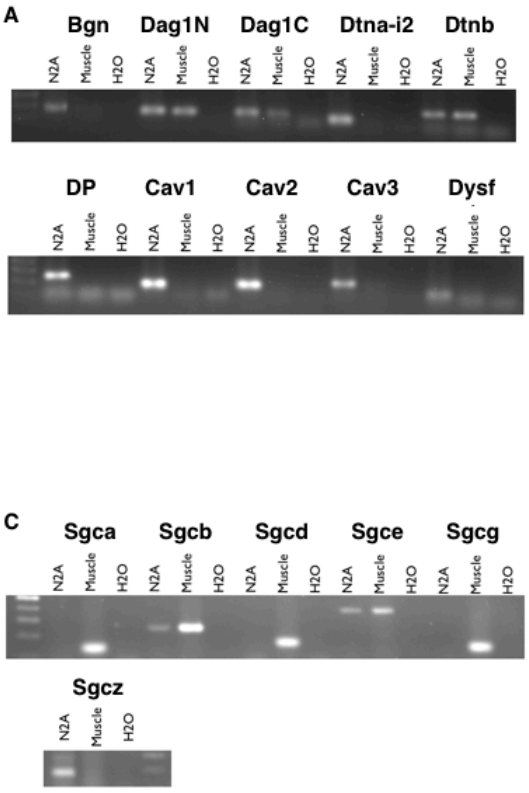

B

	N2A	N1E	NeuroS	OligoD
Sarcospan				
α-Dystroglycan				
ß-Dystroglycan				
α-Syntrophin	?	?	?	?
ß-Syntrophin	?	?	?	?
α-Dystrobrevin				
ß-Dystrobrevin				
Dysferlin				?
Biglycan				
Caveolin 1,2,3				
Dystrophin				?
nNOS	?			

D

	PNS	N2A	N1E	NeuroS	OligoD	Muscle
Sgca						
Sgcb						
Sgcd		?	?			
Sgce						
Sgcg						
Sgcz	?					

Figure 8: RT-PCR of neuroblastoma cells revealed the presence of many DGC members (A) and sarcoglycans (C). Summary tables of other cell types show presence with green, absence with white and undetermined with '?' of the DGC (B) and sarcoglycans (D).

Abbreviations

Transcripts: Biglycan (Bgn), alpha-dystroglycan (Dag1N), beta-dystroglycan (Dag1C), alpha-dystrobrevin isoform 2 (Dtna-i2), beta-dystrobrevin (Dtnb), non-isoform specific dystrophin (DP), caveolin 1, 2 and 3 (Cav1, 2, 3), Dysferlin (Dysf)
Cell Types: Neurospheres (NeuroS), Oligodendrocytes (OligD)

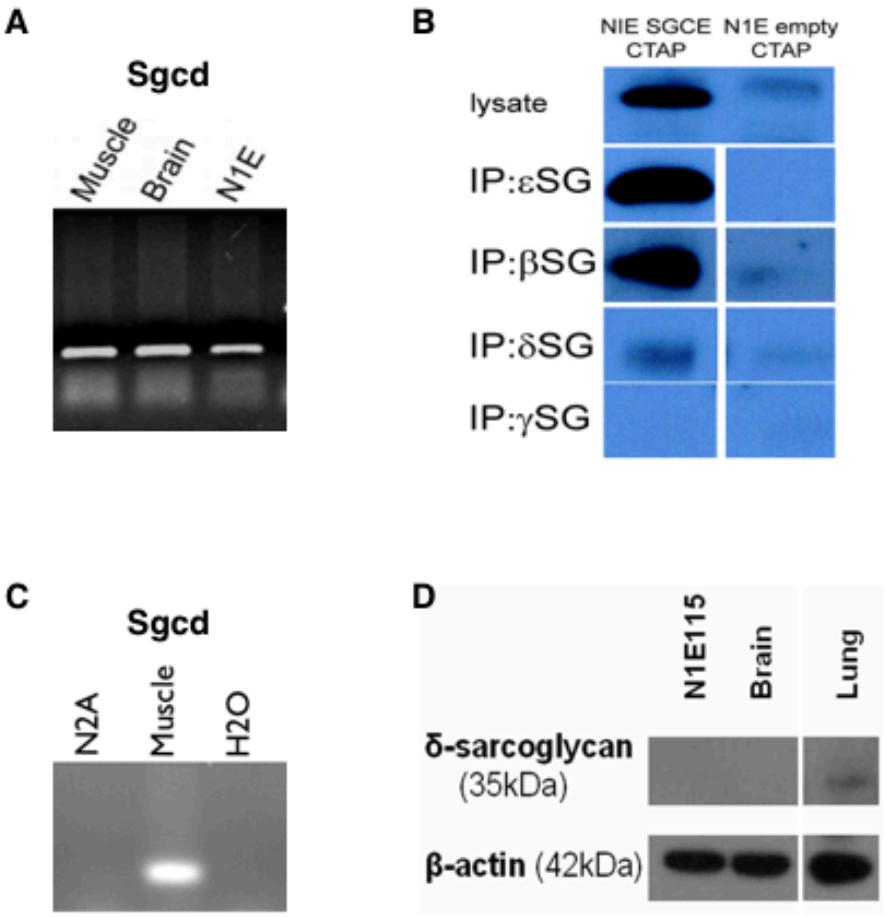

Figure 9: The expression of delta-sarcoglycan is variable in neuroblastoma cells and the brain. Sgcd transcript is present in neuroblastoma cells and brain using RT-PCR (A) and a co-IP pulling down with sgcd showed the detection of the flag protein from sgce-TAP tag transfected neuroblastoma cells (B). Sgcd transcript is not present in neuroblastoma cells using RT-PCR (C) and a WB of neuroblastoma cells and brain shows an absence (D). Figures A and B from Dr. Amanda Smith, Figure D from Dr. Nancy Laurin. In addition Lita McDonald's thesis states that her RT-PCR was negative [2].

a population of neuronal progenitor cells but any sample will include a certain level of spontaneously differentiated cells as well. These cells were shown to express DGC members by RT-PCR. Oligodendrocytes also express sgce and other DGC members. Oligodendrocytes were confirmed to express sgce by WB, both while proliferating and after differentiation (Figure 10A). IHC with these cells shows expression around the cell membrane and in the processes (Figure 10B). It is unknown which cell type(s) is concerned for the pathology of MD.

3.2.2 Development of the Flag-tag constructs

In order to investigate sgce's function in the CNS, it is important to know what complex it is part of and therefore its binding partners. Initially there was not an available and specific sgce antibody for co-IPs. Therefore a construct was designed to express sgce with an inserted flag-tag (DYKDDDDK) just after the transmembrane domain (Figure 11A, B). This construct was transfected into N1E cells but unfortunately they did not grow well or live long. It was a possibility that the inserted flag-tag interfered with normal functioning of the cell and caused these problems.

In an attempt to circumvent possible disruption of function resulting from the initial flag-tag, new constructs were designed containing the flag-tag either just before the signal peptide or just after the C-terminal (Figure 11B). It was hoped that at least one location would still allow for proper functioning. Three different flag tags were designed at both locations for a total of six constructs: a short flag tag (DYKD) hopefully minimizing structural interference, the standard flag-tag (DYKDDDK), or a 3xflag-tag (DYKDHDGDYKDHDIDYKDDDDK) in order to facilitate detection.

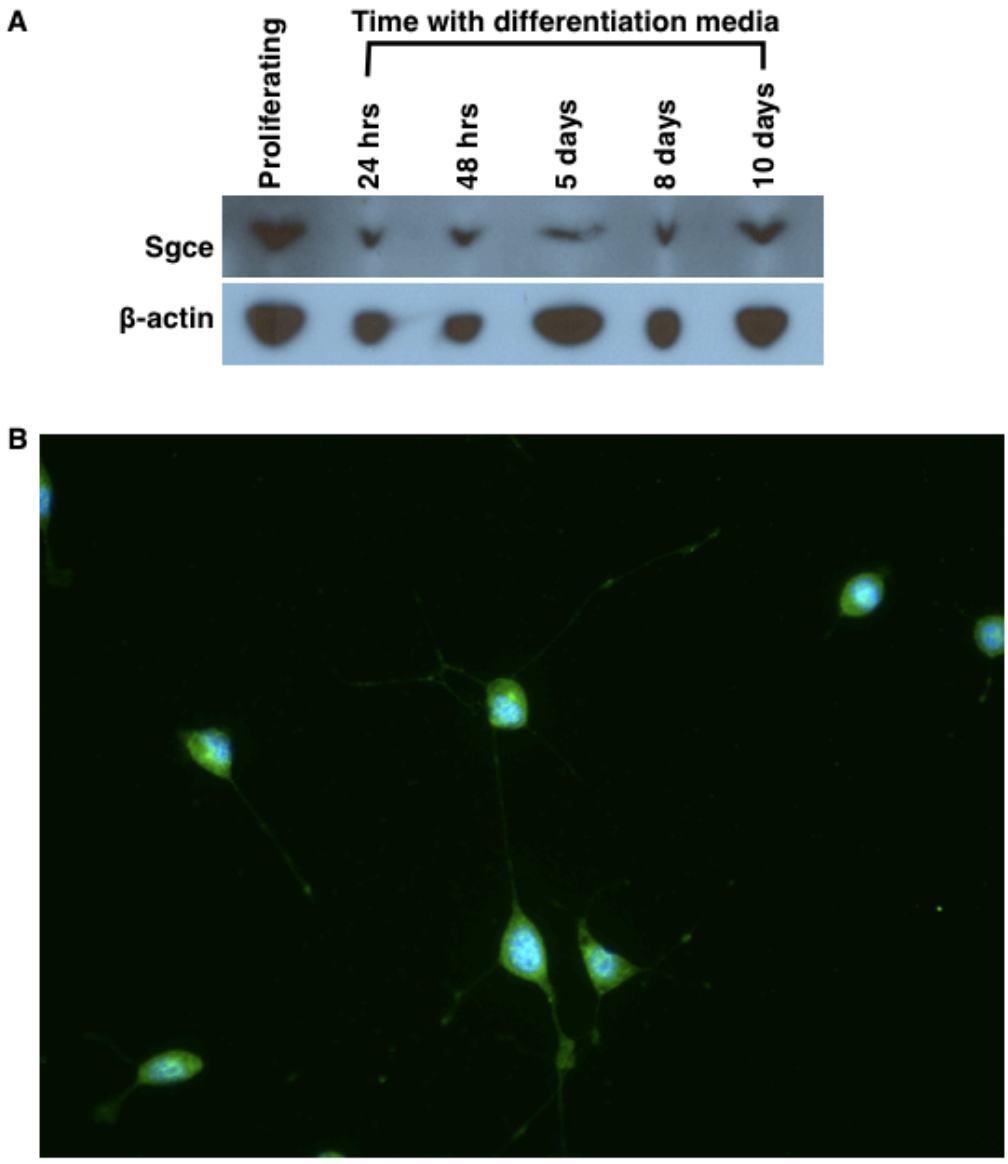

Figure 10: Oligodendrocytes express sgce protein during proliferating and differentiated states (A) around the cell membrane and in the processes (B). Oligodendrocytes were obtained from Ryan O'Meara in the Kothary Lab.

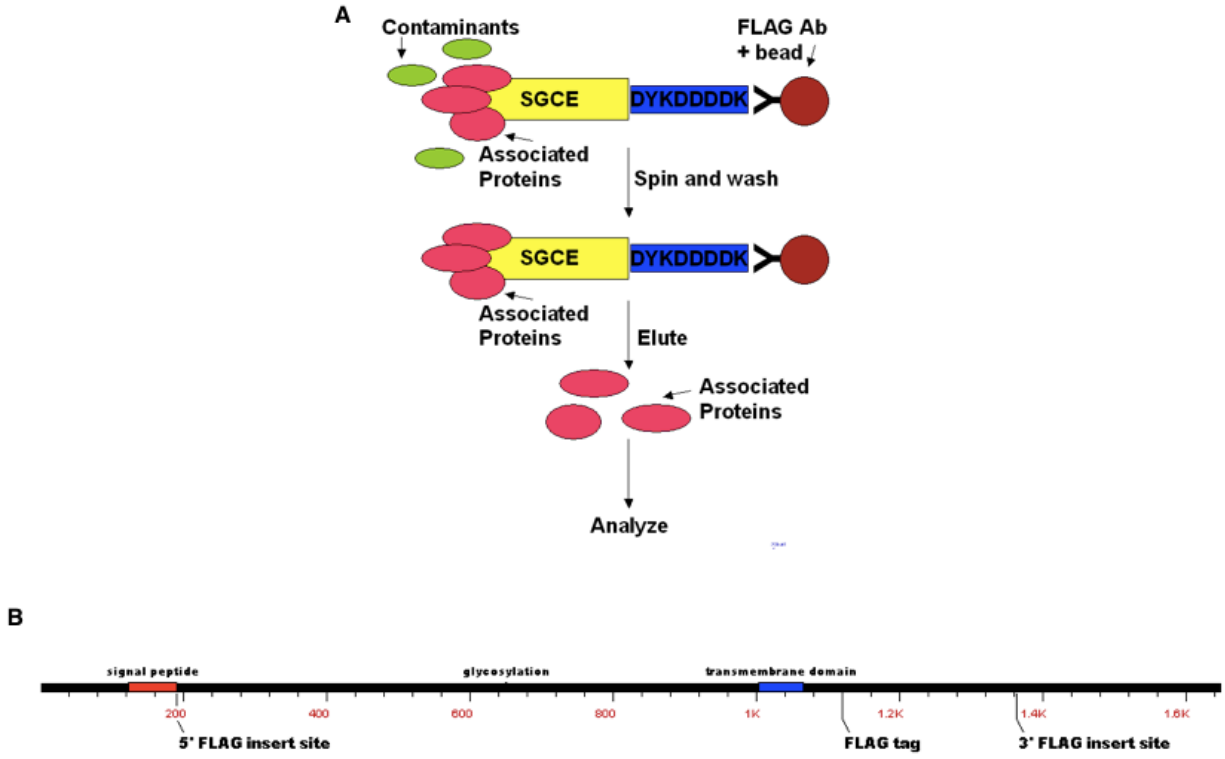

Figure 11: Sgce-Flag tag constructs. Flag-tags allow a clean pull down of associated proteins (A). The sgce coding sequence indicating where the initial flag-tag was inserted just after the transmembrane domain and where the later 3 types of flag-tags were inserted either just after the signal peptide or just before the C-terminal (B).

Of the six constructs designed, four were completed. The short flag-tag at the C-terminal and the signal peptide, the standard flag-tag at the signal peptide and the 3xflag-tag at the signal peptide were all confirmed by RE digestion and sequencing. These constructs were transfected into N1E cells but again these cells did not survive well. These observations, combined with other anecdotal observations in our lab, prompted us to look at sgce's effect on cell survival (See section 3.2.7).

To test the functionality of these flag-tag constructs they were transiently transfected into HEK293 cells. The flag-tag and 3xflag-tag at the signal peptide were easily visible by WB (Figure 12). HEK293 cells had been used to test the flag-tags in an environment without endogenous levels of sgce. In fact, HEK293 cells do have a neuronal origin and express sgce. Therefore Cos-1 cells were transfected to test these constructs in a truly sgce-null environment. Cos-1 cells showed similar results however, only the flag-tag and 3xflag-tag at the signal peptide were visible by WB (Figure 12).

In order to circumvent the lack of a proper sgce Ab for co-IP combined with the cell death seen with the over-expression of sgce, a tetracycline-inducible system for sgce expression was designed. Initially the coding sequence for sgce was excised and ligated into pTRE2. The resulting plasmid was confirmed by multiple RE digests and sequencing. Sgce-pTRE2 can be used with a Tet-On system, employing the pTK-Hyg and pTet-On plasmids, to determine the kill curve for tolerable levels of sgce in neuroblastoma cells. Tetracycline-inducible constructs containing sgce with either the short, standard or 3x flag tag inserted just before the signal peptide were also made and confirmed by RE digest. These constructs can be transfected into neuroblastoma cells and used at a tolerable level of expression for future co-IP studies.

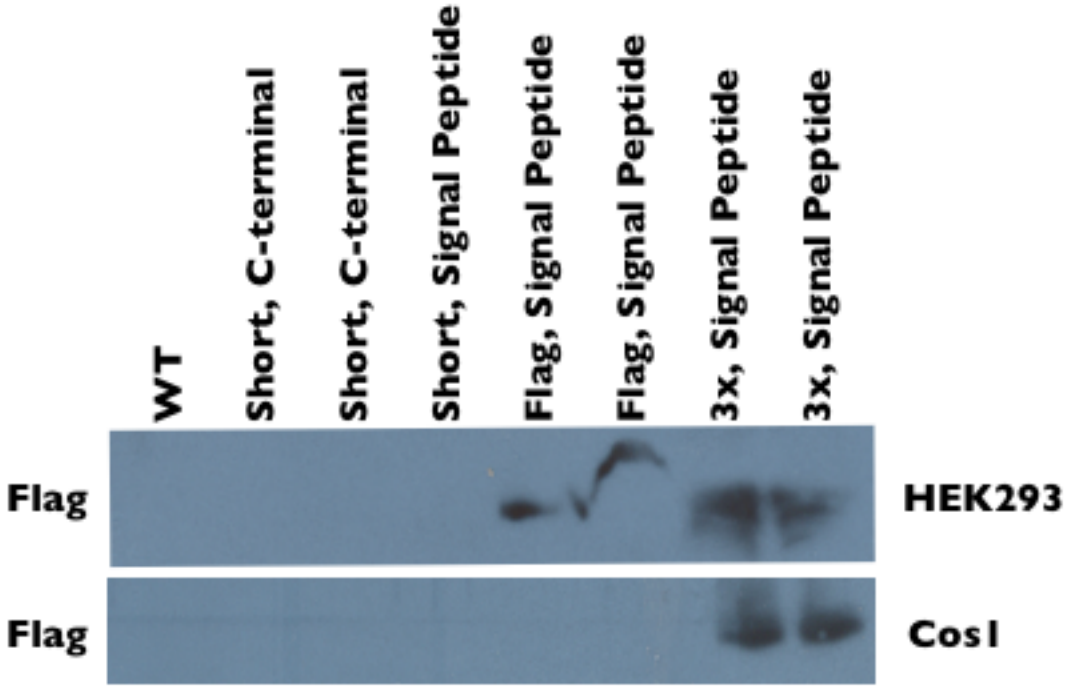

Figure 12: Transient expression of flag-tagged Sgce constructs in HEK293 and Cos1 cell lines.

Additionally, a TAP-tagged sgce construct was developed by a previous member of the lab (Dr. Nancy Laurin). This construct consists of a CTAP-His-TEV-Flag-tag from pBRIT_CTAP. This tag was used by another lab member with N1E cells (Dr. Amanda Smith). Many single clones were identified before one was found that expressed the tagged sgce at a low enough level to allow the N1E cells to survive. These cells are not as robust as the WT N1E cells or N1E cells containing the empty TAP-tag. Again, this implicated a link between sgce over-expression and cell survival.

As a complimentary model, both the empty and sgce TAP-tag constructs were transfected into N2A cells and grown under selection. Protein from pooled clones was tested by WB to confirm the presence of the Flag-tag. Unfortunately, as seen with the N1E pooled clones, it appears that single colonies will have to be expanded and tested until a tolerant line can be found.

A new Ab has been developed against sgce using the peptide ^{400}TQIPQPQTTGKWYP from the literature [26]. Future results from the flag-tag and TAP-tag experiments can now be confirmed using this sgce Ab for co-IP studies.

3.2.3 Development of the GFP-Tagged Sarcoglycans

Sgce is expressed in the brain and has been reported specifically in the olfactory bulb, the hippocampus, the pons and the cerebral cortex [20]. Using our sgce Ab, brain slices were stained and the presence of sgce in the cerebral cortex was confirmed (Figure 13A). The hippocampus appears less reactive than in published pictures but there are other unidentified structures which appear to express sgce (Figure 13A, B). This experiment should be expanded using slices throughout the brain to see all

structures and compare sagittal slices from the same plane as in the published data in order to get a clearer view.

In neuroblastoma cells sgce has been seen at the cell membrane and in the processes. Neuroblastoma cells have also been stained with Abs against sgca, sgcb, sgcd, and sgcg with variable results. None of these Abs have proven to be very effective but generally the expressed sgcs appear to also be distributed around the perimeter of the cells, as would be expected for a class of membrane bound proteins.

To circumvent the ineffective Abs, GFP-tagged sgcs were designed. Only the plasmids for sgce- and sgcb-GFP have been constructed. The coding sequence for sgce and sgcb were PCR amplified from N1E cDNA. Primers designed for this amplification included RE sites to facilitate ligation into pEGFP-N1. These primers also included extra bases where needed to maintain the reading frame during the transition from sarcoglycan to GFP. These constructs have been confirmed by RE digest and sequencing. They were then transfected into N2As and grown under kanamycin selection to obtain stable pooled clones.

Pictures of these pooled clones revealed varying visibility of the GFP-tagged sgcs (Figure 14). As expected, due to previous cell survival problems seen with over-expression of sgce, only very faint levels of sgce-GFP expression can be detected in the surviving cells and many of these pooled clones did not expand sufficiently to be used for experimentation. Results from cells transfected with the sgcb-GFP and the sgce-GFP constructs show similar distribution around the periphery as previously of the cell seen with IHC experiments (Figure 14).

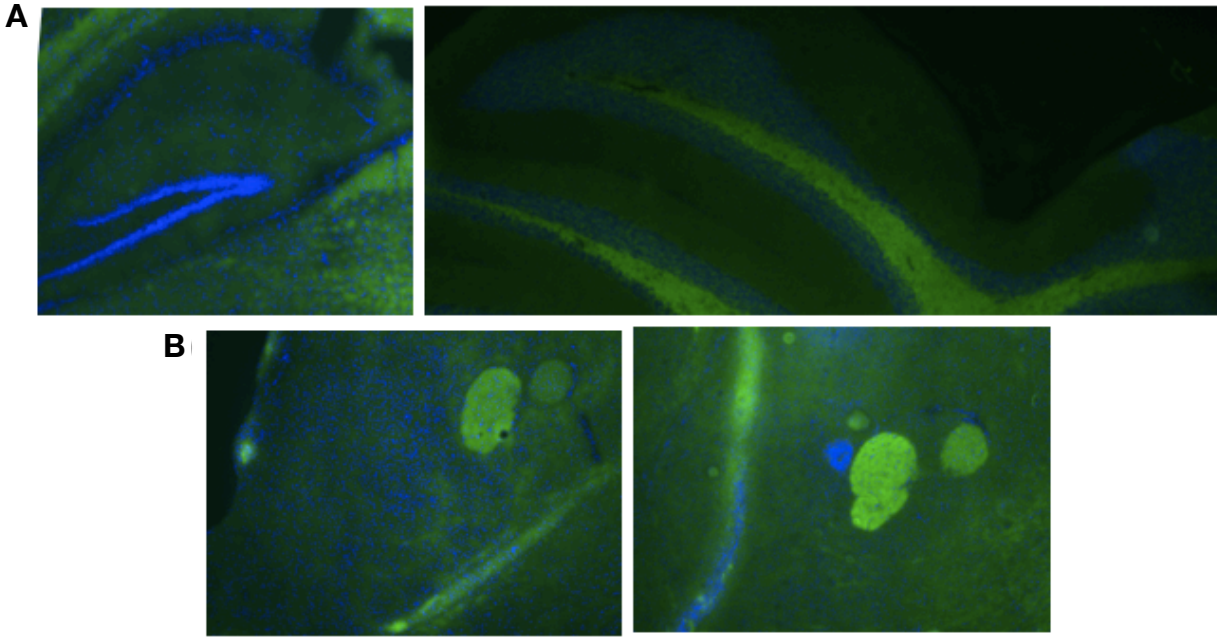

Figure 13: Sgce expression in the mouse brain. Close ups of the hippocampus and cerebral cortex (A) and two unidentified structures located below the olfactory bulb, shown in two different brain slices (B).

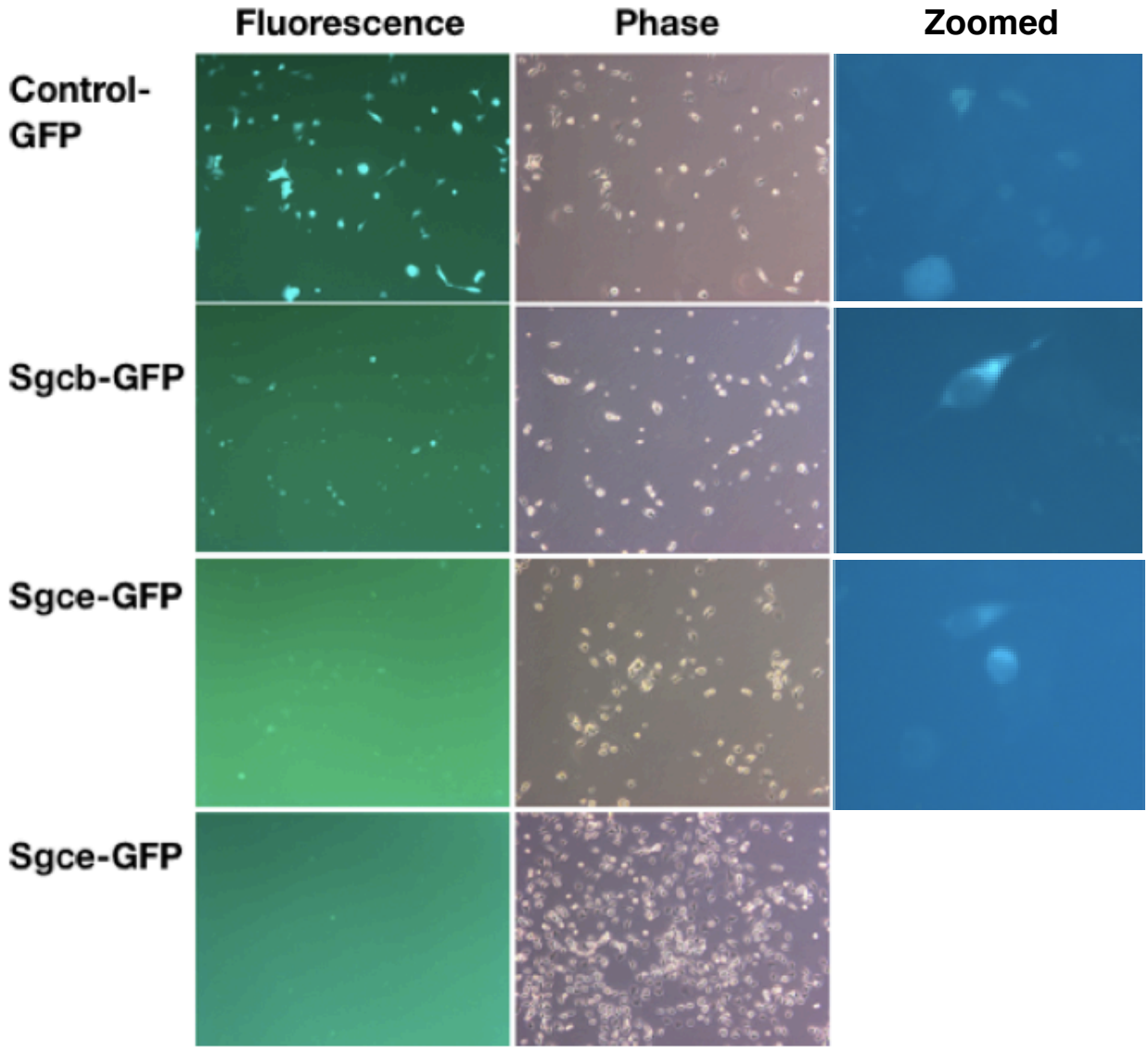

Figure 14: N2A cells expressing different GFP-tagged Sgcb and Sgce clones. This illustrates the fact that very few cells over-expressing sgce survive.

3.2.4 Development of the shRNA Constructs

To determine changes in neuronal cell functions due to the loss of sgce expression, cell lines with knocked-down (KD) sgce expression have been developed. Previously a short hairpin RNA (shRNA) was developed to knock down the expression of sgce in rat cells. This same shRNA was used in mouse N1E cells effectively. Quantification showed a 77% reduction of sgce mRNA and WB confirmed a loss of sgce protein (Figure 15A, B). This corresponded with a 50% decrease of nNOS protein and a 50% increase in cell proliferation [2] (Figure 15C, D).

Using cDNA amplified from these cells, qRT-PCR was employed to quantify changes in the mRNA transcripts of other DGC associated members. KD of sgce showed that the decrease of nNOS protein resulted in approximately a 1.5 fold up-regulation of nNOS mRNA. KD of sgce also resulted in significant increase of sgcb, αDG, βDG, β-Dtn, sspn and Snt-acid1 transcripts (Figure 16A). Several other DGC associated mRNA transcripts showed trends towards up-regulation as well. This could indicate an attempt at compensation for a lack of function due to a destabilization of the complex. The colorimetric assay for nNOS metabolites, NO_2^- and NO_3^-, further confirmed changes in nNOS activity. Only NO_2^- showed significantly reduced levels, but the lack of significance for NO_3^- may be due to extremely variable values rather than a lack of altered expression (Figure 16B).

As the original sgce-shRNA based on rat sequence was shown to be effective, the corresponding mouse sequence was used to design new oligos. Oligos were also designed to develop shRNA against sgcb, sgcd and sgcz (Table 12). Only shRNA for sgce and sgcb have been made.

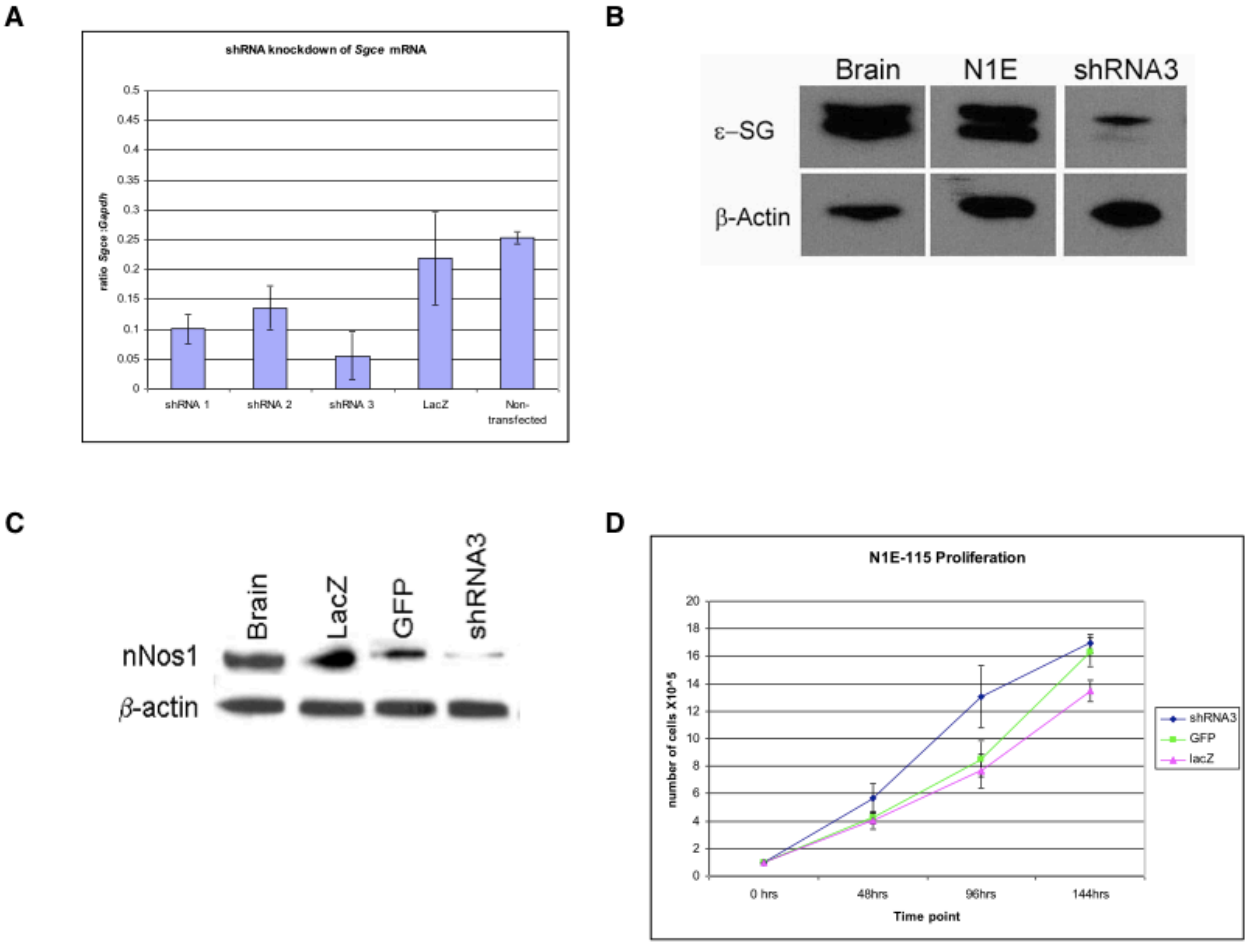

Figure 15: In N1E cells ShRNA was effective at knocking down sgce mRNA expression (A) and protein expression (B). These cells also displayed reduced expression of nNOS protein (C) and increased proliferation (D). Figures A, C and D by Lita McDonald.

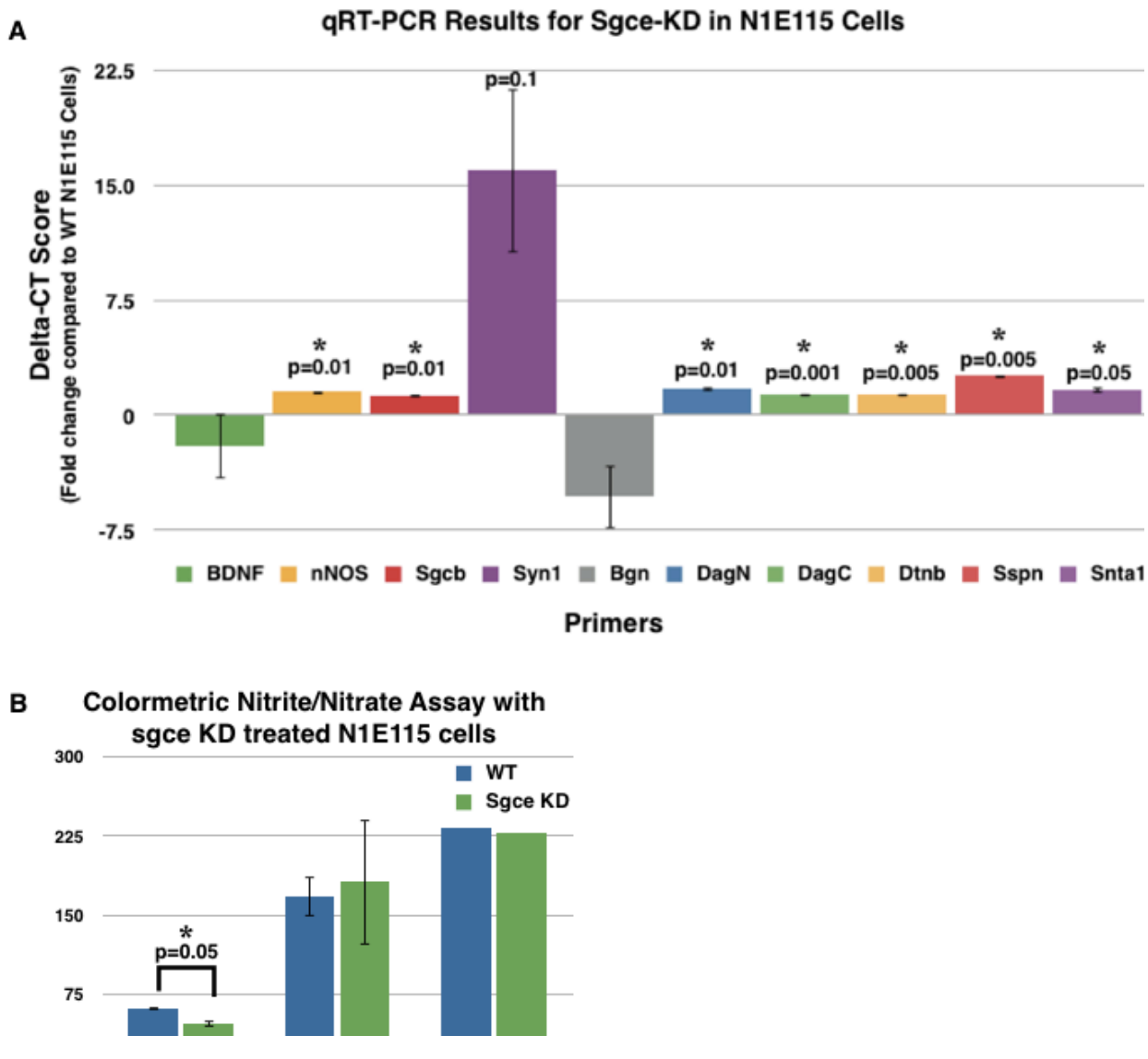

Figure 16: qRT-PCR results of sgce-KD N1E cells compared to WT (A). KD of sgce lowers nNOS metabolite levels (B).

Abbreviations: synapsin 1 (Syn1), biglycan (Bgn), alpha-dystroglycan (Dag1N), beta-dystroglycan (Dag1C), beta-dystrobrevin (Dtnb), sarcospan (Sspn), syntrophin acid 1 (Snta1).

The oligos for the sgce and sgcb targeted shRNA were annealed and ligated into plKO.1. Each construct was confirmed by RE digest and sequencing. They were then transfected into N2As and grown with puromycin selection to obtain stable pooled clones. Initial WBs suggest that sgce protein levels are decreased effectively in some of the pooled clones. KD of either sgcb or sgce appears to reduce the levels of sgce protein seen (Figure 17). This would be consistent with a stepwise formation of the SGC. For more precise experiments stable single clones should be isolated.

Changes in proliferation are not expected in these KD N2A cells due to a lack of or low levels of nNOS expression in N2A cells prior to differentiation [27,66]. Cell counts should be taken and analyzed from single clones to confirm this however.

3.2.5 Testing nNOS Interactions

KD of sgce in N1E cells results in increased proliferation, a decrease of nNOS protein and an increase of nNOS mRNA. To establish that this increased proliferation was in fact due to a decrease of nNOS protein rather than an increased turnover of protein, WT N1E cells were treated with 10^{-5} M *N* G-nitro-l-arginine methylester (L-NAME). L-NAME is a NOS inhibitor, thereby reducing the amount of NO produced.

Treatment of N1E cells with L-NAME resulted in a significantly increased number of cells counted by hemocytometer (Figure 18A). Therefore the increased proliferation seen with KD of sgce is, at least in part, due to a loss of nNOS function. L-NAME treated cells also show a trend towards increased nNOS mRNA production. Again, this may indicate an attempt at compensation for the loss of functioning nNOS protein. To further confirm the loss of NO activity, nNOS metabolites were assessed. L-NAME

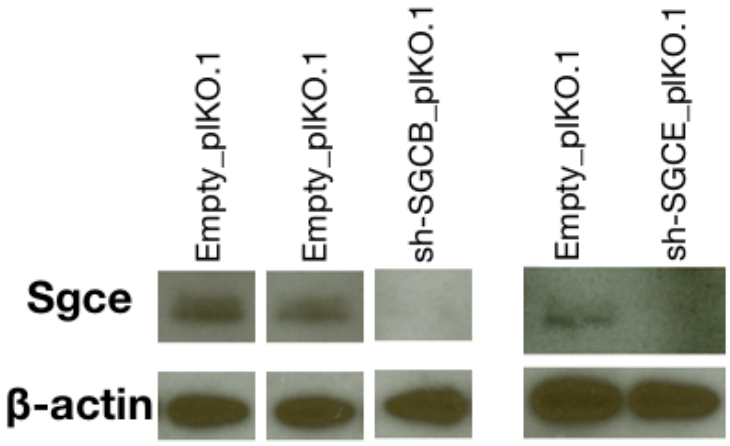

Figure 17: WB of sgce after KD of sgce and KD of sgcb in N2A cells compared with empty plasmid controls.

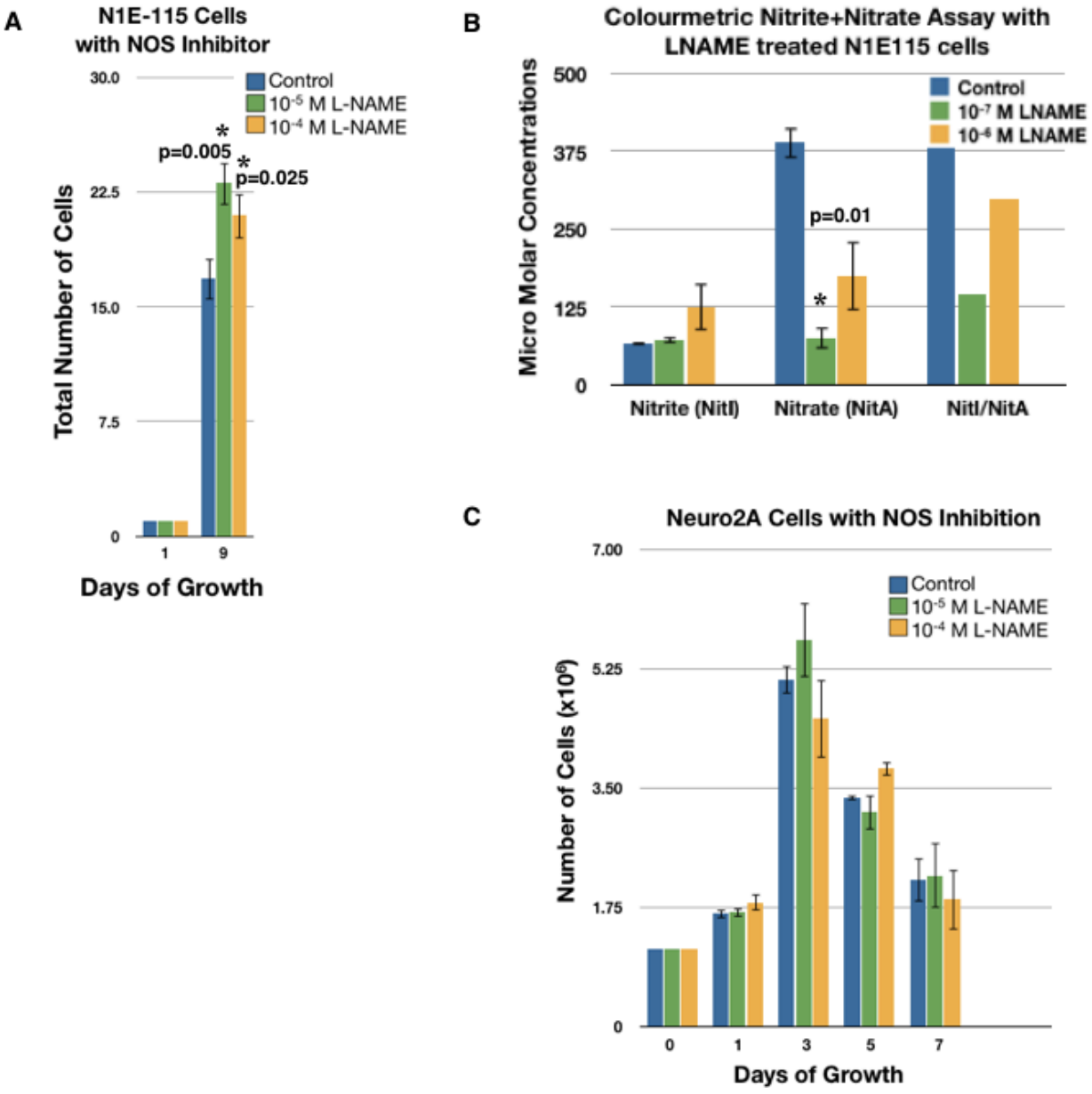

Figure 18: Reduced nNOS activity increases proliferation in N1E cells. Average growth of N1E cells treated with L-NAME (A) and corresponding reduction of nNOS metabolite, nitrate (B). N2A cells do not show a change in proliferation with treatment of L-NAME (C).

treated cells displayed a significantly decreased concentration of NO_3^- indicating a decrease in nNOS activity (Figure 18B).

Differentiated WT N1E cells showed significant decrease of nNOS mRNA transcript compared to undifferentiated WT cells. This is likely due to their more stable state and slowed proliferation. When sgce-KD N1E cells were differentiated however there was no change in the level of nNOS mRNA from the proliferating KD cells, possibly due to the same feedback about the substantial loss of NO function.

N2A cells were also treated with L-NAME. As expected, due to their low nNOS levels until differentiation, no change was see in proliferation (Figure 18C). In future, these cells can be differentiated and treated with L-NAME to confirm differences which may be seen from a loss of nNOS function. Differentiated N2A cells may provide a more accurate paradigm for studying neuronal function as well.

3.2.6 Expression Patterns of Sgce Isoforms

Sgce has two known isoforms (Figure 19C): Isoform 1 expressed in all tissues and isoform 2 expressed solely throughout the brain [4]. It is unclear whether these isoforms play different roles or form novel complexes in the brain. Both isoforms have been found throughout the brain [20]. In neurons, isoform two appears to by pre-synaptic, while the isoform one is post-synaptic [65]. Firstly, to identify which cell types in the brain contained which isoforms, N1E cells and oligodendrocytes were used for WB. It was determined that both isoforms are expressed in neuroblastoma cells while only one is expressed in oligodendrocytes (Figure 19A). The two sgce isoforms are fairly close in size with isoform 1 having a predicted size of 47 kDa while isoform 2 is predicted at 49

kDa [20]. PCR was used to confirm which isoform was present in oligodendrocytes. The transcript was identified as the common isoform 1 (Figure 19B, C). This suggests a novel role for isoform 2, specifically in neurons. The approach in experiments has been to use isoform neutral sequences for KO, KD and Ab studies. Future studies may wish to use these techniques in an isoform specific manner to tease apart their potentially separate roles.

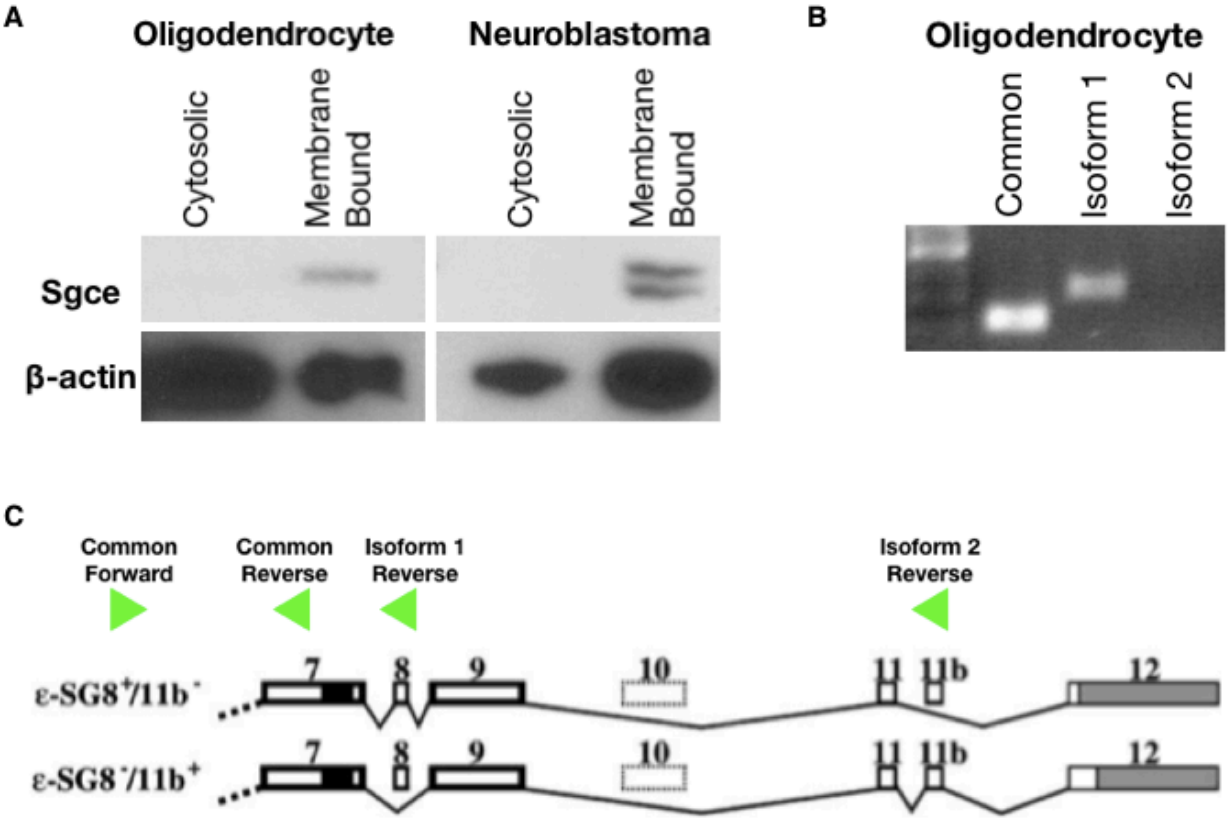

Figure 19: Isoforms of Sgce. A western blot shows the presence of two isoforms in neuroblastoma cells and one isoform in oligodendrocyes (A). PCR confirms that oligodendrocytes express isoform 1 but not isoform 2 (B). Primers for isoform PCR placed along the sgce exons (C).

3.2.7 Over-expression of Sgce in Neuronal Cells

As a compliment to the KD cells, a construct was designed to over-express sgce. This construct contained the coding sequence of sgce ligated into pcDNA3 under a CMV promoter and was transfected into N1E cells. qRT-PCR showed the expected increase of sgce transcript. They also displayed significant increases of nNOS and βDG and a significant decrease of sspn mRNA transcript. Unfortunately these cells did not grow well or live long.

Other experiments using flag-tagged, TAP-tagged, and GFP-tagged sgce in neuronal cell lines also resulted in problems with cell survival (Figure 20A). These same constructs in non neuronal cells, such as the Flag-tag in Cos1 cells and the TAP-tag in fibroblastic NIH-3T3 cells (NIH-3T3 cells grown by Dr. Nancy Laurin), were tolerated well. These observations prompted the hypothesis that over-expression of sgce may be lethal, at least in neuronal cell types.

Pursuing this idea, N1E cells were co-transfected with either pcDNA3 or the over-expressing sgce construct as well as pEGFP-N1. By comparing GFP expression it was determined that similar transfection efficiencies were obtained for both conditions. The cells containing the sgce-pcDNA3 plasmid displayed a significant decrease in total number of surviving cells by 48 hrs post transfection (Figure 20B, C). Further investigation revealed a significant increase of TUNEL (Terminal deoxynucleotidyl transferase dUTP nick end labeling) staining at 72 hrs. TUNEL stain is used to detect DNA fragmentation resulting from apoptotic signaling cascades. This result therefore suggests an increase in apoptosis in these cells (Figure 20D).

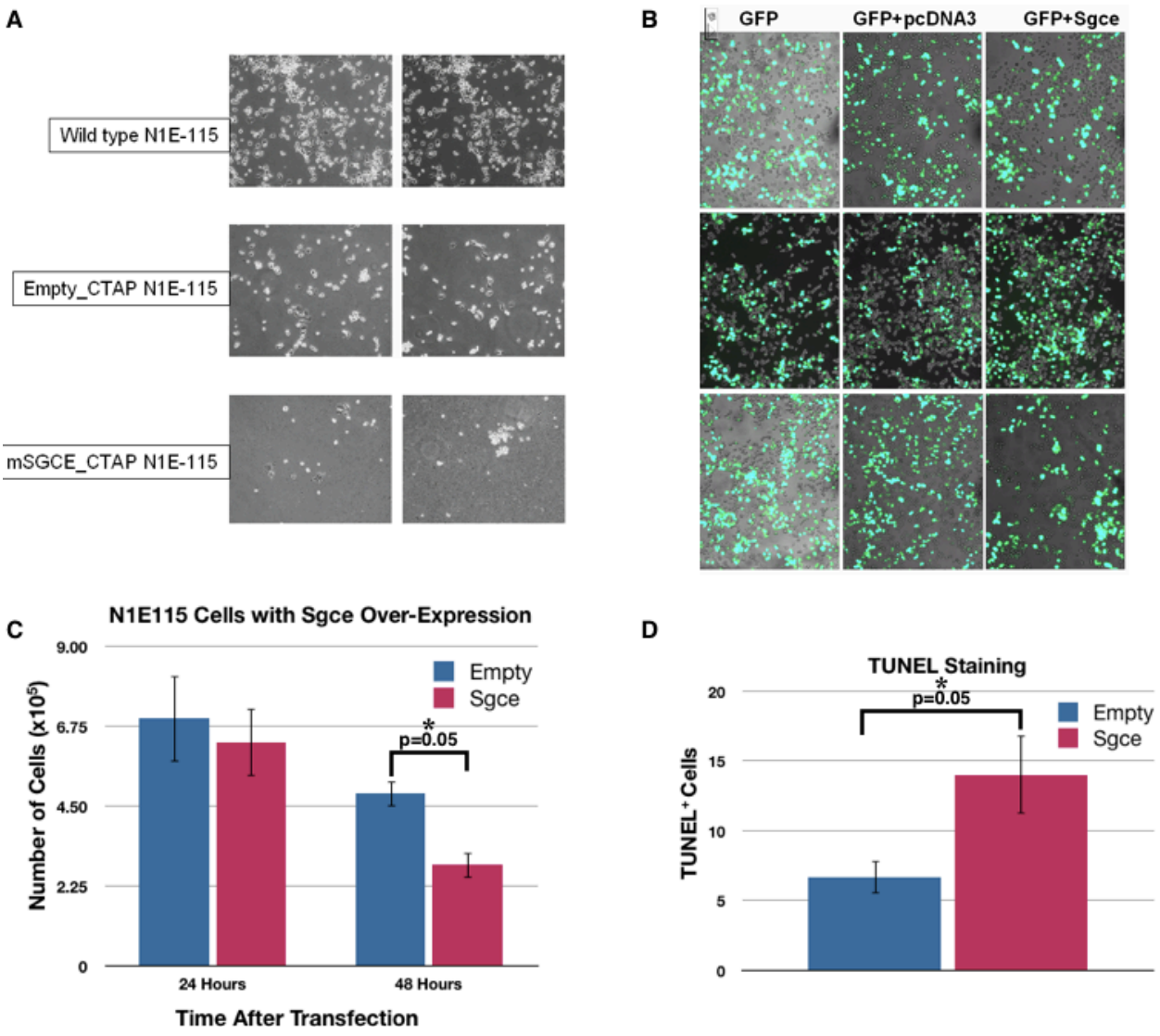

Figure 20: Over-expression of sgce in neuroblastoma cells causes cell death. This was seen anecdotally during experiments with the sgce-TAP-tag in N1E cells (A). To quantify sgce-pcDNA3 was transfected with GFP into N1E cells to assess transfection efficiency (B). The surviving cells were counted at two time points (C) and stained with TUNEL (D). Figure A by Dr. Nancy Laurin.

It has been our experience that over-expression of sgce is not tolerated in cells which already have an endogenous level of sgce expression. Conversely, sgce can be expressed at high levels in cells which do not express sgcs naturally, such as Cos-1 cells. A similar observation was reported for sgca in muscle [28]. At the time, the authors postulated that over-expression of sgca was cytotoxic due to the hierarchal order of assembly of the SGC. Given the fact that sgca and sgce are paralogs, it is likely that there was also an increase in apoptosis. Further experimentation with over-expression of sgce is not directly relevant to the MD disease pathology, as the disease phenotype is due to an absence of sgce rather than an abundance, but it may still give some insight into the functional roles of sgce.

3.2.8 Cell Adhesion

Over time, as the experiments manipulating sgce's expression levels proceeded, it was anecdotally noted during tissue culture that some conditions appeared to result in more or less cell adherence to the dishes. Furthermore, when counting cells under the microscope with the hemocytometer, some conditions appeared to result in varying ratios of clumped cells to single cells. Therefore, while studying the over-expression of sgce in N1E cells, as described above, the number of clumps of cells seen on the hemocytometer were also recorded and grouped by clumps of 2, 3-10, or 11^+ cells. The over-expression of sgce resulted in a significant increase of clumps in both the 3-10 and the 11^+ cell categories (Figure 21).

It is likely that this clumping is related to the overall low health of these cells rather than any particular function of sgce. It is interesting to note however that when

neurospheres are treated with ETOH, a treatment which is known to ameliorate MD symptoms in many cases, and they increase their sgce expression levels, these neurospheres also increase their level of expression for laminins and ß-Integrins [4]. Furthermore, the ETOH treated neurospheres increase in size. It was demonstrated that this increase was independent of cell cycle stimulation, perhaps indicating an increased tendency for the cells to stay adhered to the sphere. This suggests that sgce's role in cell adhesion may be of interest for further study.

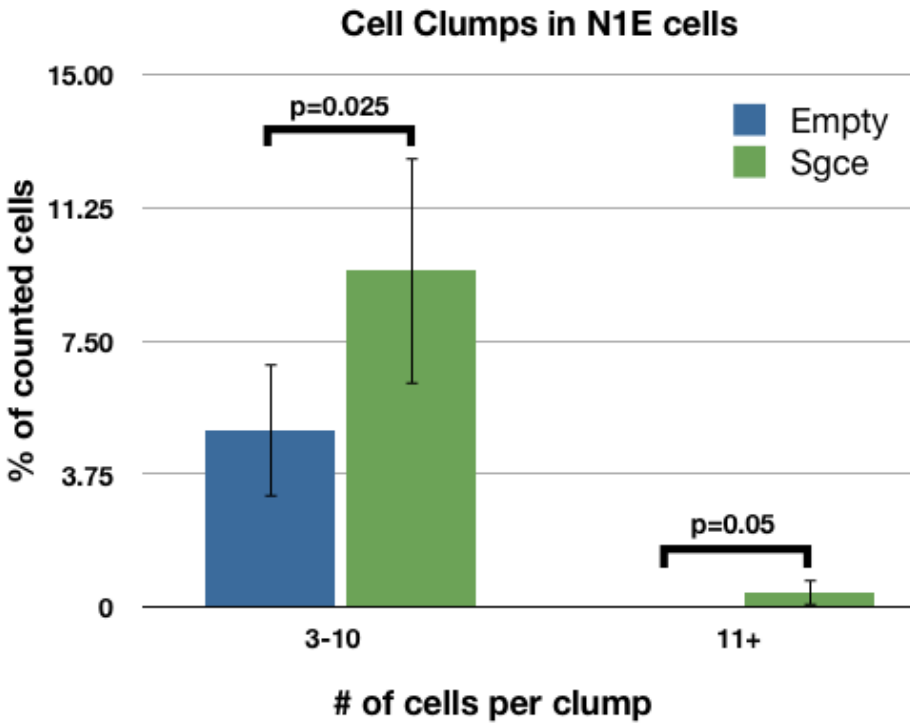

Figure 21: Over-expression of sgce leads to more cell clumping.

3.3 Discussion and Future Directions

In vitro I showed that the mRNA is present in neuronal cells for many of the DGC associated proteins. I also confirmed that the KD of sgce results in a reduction of nNOS protein and in increased proliferation of NIE cells. By using a nitrite/nitrate assay as well as studies with L-NAME, I was able to confirm that this increased proliferation was in fact due to a lack of nNOS function. I also showed that these proliferation changes do not occur in N2A cells, which do not express high levels of nNOS during proliferation, further confirming nNOS's role in the proliferation changes. Using qRT-PCR I found that KD of sgce resulted in significant changes in the transcript levels for many DGC associated proteins. This suggests that a DGC-like complex is forming in neuronal cells. Also, as a result of difficulties with my research, I became aware that over-expression of sgce causes cell death. I quantified this observation using cell counts and TUNEL staining, both showing significant results.

Additionally, I have created several new constructs which will hopefully be of use for future students wanting to study sgce's functions. New shRNA targeting sgce and sgcb have been made and both constructs result in reducing the expression of sgce. I also created 7 different flag-tagged sgces and have transferred some of these into a tet-inducible system, which should circumvent the problem of over-expression. Finally GFP-tagged constructs for sgce and sgcb have been made and pooled clones have been developed. These tools will hopefully enable future students to continue to tease apart sgce's function(s).

The expression of sgcd mRNA in neuronal cells is somewhat controversial. If sgcd is present in neurons, it would suggest that one of the known heterotetrameric

SGCs forms is present in neuronal cells, but if sgcd is absent it would point towards a novel SGC in the CNS. In muscle sgcd is thought to be necessary for formation and localization of the SGC [14]. This may not be a definite rule however, as a mildly effected LGMD2F patient whose muscle biopsy only showed significant deficiency for sgcd, while maintaining sgca, sgcb and sgcg at the muscle membrane [25]. The seemingly variable sgcd levels may indicate low levels of the known heterotetrameric complex along with the formation of a novel sgce complex in neuronal tissues.

KD N2A cells should be differentiated in the future, which should allow for the detection of potential changes in nNOS protein and mRNA expression. nNOS activity assays may also be employed. It can be predicted that a decrease in nNOS protein will result due to a destabilization of the SGC. Experiments may also compare these KD cells against WT N2A cells treated with L-NAME, to confirm which differences seen are attributable to disrupted nNOS activity.

These experiments were done *in vitro*. Although this allows for ease of manipulation, it does not represent the delicate balance found within the CNS. In the brain many different neuronal cell types interact and exchange information. Neuronal type cells, such as neuroblastoma cells and neurospheres, as well as oligodendrocytes were used independently in these studies. It is also important to remember that many of these experiments used neuroblastoma cells in a proliferative state. Expression patterns may change once these cells are differentiated.

It is possible that sgce is important for cell-cell interactions or adhesion and may aide in stabilization at the oligodendrocyte-neuron connections or neuron-neuron synapses. Any findings with tissue culture should be confirmed in an *in vivo* model.

Completing the *in vivo* mouse models will allow for further insight into the pathology of MD.

The two isoforms of SGCE likely play different roles, as they display different localization. Patient mutations which result in the null sgce phenotype effect both isoforms. To truly understand the pathology of MD and therefore how to best target treatment, it will be important to understand the functional roles of both isoforms. It is possible that one isoform disrupts the pathway causing the myoclonic jerks and/or dystonia while the other isoform is involved in disrupting pathways leading to OCD or other psychological phenotypes. For effective and complete treatment it will be necessary to understand all potentially effected pathways.

The studies on over-expression of sgce resulted from difficulties encountered in the lab. It will be important for future researchers to be aware of these hurdles when planning experiments involving the manipulation of sgce. Although over-expression of sgce is the opposite phenotype from that seen in the disease, future experiments to determine the cause of this cell death may aid in elucidating sgce's function.

4. General Discussion

MD is a neurologically based movement disorder characterized by bilateral myoclonic jerks paired with dystonia [1]. Mutations have been mapped to the *SGCE* gene in about 40% of patients [2]. Examining the properties of SGCE in the CNS will aid to elucidate the pathology of MD. Although Sgce is a member of the SGC in other tissues, little is known about its interactions in the CNS. The vast majority of mutations in SGCE result in the patients with MD being effectively null for sgce expression.

During my time on this project I used recombineering to complete the constructs for two transgenic mouse models: One model for the KO of exon 4 of sgce and one for the cGR in intron 1. Originally two chimeras existed from a previous student but, after breeding these chimeras containing the cKO for exon 1 and genotyping their offspring for over a year, I had to conclude that they were not viable. I therefore created primary neurosphere lines from both chimera 1 and 2, as well as from a WT mouse. These transgenic constructs and neurosphere cell lines allowed me to compare my RT-PCR results from neurospheres to a heterogeneous neurological cell population and will hopefully be of use for future students in the lab.

In vitro I showed that the mRNA is present in neuronal cells for many of the DGC associated proteins. I also confirmed that the KD of sgce results in a reduction of nNOS protein and in increased proliferation of NIE cells. By using a nitrite/nitrate assay as well as studies with L-NAME, I was able to confirm that this increased proliferation was in fact due to a lack of nNOS function. I also showed that these proliferation changes do not occur in N2A cells, which do not express high levels of nNOS during proliferation, further confirming nNOS's role in the proliferation changes. Using qRT-PCR I found that

KD of sgce resulted in significant changes in the transcript levels for many DGC associated proteins. This suggests that a DGC-like complex is forming in neuronal cells. Also, as a result of difficulties with my research, I became aware that over-expression of sgce causes cell death. I quantified this observation using cell counts and TUNEL staining, both showing significant results.

Additionally, I have created several new constructs which will hopefully be of use for future students wanting to study sgce's functions. New shRNA targeting sgce and sgcb have been made and both constructs result in reducing the expression of sgce. I also created 7 different flag-tagged sgces and have transferred some of these into a tet-inducible system, which should circumvent the problem of over-expression. Finally GFP-tagged constructs for sgce and sgcb have been made and pooled clones have been developed. These tools will hopefully enable future students to continue to tease apart sgce's function(s).

Sgce KO models were created as they should approximate MD conditions *in vivo.* Two constructs have been designed: one to conditionally KO sgce and one to conditionally repair sgce. These constructs will hopefully be used to produce chimeras and stable mouse lines in the future. Conditionally removing sgce in tissue and temporally specific manners will further elucidate the progression of the disorder and help target future treatment attempts.

The rationale behind developing both the cKO and the cGR mouse model is that they can work in tandem. The cKO model can tell us at which point during development the loss of sgce results in MD symptoms. Conversely, the cGR model will tell us by which point sgce's function must be restored for a full recovery. It is possible the KO

even in adulthood or old age will produce the same symptoms and that functional restoration at any point during development or life will result in complete cessation of symptoms. Knowing this however gives very important information for future diagnostic and treatment planning.

In the same manner, these two models can be used together to elucidate the specific cell type responsible for the pathology of MD. By systematically removing sgce in more specific areas it can be determined that this disorder is a solely neurologically based movement disorder, as it has always been believed to be. It is also possible to show which cell type(s) specifically requires the restoration of sgce function for a full recovery. Again this information may be very useful for the planning of diagnostics and treatments in the future.

Behavioral studies will greatly elucidate sgce's functions. Previous studies have shown sgce expressed throughout the mouse brain. Higher expression was seen in certain areas however, including the olfactory bulb. Behavioral analysis will evaluate if the KO mice experience any dysfunction in olfaction. If a change is seen it will be interesting to clinically test olfaction in MD human patients. Although no reported cases of smell dysfunction are reported with MD, olfaction is not a highly relied upon sense for humans. Small changes may not be personally apparent or disabling. Other behavioral experiments, such as the Morris water maze, allow for functions of spatial memory and the hippocampus to be analyzed. It would be prudent to put these mice through a battery of tests, as experiments which are not easily feasible in human patients may give insight into the pathology of this disease.

Future study with these conditionally transgenic mice should also investigate the function of the BG as it is possible that the BG are involved in the pathology of MD. MD is often thought to be cortically related and a hyperdopaminergic disease. Increased levels of DA, usually as a side effect of Levodopa, are known to produce both myoclonus and dystonia. Furthermore, a previous sgce KO model showed increased DA in the striatum and one MD family has a mutation in the D2R gene.

Unfortunately I had a number of difficulties in getting a MD mouse model off the ground. The original chimeras for cKO of sgce's exon 1 were bred for a year, yielding 325 WT pups between them. Of these WT pups a number of them should have displayed a brown coat color. This should have happened even if PEG10's dysfunction was responsible for the lack of mutant pups. This indicates that there may have been something wrong with the cells used for blastocyst injection.

Another possible, yet unlikely, problem with these chimeras could have come from the Neo cassette. The Neo gene is located in the intron and does not usually interfere with normal cell functioning. It is possible though that it was located in an unknown promoter site or interfered in another unforeseen way. After recombination into ES cells, it is possible to remove the Neo cassette before blastocyst injection. The main advantage to keeping it in, apart from less handling of the cells prior to injection, is that it allows for selection of primary cell lines later on; as was done when developing the neurosphere line.

For both the cKO of sgce's exon 4 and the cGR models the road block was with the homologous recombination after electroporation. Significant time was spent troubleshooting this step. Both constructs were re-sequenced, the database sequence

was checked, protocols were gone over, transfection efficiencies assessed and the selection cassette was tested. The source of this problem has yet to be confirmed. In future, it would be sensible to try different ES cell lines. The BAC used for retrieval of the sgce gene and subsequent targeting comes from a 129S6 strain of mouse, it is possible that using ES cells for electroporation from a similar background would aid in homologous recombination. Potential cell lines to try in future could be R1 or J1 ES cells, which come from 129X1/129S1 and 129S4 origins respectively.

In the CNS, sgce may form a complex similar to the DGC found in muscle. KD of sgce in neuronal cells results in destabilization of nNOS and its activity, likely due to a disruption of the SGC. KD of sgcb appears to result in lowered sgce protein expression as well, possibly indicating a hierarchal assembly similar to that found in muscle. Interestingly sgcd may not play a prevalent role in the neuronal SGC as it appears to only be expressed intermittently.

To determine the pathology of MD it will be important to conclude which proteins sgce is forming a complex with as well as this complex's function(s). It is possible that sgce forms the heterotetrameric complex known from muscle, along with sgcb, sgcd, and sgcz. Sgcz is known to be highly expressed in the CNS and sgcb is present in neuronal cells. Sgcd also appears to be present to some extent in neuronal cells. It also seems logical that this heterotetramer would interact with a DGC-like complex as many of the known DGC members from muscle are also present in neuronal cells. Furthermore, it appears that KD of sgcb also results in a reduction of sgce. This suggests some interaction between these two proteins. It is possible that the sgce which

would have formed part of this complex was unable to make its way to the membrane and was therefore degraded.

It is also likely that novel complexes containing sgce are being formed in the CNS. The stoichiometry of the sgcs does not promote the theory of all sgce forming the known heterotetramer. Sgce and sgcz are known to have significantly higher expression than other sgcs in the CNS. Also, sgcd is necessary for the known heterotetramer to form and its expression is low and inconsistent. This suggests that the known complex, if it is forming, may be playing a minor role in the CNS. As antibodies become available for sgcz it will be interesting to perform co-localization and co-IP studies to decipher if these two sgcs are forming their own novel complexes.

Another indication that the known SGC from muscle is not the only complex for neuronal sgce is that loss of sgcb does not cause MD. It has been shown that loss of sgcb is sufficient to prevent the formation of the SGC at the membrane. If all sgc-containing complexes in the brain were not being formed in patients with sgcb deficiencies, we would expect to see LGMD as well as MD symptoms. As sgcb is the most unique sgc, it is unlikely that it is being compensated for by another protein.

Furthermore, two main isoforms of sgce exist: one is expressed ubiquitously while the other appears to be neuron specific. These isoforms may themselves join distinct complexes. As most of the studies here were performed with materials which were not isoform specific, it is possible that the results in these experiments pertain to only one or both isoforms. KD of each isoform at a time would allow for the determination of which one is effecting nNOS levels etc. This would also indicate if one isoform is more likely to form the known SGC than the other.

Decreases of nNOS are seen in response to KO or KD of sgce as well as several other DGC associated proteins [9,93]. This is thought to be due to a lack of the SGC reaching the membrane, which effects nNOS's ability to anchor via Syn. nNOS synthesizes the free radical NO, an important signalling molecule involved in many physiological functions. It is also, unfortunately, very difficult to measure directly as it has the very short half life of a couple seconds. Other methods can be employed as indirect readings for NO levels. One method was described and variations on this method should be used with future *in vivo* and *in vitro* studies. Another reason NO is difficult to measure is that, in the CNS, it is able to act like a neurotransmitter and disperse widely to neighbouring neurons. NO is an unusual neurotransmitter in that it can freely enter nearby cells without having to go through the synapse and, although nNOS is only expressed in about 1% of neurons, it is predicted that virtually every cell in the brain is exposed to NO [56,95]. It is therefore possible that if the sgce containing complex destabilizes, resulting in the degradation of nNOS and a loss of NO in the environment, it actually effects change in nearby cells which may not even be expressing sgce.

An unexpected finding was the effect of over-expression of sgce. Over the course of many experiments it became clear that neuronal cells did not live well once transfected with an sgce containing plasmid. Over-expression of sgce was shown by TUNEL staining to induce apoptosis and further digging in the literature found that a similar process may take place with high levels of sgca [28]. Although nNOS/NO levels were not assessed in these over-expressing cells, it is interesting to note that increased

levels of NO is known to induce energy depletion induced necrosis [58]. As KD of sgce causes a reduction in nNOS it would be interesting to see if the reverse is also true.

Further study both *in vivo* and *in vitro* are necessary to look at the SGC assembly and its binding partners. Functional changes occurring in response to a loss of sgce will not only provide insight into the pathology of MD but will also give us further insight into the functioning of the mammalian CNS.

5. Bibliography

1. C Klein (2005) Movement disorders: Classifications. *Journal of Inherited Metabolism Disorders* **28**:425-439.
2. L McDonald (2007) The establishment of in vivo and in vitro models for Myoclonus Dystonia. *Department of Biochemistry, Microbiology and Immunology*.
3. Esapa CT, Waite A, Locke M, Benson MA, Kraus M, McIlhinney RA, et al. SGCE missense mutations that cause myoclonus-dystonia syndrome impair epsilon-sarcoglycan trafficking to the plasma membrane: modulation by ubiqui- tination and torsinA (2007) *Human Molecular Genetics* **16**:327-342.
4. Vangipuram, SA, Grever, WE, Parker, C, & WD Lyman (2008) Ethanol increases fetal human neurosphere size and alters adhesion molecule gene expression. *Alcoholism: Clinical and Experimental Research* **32(2)**:339-347.
5. Grimes, DA, Han, F, Lang, AE, St George-Hyssop, P, Racacho, L, & DE Bulman (2002) A novel locus for inherited myoclonus-dystonia on 18p11. *Neurology* **59(8)**: 1183-1186.
6. Zacaria, ML, Di Tommaso, F, Brancaccio, A, Paggi, P, & TC Petrucci (2001) Dystroglycan distribution in adult mouse brain: A light and electron microscopy study. *Neuroscience* **104(2)**:311-324.
7. Peter, AK, Marshall, JL, & RH Crosbie (2008) Sarcospan reduces dystrophic pathology: stabilization of the utrophin-glycoprotein complex. *Journal of Cell Biology* **183(3)**:419-427.
8. Waite, A, Tinsley, CL, Locke, M, & DJ Blake (2009) The neurobiology of the dystrophin-associated glycoprotein complex. *Annals of Medicine* **41(5)**:344-359.
9. Crosbie, RH, Barresi, R, KP Campbell (2002) Loss of sarcolemma nNOS in sarcoglycan-deficient muscle. *FASEBJ* **16(13)**:1786-1791.
10. Rees, ML, Lien CF, & DC Gorecki (2007) Dystrobrevins in muscle and non-muscle tissues. *Neuromuscular Disorders* **17(2)**:123-134.
11. Hack, AA, Groh, ME, & EM McNally (2000) Sarcoglycans in muscular dystrophy. *Microscopy research and technique* **48(3-4)**:167-180.
12. Wheeler (2003) Sarcoglycans in vascular smooth and striated muscle. *Trends in Cardiovascular Medicine* **13**:238-43.
13. Lancioni, A et al. (2011) Combined deficiency of alpha and epsilon sarcoglycan disrupts the cardiac dystrophin complex. *Human Molecular Genetics* [Epub ahead of print].
14. Shi, W, Chen, Z, Schottenfeld, J, Stahl, RC, Kunkel, LM, & YM Chan (2004) Specific assembly pathway of sarcoglycans is dependent on beta- and delta-sarcoglycan. *Muscle and Nerve* **29(3)**:409-419.
15. Imamura, M, Araishi, K, Noguchi, S, & E Ozawa (2000) A sarcoglycan-dystroglycan complex anchors Dp116 and utrophin in the peripheral nervous system. *Human Molecular Genetics* **9(20)**:3091-3100.
16. Sassoe-Pognetto, M, Froia, E, Pregno, G, Briatore, F, & A Patrizi (2011) Understanding the molecular diversity of GABAergic synapses. *Frontiers in Cellular Neuroscience* [Epub ahead of print].

17. Sugita, S, Saito, F, Tang, J, SAtz, J, Campbell, K, & TC Sudhof (2001) A stoichiometric complex of neurexins and dystroglycans in the brain. *The Journal of Cell Biology* **154(2)**:435-445.
18. Xiao, J, & MS Le Doux (2003) Cloning, developmental regulation and neural localization of rat epsilon-sarcoglycan. Brain Research. *Molecular Brain Research* **119(2)**:132-143.
19. Ettinger, AJ, Guoping, F, & JR Sanes (1997) ε-sarcoglycan, a broadly expressed homologue of the gene mutated in limb-girdle muscular dystrophy. *The Journal of Biological Chemistry* **272(51)**:32534-32538.
20. Nishiyama, A, Endo, T, Takeda, S, & M Imamura (2004) Identification and characterization of epsilon-sarcoglycans in the central nervous system. Brain Research. *Molecular Brain Research* **125(1-2)**:1-12.
21. Zhao, Y, Lu, S, Wu, L, Chai, G, Chen, Y, Sun, J, Yu, Y, Zhou, W, Zheng, Q, Wu, M, Otterson, GA, & WG Zhu (2006) Acetylation of p53 at lysine 373/382 by the histone deacetylase inhibitor depsipeptide induces expression of p21 (Waf1/Cip1). *Molecular and Cellular Biology* **26(7)**:2782-2790.
22. Yokoi, F, Dang, MT, Li, J, & Y Li (2006) Myoclonus, motor deficits, alterations in emotional responses and monoamine metabolism in epsilon-sarcoglycan deficient mice. *Journal of Biochemistry* **140(1)**:141-146.
23. Liu, P, Jenkins, N, & N Copeland (2003) A highly efficient recombineering-based method for generating conditional knockout mutations. *Genome Research* **13**:476-484.
24. Liou, JY, Ko, BS, & TC Chang (2010) An efficient transfection method for mouse embryonic stem cells. *Methods in Molecular Biology* **650**:145-153.
25. Gouveia, TL, Kossugue, PM, Paim, JF, Zatz, M, Anderson, LV, Nigro, V, & M Vainzof (2007) A new evidence for the maintenance of the sarcoglycan complex in muscle sarcolemma in spite of the primary absence of delta-SG protein. *Journal of Molecular Medicine (Berlin, Germany)* **85(4)**:415-420.
26. Cai, H, Erdman, RA, Zweier, L, Shaw, JH, Baylor, KA, Stecker, MM, Carey, DJ, & YM Chan (2007) The Sarcoglycan complex in Schwann cells and its role in myelin stability. *Experimental Neurology* **205(1)**:257-269.
27. Evangelopoulos, ME, Wuller, S, Weis, J, & A Kruttgen (2010) A role of nitric oxide in neurite outgrowth of neuroblastoma cells triggered by mevastatin or serum reduction. *Neuroscience Letters* **468(1)**:28-33.
28. Dressman, D, Araishi, K, Imamura, M, Sasaoka, T, Liu, LA, Engvall, E, & EP Hoffman (2002) Delivery of α- and β-sarcoglycan by recombinant adeno-associated virus: Efficient rescue of muscle, but differential toxicity. *Human Gene Therapy* **13**:1631-1646.
29. Truett, GE, Heeger, P, Mynatt, RL, Truett, AA, Walker, JA, & ML Warman (2000) Preparation of PCR-quality mouse genomic DNA with hot sodium hydroxide and tris (HotSHOT). *Biotechniques* **29(1):**52-54.
30. Alderton, WK, Cooper, CE, & RG Knowles (2001) Nitric oxide synthase: structure function and inhibition. *The Biochemical Journal* **357(3):**593-615.
31. AL Joyner (2000) *Gene targeting : a practical approach.* 2nd ed. Oxford University Press, Oxford ; New York.

32. Ono, R et al. (2006) Deletion of Peg10, an imprinted gene acquired from a retrotransposon, causes early embryonic lethality. *Nature Genetics* **38(1):**101-106.
33. Bernocco, S, Fondelli, C, Matteoni, S, Gotta, S, Terstappen, GC, & R Raggiaschi (2008) Sequential detergent fractionation of primary neurons for proteomics studies. *Proteomics* **8(5):**930-938.
34. Sugita, S, Saito, F, Tang, J, Satz, J, Campbell, K, & TC Sudhof (2001) A stoichiometric complex of neurexins and dystroglycan in brain. *The Journal of Cell Biology* **154(2):**435-445.
35. Powell, SK, & HK Kleinman (1997) Neuronal laminins and their cellular receptors. *The International Journal of Biochemistry and Cell Biology* **29(3):**401-414.
36. www.*omim.org* Online Mendelian Inheritance in Man: An Online Catalog of Human Genes and Genetic Disorders. Last updated 14 August 2012
37. www.*ninds.nih.gov* National Institute of Neurological Disorders and Stroke, National Institute of Health.
38. Gorecki, DC, Monaco, AP, Derry, JMJ, Walker, AP, Barnard, EA, & PJ Barnard (1992) Expression of four alternative dystrophin transcripts in brain regions regulated by different promoters. *Human Molecular Genetics* **1(7):**505-510.
39. Holder, E, Maeda, M, & RD Bies (1996) Expression and regulation of the dystrophin Purkinje promoter in human skeletal muscle, heart, and brain. *Human Genetics* **97:**232-239.
40. Lidov, HGW, Selig, S, & LM Kunke (1995) Dp140: a novel 140 kDA CNS transcript from the dystrophin locus. *Human Molecular Genetics* **4(3):**329-335.
41. Lidov, HGW, Byers, TJ, Watkins, SC, & LM Kunkel (1990) Localization of dystrophin to postsynaptic regions of central nervous system cortical neurons. *Nature* **348:**725-728.
42. Austin, RC, Howard, PL, D'Souza, VN, KIamut, HJ, & PN Ray (1995) Cloning and characterization of alternatively spliced isoforms of Dp71. *Human Molecular Genetics* **4(9):**1475-1483.
43. Nudel, U, Zuk, D, Einat, P, Zeelon, E, Levy, Z, Neuman, S, and D Yaffe (1989) Duchenne muscular dystrophy gene product is not identical in muscle and brain. *Nature* **337:**76-78.
44. Boyce, FM, Beggs, AH, Feener, CA, and LM Kunkel (1991). Dystrophin is transcribed in brain from a distant upstream promoter. *Proceedings from the National Academy of Sciences of the United States of America* **88:**1276-1280.
45. Bansal, D, Miyake, K, Vogel, SS, Groh, S, Chen. CC, Williamson, R, McNeil, PL, & KP Campbell (2003) Defective membrane repair in dysferlin-deficient muscular dystrophy. *Nature* **423(6936):**168-172.
46. Hagiwara, Y, Sasaoka, T, Araishi, K, Imamura, M, Yorifuji, H, Nonaka, I, Ozawa, E, & T Kikuchi (2000) Caveolin-3 deficiency causes muscle degeneration in mice. *Human Molecular Genetics* **9(20):**3047-3054.
47. Hoffman, EP, & LM Kunkel (1989) Dystrophin abnormalities in Duchenne/Becker muscular dystrophy. *Neuron* **2(1):**1019-1029.
48. S Fahn (2000) The spectrum of levodopa-induced dyskinesias. *Annals of Neurology* **47(4 Sup1):**S2-9.

49. Todd, RD, & JS Perlmutter (1998) Mutational and biochemical analysis of dopamine in dystonia: evidence for decreased dopamine D2 receptor inhibition. *Molecular Neurobiology* **16(2):**135-147.
50. Klein, C, Gurvich, N, Sena-Esteves M, Bressman, S, Brin, MF, Ebersole, BJ, Fink, S, Forsgren, L, Friedman, J, Grimes, D, Holmgren, G, Kyllerman, M, Lang, AE, de Leon, D, Leung, J, Prioleau, C, Raymond, D, Sanner, G, Saunders-Pullman, R, Vieregge, P, Wahlstrom, J, Breakefield, XO, Kramer, PL, Ozelius, LJ, & SC Sealfon (2000) Evaluation of the role of the D2 dopamine receptor in myoclonus dystonia. *Annals of Neurology* **47(3):**369-373.
51. Klein C, Brin MF, Kramer P, Sena-Esteves, M, de Leon, D, Doheny, D, Bressman, S, Fahn, S, Breakfield, XO, & LJ Ozelius (1999) Association of a missense change in the D2 dopamine receptor with myoclonus dystonia. *Proceedings from the National Academy of Sciences of the United States of America* **96:**5173–5176.
52. Stocco, A, Lebiere, C, & JR Anderson (2010) Conditional Routing of Information to the Cortex: A Model of the Basal Ganglia's Role in Cognitive Coordination. *Psychological Review* **117(2):**541-574.
53. EM Southern (1975) Detection of specific sequences among DNA fragments separated by gel electrophoresis. *Journal of Molecular Biology* **98(3):**503-517.
54. Feinberg, AP, & B Vogelstein, (1983) A technique for radiolabeling DNA restriction endonuclease fragments to high specific activity. *Analytical Biochemistry* **132(1):** 6-13.
55. Cai, Q, Patel, M, Coling, D, & BH Hu (2012) Transcriptional changes in adhesion-related genes are site-specific during noise-induced cochlear pathogenesis. *Neurobiology of Disease* **45(2):**723-732.
56. Förstermann, U, & WC Sessa (2012) Nitric oxide synthases: regulation and function. *European Heart Journal* **33(7):**829-837.
57. Bellefontaine, N, Hanchate, NK, Parkash, J, Campagne, C, de Seranno, S, Clasadonte, J, d'Anglemont de Tassigny, X, & V Prevot (2011) Nitric oxide as key mediator of neuron-to-neuron and endothelia-to-glia communication involved in the neuroendocrine control of reproduction. *Neuroendocrinology* **93(2):**74-89.
58. GC Brown (2010) Nitric oxide and neuronal death. *Nitric oxide : biology and chemistry / official journal of the Nitric Oxide Society* **23(3):**153-165.
59. Dragatsis, I, & S Zeitlin (2001) A method for the generation of conditional gene repair mutations in mice. *Nucleic Acids Research* **29(3):**E10.
60. Hjermind, LE, Vissing, J, Asmus, F, Krag, T, Lochmuller, H, Walter, MC, Erdal, J, Blake, DJ, & JE Nielsen (2008) No muscle involvement in myoclonus-dystonia caused by ε-sarcoglycan gene mutations. *European Journal of Neurology* **15:**525-529.
61. Waite, A, De Rosa, MC, Brancaccia, A, & DJ Blake (2011) A gain-of-glycosylation mutation associated with myoclonus dystonia syndrome affects trafficking and processing of mouse ε-sarcoglycan in the late secretory pathway. *Human Mutations* **32(11):**1246-1258.
62. Yokoi, F, Dang, MT, Yang, G, Li, JD, Doroodchi, A, Zhou, T, & Y Li (2011) Abnormal nuclear envelope in the cerebellar Purkinje cells and impaired motor learning in DYT11 myoclonus-dystonia mouse models. *Behavioural Brain Research* **227(1):** 12-20.

63. Yokoi, F, Dang, MT, Zhou, T, & Y Li (2012) Abnormal nuclear envelopes in the striatum and motor deficits in DYT11 myoclonus-dystonia mouse models. *Human Molecular Genetics* **21(4):**916-925.
64. Peall, KJ, Waite, A, Blake, DJ, Owen, MJ, & HR Morris (2011) Psychiatric disorders, myoclonus dystonia, and the epsilon-sarcoglycan gene: a systematic review. *Movement Disorders* **26(10):**1939-1942.
65. Ritz, K, van Schaik, BDC, Jakobs, ME, van Kampen, AH, Aronica, E, Tijssen, MA, & F Baas (2011) SGCE isoform characterization and expression in human brain: implications for myoclonus-dystonia pathogenesis? *European Journal of Human Genetics* **19:**438-444.
66. Grant, MKO, Cuadra, AE, & EE El-Fakahany (2002) Endogenous expression of nNOS protein in several neuronal cell lines. *Life Sciences* **71:**813-817.
67. Allikian, MJ, Hack, AA, Mewborn, S, Mayer, U, & EM McNally (2004) Genetic compensation for sarcoglycan loss by integrin α7β1 in muscle. *Journal of Cell Science* **117:**3821-3830.
68. Yoshida, T, Pan, Y, Hanada, H, Iwata, Y, & M Shigekawa (1998) Bidirectional signaling between sarcoglycans and the integrin adhesion system in cultured L6 myocytes. *The Journal of Biological Chemistry* **273(3):**1583-1590.
69. L Defebvre (2007) Myoclonus and extrapyramidal diseases. *Neurophsiologie Clinique* **36:**319-325.
70. Dang, MT, Yokoi, F, McNaught, K, Jengelley, TA, Jackson, T, Li, J, & Y Li (2005) Generation and characterization of Dyt1 ΔGAG knock-in mouse as a model for early-onset dystonia. *Experimental Neurology* **196:**452-463.
71. M Hallett (2004) Dystonia: abnormal movements result from loss of inhibition. *Dystonia 4: Advances in Neurology* **94:**1-9.
72. SB Bressman (2004) Dystonia genotypes, phenotypes and classification. *Dystonia 4: Advances in Neurology* **94:**101-107.
73. Saunders-Pullman, R, Shriberg, J, Shanker, V, & SB Bressman (2004) Penetrance and expression of dystonia genes. *Dystonia 4: Advances in Neurology* **94:**121-125.
74. Beukers, RJ, van der Meer, JN, van der Salm, SM, Foncke, EM, Veltman, DJ, & MAJ Tijssen (2011) Severity of dystonia is correlated with putaminal gray matter changes in myoclonus-dystonia. *European Journal of Neurology* **18(6):**906-912.
75. Hartmann, CJ, Leube, B, Wojtecki, L, Betz, B, Groiss, SJ, Bauer, P, Schnitzler, A, & M Südmeyer (2011). A novel mutation of the SGCE-gene in a german family with myoclonus-dystonia syndrome. *Journal of Neurology* **258(6):**1186-1188.
76. Kowarik, MC, Langer, S, Keri, C, Hemmer, B, Oexle, K, & J Winkelmann (2011) Myoclonus-dystonia in 18p deletion syndrome. *Movement Disorders* **26(3):** 560-561.
77. Beukers, RJ, Foncke, EM, van der Meer, JN, Nederveen, AJ, de Ruiter, MB, Bour, LJ, Veltman, DJ, & MAJ Tijssen (2010) Disorganized sensorimotor integraiton in mutation-positive myoclonus-dystonia. *Archives of Neurology* **67(4):**469-474.
78. Wong, SH, Steiger, MJ, Larner, AJ, & NA Fletcher (2010) Hereditary myoclonus dystonia (DYT11): a novel sgce gene mutation with intrafamilial phenotypic heterogeneity. *Movement Disorders* **25(7):**956-957.
79. Ritz, K, Gerrits, MCF, Foncke, EMJ, van Ruissen, F, van der Linden, C, Vergouwen, MDI, Bloem, BR, Vandenberghe, W, Crols, R, Speelman, JD, Baas, F,

& MA Tijssen (2009) Myoclonus-dystonia: clinical and genetic evaluation of a large cohort. *Journal of Neurosurgery and Psychiatry* **80:**653-658.
80. Kinugawa, K, Vidailhet, M, Clot, F, Apartis, E, Grabli, D, & E Roze (2009) Myoclonus-dystonia: an update. *Movement Disorders* **24(4):**479-489.
81. Lewis, C, Carberry, S, & K Ohlendieck (2009) Proteomic profiling of x-linked muscular dystrophy. *Journal of Muscle Research and Cell Motility* **30(7-8):**267-269.
82. Thümmler, S, Giuliano, F, Pincemaille, O, Saugier-Veber, P, & S Perelman (2009) Myoclonus in fraternal twin toddlers a French family with a novel mutation in the SGCE gene. *European Journal of Paediatric Neurology* **13(6):**559-561.
83. Meunier, S, Lourenco, G, Roze, E, Apartis, E, Trocello, JM, & M Vidailhet (2008) Cortical excitability in DYT-11 positive myoclonus dystonia. *Movement Disorders* **23(5):**761-764.
84. Chen, XP, Zhang, YW, Zhang, SS, Chen, Q, Burgunder, JM, Wu ,SH, Yang, Y, Luo, ZM, & HF Shang (2008) A novel mutation of the epsilon-sarcoglycan gene in a Chinese family with myoclonus-dystonia syndrome. *Movement Disorders* **23(10):** 1472-1475.
85. Bonnet, C, Grégoire, MJ, Vibert, M, Raffo, E, Leheup, B, & P Jonveaux (2008) Cryptic 7q21 and 9p23 deletions in a patient with apparently balanced de novo reciprocal translocation t(7;9)(q21;p23) associated with a dystonia-plus syndrome: paternal deletion of the epsilon-sarcoglycan (SGCE) gene. *Journal of Human Genetics* **53(10):**876-885.
86. Beukers, RJ, Booij, J, Weisscher, N, Zijlstra, F, van Amelsvoort, TA, & MA Tijssen (2009) Reduced striatal D2 receptor binding in myoclonus-dystonia. *European Journal of Nuclear Medicine and Molecular Imaging* **36(2):**269-274.
87. Hess, CW, Raymond, D, Aguiar Pde, C, Frucht, S, Shriberg, J, Heiman, GA, Kurlan, R, Klein, C, Bressman, SB, Ozelius, LJ, & R Saunders-Pullman (2007) Myoclonus-dystonia, obsessive-compulsive disorder, and alcohol dependence in SGCE mutation carriers. *Neurology* **68:**522-524.
88. Asmus, F, & T Gasser (2004) Inherited myoclonus-dystonia. *Dystonia 4: Advances in Neurology* **94:**113-119.
89. Han, F, Lang, AE, Racacho, L, Bulman, DE, & DA Grimes (2003) Mutations in the epsilon-sarcoglycan gene found to be uncommon in seven myoclonus-dystonia families. *Neurology* **61(2):**244-246.
90. Müller, B, Hedrich, K, Kock, N, Dragasevic, N, Svetel, M, Garrels, J, Landt, O, Nitschke, M, Pramstaller, PP, Reik, W, Schwinger, E, Sperner, J, Ozelius, L, Kostic, V, & C Klein (2002) Evidence that paternal expression of the epsilon-sarcoglycan gene accounts for reduced penetrance in myoclonus-dystonia. *American Journal of Human Genetics* **71(6):**1303-1311.
91. Grabowski, M, Zimprich, A, Lorenz-Depiereux, B, Kalscheuer, V, Asmus, F, Gasser, T, Meitinger, T, & TM Strom (2002) The epsilon-sarcoglycan gene (SGCE), mutated in myoclonus-dystonia syndrome, is maternally imprinted. *European Journal of Human Genetics* **11(2):**138-144.
92. Zimprich A, Grabowski M, Asmus F, Naumann M, Berg D, Bertram M, Scheidtmann K, Kern P, Winkelmann J, Müller-Myhsok B, Riedel L, Bauer M, Müller T, Castro M, Meitinger T, Strom TM, & T Gasser (2001) Mutations in the gene encoding epsilon-sarcoglycan cause myoclonus-dystonia syndrome. *Nature Genetics* **29(1):**66-69.

93. Finanger Hedderick, EL, Simmers, JL, Soleimani, A, Andres-Mateos, E, Marx, R, Files, DC, King, L, Crawford, TO, Corse, AM, & RD Cohn (2011) Loss of sarcolemmal nNOS is common in acquired and inherited neuromuscular disorders. *Neurology* **76(11):**960-967.
94. Adams, ME, Anderson, KN, & SC Froehner (2010) The alpha-syntrophin PH and PDZ domains scaffold acetylcholine receptors, utrophin, and neuronal nitric oxide synthase at the neuromuscular junction. *The Journal of Neuroscience* **30(33):** 11004-11010.
95. Y Gao (2010) The multiple actions of NO. *European Journal of Physiology* **459:**829-839.
96. Hsieh, HY, Robertson, CL, Vermehren-Schmaedick, A, & A Balkowiec (2010) Nitric oxide regulates BDNF release from nodose ganglion neurons in a pattern-dependent and cGMP-independent manner. *Journal of Neuroscience Research* **88(6):**1285-97.
97. Li, M, Wang, L, Peng, Y, Wang, JC, & LH Zhou (2010) Knockdown of the neuronal nitric oxide synthase gene retard the development of the cerebellar granule neurons in vitro. *Developmental Dynamics* **239:**474-481.
98. Zhang, L, Yokoi, F, Parsons, DS, Standaert, DG & Y Li (2012) Alteration of Striatal Dopaminergic Neurotransmission in a Mouse Model of DYT11 Myoclonus-Dystonia. *Public Library of Science* **7(3):**e33669.